UC Irvine
UC Irvine Previously Published Works

Title

Calibration of the jet energy scale and resolution of small-radius jets using semileptonic $t\bar{t}$ events with the ATLAS detector

Permalink

https://escholarship.org/uc/item/19s613bs

Journal

European Physical Journal C, 86(8)

ISSN

1434-6044

Authors

Aad, G

Aakvaag, E

Abbott, B

et al.

Publication Date

2026-08-07

DOI

10.1140/epjc/s10052-026-15692-2

Copyright Information

This work is made available under the terms of a Creative Commons Attribution License, available at https://creativecommons.org/licenses/by/4.0/

Peer reviewed

eScholarship.org Powered by the California Digital Library
University of California

Eur. Phys. J. C (2026) 86:943
https://doi.org/10.1140/epjc/s10052-026-15692-2

THE EUROPEAN PHYSICAL JOURNAL C

Regular Article - Experimental Physics

Calibration of the jet energy scale and resolution of small-radius jets using semileptonic $t\bar{t}$ events with the ATLAS detector

ATLAS Collaboration[⋆]

CERN, 1211 Geneva 23, Switzerland

Received: 22 December 2025 / Accepted: 11 April 2026
© CERN for the benefit of the ATLAS Collaboration 2026, modified publication 2026

Abstract A measurement of correction factors for the hadronic jet energy scale and resolution in the ATLAS detector is presented. These correction factors account for differences between simulated and observed data. They are obtained by analysing a selection of top quark events collected in proton–proton collisions by ATLAS between the years 2015 and 2018 at a centre-of-mass energy $\sqrt{s} = 13$ TeV as well as in 2022 and 2023 at $\sqrt{s} = 13.6$ TeV. The impact of different jet energy scale or resolution corrections on the reconstructed mass of the hadronically decaying W boson from top-quark decays in simulation is quantified. The correction factors are extracted from a fit to the parameterised reconstructed W-boson mass distribution to data. The energy scale and resolution corrections are measured as a function of the jet transverse momentum between 20 and 200 GeV and absolute pseudorapidity less than 0.8. The uncertainties in the energy scale range from about 0.93% to about 1.7% for jets between 35 and 200 GeV, while for the energy resolution the uncertainties range from about 14 to 28%. The method presented will be used in conjunction with other techniques to further improve ATLAS jet energy scale and resolution precision.

1 Introduction

In quantum chromodynamics (QCD), the theory of strong interactions, the quarks and gluons carry colour charge. Because of the confinement properties of QCD, they cannot be detected directly but instead form collimated sprays of hadrons, called jets. Jets are produced abundantly at the Large Hadron Collider (LHC) [1] and are an important signature for many processes. The measurement of the jet energy plays a vital role in all jet-based analyses with the ATLAS detector, with the uncertainty in the energy calibrations often being one of the largest uncertainties in precision measurements [2–6].

In ATLAS, the jet energy is evaluated through a series of corrections starting from the correction to the energy of the individual jet's constituents [7–11]. The calibration of the average jet transverse momentum (p_{T}) is called the 'jet energy scale' (JES) and the calibration of the p_{T} resolution is called the 'jet energy resolution' (JER). The jet energy corrections are based on Monte Carlo (MC) simulations modelling the detector response and on assessing *in situ* how well the MC simulations describe data. The corrections ensure that the reconstructed jet p_{T} equals, on average, the p_{T} of the corresponding particle-level jet, i.e. the event generator output after the hadronisation and before the detector simulation. Several effects are corrected including the non-compensating nature of the ATLAS calorimeter (i.e. a lower response to hadrons than to electrons or photons), energy deposits outside jets and energy losses in dead material before and in-between the calorimeters. The jet response is usually expressed as a function of variables, such as the energy fraction in the hadronic calorimeter or the number of charged-particle tracks associated to a jet, that are sensitive to jet fragmentation.

A subsequent set of *in situ* jet calibrations are applied to ensure that the jet p_{T} evaluated in data matches the simulation. These corrections are obtained by exploiting the p_{T}-balance in certain event topologies where the jet recoils against a well-measured object like a photon or a Z boson decaying into electron or muon pairs (Z/γ+jet), dijet or multijet events, and by comparing the p_{T}-balance in simulation with that in data.

The 'Z/γ+jet' method was also used for JER measurements in previous ATLAS calibrations [7]. Currently, ATLAS JER measurements rely on two methods. Firstly, the 'dijet-balance' method [10], where the scalar balance of the p_{T} of the jets in dijet events, is exploited. Secondly, the 'random cones' technique [10], in which energy deposits in the calorimeter are summed in circular areas analogous to the jet area for anti-k_t jets [12], providing the best precision for low p_{T} jets.

⋆ e-mail: atlas.publications@cern.ch

Published online: 07 August 2026

This paper focuses on a complementary technique to improve the current *in situ* calibration for the JES and JER by measuring jets in top-quark pair-production ($t\bar{t}$) events, where one of the top-quark decays includes a lepton from the W boson (semileptonic $t\bar{t}$ events). Semileptonic $t\bar{t}$ events are chosen due to the presence of a hadronically decaying W boson whose lineshape distribution is sensitive to JES and JER. Additionally, semileptonic $t\bar{t}$ events contain a high-momentum charged lepton that provides a clear signal for the trigger to accept the events. Finally, the $t\bar{t}$ production cross-section is large at the LHC and the decay products provide a signature with an isolated lepton and b-jet in the final state that leads to an experimental signature with minimal background. The ATLAS Collaboration previously used $t\bar{t}$ events as a cross-check of the JES calibration [13]. Moreover, top-quark mass measurements performed at Tevatron and LHC experiments exploited the W-boson lineshape distribution to control the JES uncertainties [5,14–18], demonstrating the potential of W-boson mass distribution as a powerful probe of the jet response. However, the obtained corrections to the JES in the previous top-quark mass measurements are not considered universal as they are not binned in jet p_{T} and jet η but are specific to each measurement's selections, and are used only within their respective measurements. This paper presents the measurement of the JES corrections as a function of jet p_{T} and jet $|\eta|$ making the calibration universal and not relying on the kinematics of the calibration dataset. The selection of the events in the presented measurement is orthogonal to the selection with the established jet calibration techniques. The dominant uncertainties of the presented measurement originate from the uncertainty in the modelling of the $t\bar{t}$ events, making the systematic uncertainties decorrelated from the standard calibration techniques. Additionally, the jets from the W-boson decay are quark-initiated, compared to mostly gluon-initiated jets from the established JER calibration techniques providing complementary information about jet calibrations.

This paper presents a measurement of the correction factors between simulation and data for the JES and the JER, targeting jets clustered with the anti-k_t algorithm with a radius parameter $R = 0.4$ using the proton–proton collision data collected by the ATLAS detector in Run 2, i.e. between the years 2015 and 2018 at a centre-of-mass energy of $\sqrt{s} = 13$ TeV and, separately, for data collected in Run 3 in the years 2022 and 2023 at $\sqrt{s} = 13.6$ TeV.

The forward-folding formula [19] is applied to individual jets to generate templates representing different JES or JER assumptions. The forward-folding technique is used because of its better precision compared to the background suppression technique [19]. The two jets originating from the hadronically decaying W boson are identified and the templates for the invariant mass of the two jets are constructed. Only central jets in the pseudorapidity region of $|\eta| < 0.8$[1] are considered to facilitate the future combination with other *in situ* measurements. A likelihood fit of the generated templates to the observed data is performed to find the optimal values for the JES and JER parameters together with their uncertainties.

2 ATLAS detector

The ATLAS detector [20,21] at the LHC covers nearly the entire solid angle around the collision point. It consists of an inner tracking detector surrounded by a thin superconducting solenoid, electromagnetic and hadronic calorimeters, and a muon spectrometer incorporating three large superconducting air-core toroidal magnets.

The inner-detector system (ID) is immersed in a 2 T axial magnetic field and provides charged-particle tracking in the range of $|\eta| < 2.5$. The high-granularity silicon pixel detector covers the vertex region and typically provides four measurements per track, the first hit generally being in the insertable B-layer (IBL). It is followed by the semiconductor tracker (SCT), which usually provides eight measurements per track. These silicon detectors are complemented by the transition radiation tracker (TRT), which enables radially extended track reconstruction up to $|\eta| = 2.0$. The TRT also provides electron identification information based on the fraction of hits (typically 30 in total) above a higher energy-deposit threshold corresponding to transition radiation.

The calorimeter system covers the pseudorapidity range $|\eta| < 4.9$. Within the region $|\eta| < 3.2$, electromagnetic calorimetry is provided by barrel and endcap high-granularity lead/liquid-argon (LAr) calorimeters, with an additional thin LAr presampler covering $|\eta| < 1.8$ to correct for energy loss in material upstream of the calorimeters. Hadronic calorimetry is provided by the steel/scintillator-tile calorimeter, segmented into three barrel structures within $|\eta| < 1.7$, and two copper/LAr hadronic endcap calorimeters. The solid angle coverage is completed with forward copper/LAr and tungsten/LAr calorimeter modules optimised for electromagnetic and hadronic energy measurements, respectively.

The muon spectrometer (MS) comprises separate trigger and high-precision tracking chambers measuring the deflection of muons in a magnetic field generated by the supercon-

[1] ATLAS uses a right-handed coordinate system with its origin at the nominal interaction point (IP) in the centre of the detector and the z-axis along the beam pipe. The x-axis points from the IP to the centre of the LHC ring, and the y-axis points upwards. Polar coordinates (r, ϕ) are used in the transverse plane, ϕ being the azimuthal angle around the z-axis. The pseudorapidity is defined in terms of the polar angle θ as $\eta = -\ln\tan(\theta/2)$ and is equal to the rapidity $y = \frac{1}{2}\ln\left(\frac{E+p_z}{E-p_z}\right)$ in the relativistic limit. Angular distance is measured in units of $\Delta R \equiv \sqrt{(\Delta y)^2 + (\Delta\phi)^2}$.

ducting air-core toroidal magnets. The field integral of the toroids ranges between 2.0 and 6.0 T m across most of the detector. Three layers of precision chambers, each consisting of layers of monitored drift tubes, cover the region $|\eta| < 2.7$. These were complemented in the innermost layer of the endcap region by cathode-strip chambers in Run 2, which were replaced in Run 3 by layers of small-strip thin-gap chambers and Micromegas chambers, both providing precision tracking in the region $1.3 < |\eta| < 2.7$. The muon trigger system covers the range $|\eta| < 2.4$ with resistive-plate chambers in the barrel region, thin-gap chambers in the endcap regions, and, in Run 3, the small-strip thin-gap chambers and Micromegas chambers in the innermost layer of the endcap.

The luminosity is measured mainly by the LUCID–2 detector [22] that records Cherenkov light produced in the quartz windows of photomultipliers located close to the beampipe.

Events were selected by the first-level trigger system implemented in custom hardware, followed by selections made by algorithms implemented in software in the high-level trigger [23,24]. The first-level trigger accepted events from the 40MHz bunch crossings at a rate close to 100kHz, which the high-level trigger further reduced in order to record complete events to disk at about 1.25 kHz and 3 kHz in Run 2 and Run 3, respectively.

The Run 3 detector configuration benefits from several upgrades compared with that of Run 2 to maintain high detector performance at the higher pile-up levels of Run 3. The improvements include a new innermost layer of the muon spectrometer in the endcap region, which provides higher redundancy and a large reduction in fake muon triggers. The trigger system also benefits from new digital electronics readout of the LAr calorimeters with significantly increased granularity. Other updates and further details are provided in Ref. [21].

A software suite [25] is used in data simulation, in the reconstruction and analysis of real and simulated data, in detector operations, and in the trigger and data acquisition systems of the experiment.

3 Data and Monte Carlo samples

This analysis uses two data samples collected by ATLAS. Only events recorded when LHC beams were stable and all ATLAS detector systems were operational are selected [26]. The first sample consists of the full LHC Run 2 data collected in 13 TeV proton–proton (pp) collisions during 2015–2018, corresponding to an integrated luminosity of 140 fb^{-1} [27]. The second consists of LHC Run 3 pp data collected during 2022 and 2023, corresponding to an integrated luminosity of 52 fb^{-1}. The uncertainty in the total integrated luminosity is 0.83% for the Run 2 data-taking and 2% for the Run 3 data-taking [27,28]. The mean average number of interactions per bunch crossing was 33.7 for Run 2 and 42.5 and 51.2 during Run 3 data-taking in 2022 and 2023 respectively.

Only data events selected by the single-electron or single-muon trigger [29,30] are used in the presented analysis. The electron trigger reached the efficiency plateau region for electrons with reconstructed $p_{\mathrm{T}} > 25$ GeV in 2015 and for $p_{\mathrm{T}} > 27$ GeV in 2016–2023. The corresponding thresholds for the muon trigger were 21 GeV in 2015, 27 GeV in 2016–2018 and 25 GeV in 2022–2023.

The top-quark mass was set to $m_t = 172.5$ GeV in all simulated processes, unless stated otherwise. The decays of bottom and charm hadrons were performed by EvtGen 1.6.0 [31] in the Run 2 simulation and by EvtGen 2.1.1 in the Run 3 simulation.

The production of $t\bar{t}$ events was simulated using the Powheg Box v2 [32–35] generator at next-to-leading order (NLO) with the NNPDF3.0 NLO [36] parton distribution function (PDF) set and the h_{damp} parameter[2] set to $1.5\,m_t$ [37]. The $t\bar{t}$ sample was normalised to the cross-section prediction at next-to-next-to-leading order (NNLO) in QCD including the resummation of next-to-next-to-leading-logarithmic (NNLL) soft-gluon terms calculated using Top++ 2.0 [38–44].

The associated production of top quarks with W bosons (tW) was simulated by the Powheg Box v2 [33–35,45] generator at NLO in QCD using the five-flavour scheme and the NNPDF3.0NLO set of PDFs. The functional form of the renormalisation and factorisation scales was set to a dynamic scale with $\mu = H_{\mathrm{T}}/2 = (m_{\mathrm{T,top}} + m_{\mathrm{T},W} + p_{\mathrm{T,j1}})/2$, where $m_{\mathrm{T,top}}$ and $m_{\mathrm{T},W}$ are the transverse masses of top quark and W boson, respectively, and $p_{\mathrm{T,j1}}$ is the transverse momentum of the leading jet. The diagram removal scheme [46] was used to remove interference and overlap with $t\bar{t}$ production. The inclusive cross-section was corrected to the theory prediction calculated at NLO in QCD with NNLL soft-gluon corrections [47,48]. The tW process dominates the contribution of the single-top processes in the analysis selection described below.

Single-top t-channel and s-channel production was simulated using the Powheg Box v2 [49,50] generator at NLO in QCD using the four-flavour (five-flavour) scheme for the t-channel (s-channel) and the corresponding NNPDF3.0 NLO set of PDFs.

For all nominal simulated $t\bar{t}$ and single-top samples, the events were interfaced to Pythia 8.230 [51] for the Run 2 simulation and interfaced to Pythia 8.308 for the Run 3 simulation to model the parton shower, hadronisation, and under-

[2] The h_{damp} parameter is a resummation damping factor and one of the parameters that controls the matching of Powhegmatrix elements to the parton shower. It essentially regulates the high-p_{T} radiation against which the $t\bar{t}$ system recoils.

lying event, with parameters set according to the A14 set of tuned parameters (tune) [52] and using the NNPDF2.3LO set of PDFs [53]. Several alternative MC generators are used to estimate the uncertainty in the modelling of the $t\bar{t}$ and tW events as described in Sect. 6.

The production of (Z/W)+jets events was simulated with the SHERPA 2.2.11 and SHERPA 2.2.14 [54] generators using NLO matrix elements (ME) for up to two partons, and leading-order (LO) matrix elements for up to four (five) partons in the Run 2 (Run 3) simulation calculated with the Comix [55] and OPENLOOPS [56–58] libraries. They were matched to the SHERPA parton shower [59] using the MEPS@NLO prescription [60–63] with the set of tuned parameters developed by the SHERPA authors. The NNPDF3.0NNLO set of PDFs [36] was used and the samples were normalised to an NNLO prediction [64].

Samples of diboson final states (VV) were simulated with SHERPA 2.2.11 or SHERPA 2.2.12 for the Run 2 simulation, and SHERPA 2.2.14 or SHERPA 2.2.16 for the Run 3 simulation, depending on the process, including off-shell effects and Higgs boson contributions, where appropriate. Fully leptonic final states and semileptonic final states, where one boson decays leptonically and the other hadronically, were simulated using matrix elements at NLO accuracy in QCD for up to one additional parton and at LO accuracy for up to three additional parton emissions.

Simulated $t\bar{t}$ events with both W bosons decaying hadronically are used to estimate the contribution of the fake and non-prompt lepton background. The flavour-tagging requirements with the kinematic reconstruction presented in Sect. 5 significantly suppress the other sources of the fake and non-prompt backgrounds and the contribution is expected to be dominated by the $t\bar{t}$ events.

The effect of pile-up was modelled by overlaying [65] the simulated hard-scattering event with inelastic pp events generated from a mix of EPOS 2.0.1.4 [66] and PYTHIA 8.308 [67]. The EPOS events were generated with the EPOS LHC tune [68] and the PYTHIA events with the A3 tune [69] and the NNPDF2.3LO set of PDFs. PYTHIA pile-up events include either a high p_{T} jet, a prompt photon, or a lepton from a B-hadron decay, while EPOS was filtered to simulate all remaining pile-up events in the overlay sample. The individual simulations were first reweighted to ensure a smooth connection across jet p_{T}, then the combination reweighted to match the distribution of the actual number of interactions per bunch crossing measured in data.

The ATLAS detector response was simulated using the GEANT4 toolkit [70] with the full simulation of the ATLAS detector [71] for most of the samples. For some of the systematic variations affecting the measurement of the JES and JER correction factors, a fast detector simulation based on a parametric description of the calorimeter showers [72] was used. The samples with fast detector simulations are always compared only to nominal samples with the same fast detector simulations.

4 Object definitions and forward-folding method

Electrons are reconstructed from energy deposits in the electromagnetic calorimeter matched to a track in the ID. The electrons are required to satisfy the 'tight' likelihood-based identification working point and to be well isolated [73,74]. These electrons are required to have $p_{\mathrm{T}} > 27$ GeV and $|\eta| < 2.47$ while excluding the transition region between the barrel and endcap calorimeters ($1.37 < |\eta| < 1.52$). Muons are reconstructed from a track in the ID and a matched track from the MS. The muons are required to satisfy the 'medium' identification working point and to be well isolated [75,76]. The muons are required to have $p_{\mathrm{T}} > 27$ GeV and $|\eta| < 2.5$. The identification, isolation and trigger efficiencies of the electrons and muons are corrected in simulation via scale factors to match the efficiencies measured in data [29,30,74].

Electron (muon) candidates are matched to the reconstructed position of the main interaction point, the primary vertex [77], by requiring that the significance of their transverse impact parameter, d_0,[3] satisfies $|d_0/\sigma(d_0)| < 5$ (3), where $\sigma(d_0)$ is the measured uncertainty in d_0, and by requiring that their longitudinal impact parameter, z_0,[4] satisfies $|z_0 \sin\theta| < 0.5$ mm.

The jets are reconstructed from particle flow objects [8] using the anti-k_t clustering algorithm with a radius parameter $R = 0.4$, implemented in the FASTJET software package [78]. Only jets that have $p_{\mathrm{T}} > 15$ GeV and $|\eta| < 2.5$ are considered for the selection, while only jets with $p_{\mathrm{T}} > 20$ GeV and $|\eta| < 0.8$ are used for the JES and JER correction measurement. To suppress jets originating from pile-up, jets with $p_{\mathrm{T}} < 60$ GeV are required to satisfy a neural-network-based jet vertex tagger (NNJVT) discriminant, a successor to the jet vertex tagger algorithm [79]. The reconstructed jets are calibrated in two different ways for use in this measurement, once with no *in situ* corrections applied for examining the JES and once with the currently used *in situ* corrections [10] for examining the JER. In both cases, the MC-based JES correction is applied. Using these two separate calibrations for the different studies ensures that the results can be compared with other *in situ* calibration techniques, and that the best-available calibration is used as the basis for each step.

Jets that include B-hadrons (b-tagged jets) are identified by the GN2 flavour tagging algorithm [80] with a working

[3] The transverse impact parameter, d_0, is defined in the x–y plane as the distance of closest approach of the track to the beamline.

[4] The longitudinal impact parameter, z_0, is defined as the distance in z between the primary vertex and the point on the track used to evaluate d_0.

point corresponding to an efficiency of 85% for selecting a true b-jet in a $t\bar{t}$ reference sample. Scale factors are applied to simulation to match the efficiency of the b-tagging measured in data [81–83].

The missing transverse momentum is defined as the negative vector sum of the transverse momenta of all selected and calibrated physics objects, including a term to account for the momenta of soft particles that are not associated with any of the selected objects [84]. This soft term is calculated from ID tracks matched to the primary vertex. The magnitude of the missing transverse momentum vector is denoted by $E_{\mathrm{T}}^{\mathrm{miss}}$.

To avoid any double-counting of physics objects, a dedicated sequential overlap-removal procedure is applied to resolve the ambiguities. Jets within $\Delta R = 0.2$ of an electron or muon are discarded and electrons with $0.2 < \Delta R < 0.4$ to the remaining jets are rejected. Jets with fewer than three tracks are removed if they overlap with a muon within $\Delta R = 0.4$.

For the forward-folding procedure [19,85,86], particle-level objects need to be identified, using the MC particle-level record in simulation. Particle-level leptons are selected as leptons originating from the decay of a W or Z boson. The four-momentum of an electron or muon is summed with the four-momenta of all radiated photons within a cone of size $\Delta R = 0.1$ around its direction, excluding photons from hadron decays. The particle-level jets are reconstructed with the anti-k_t algorithm with a radius parameter of $R = 0.4$, using all stable particles ($c\tau > 10$ mm) except for the selected electrons, muons, and photons used in the definition of the selected leptons, and neutrinos originating from the Z boson or W bosons. The particle-level jets are required to have $p_{\mathrm{T}} > 10$ GeV and $|\eta| < 2.5$.

The forward-folding method is used to simulate the changes to the p_{T} of the selected jets due to alternative assumptions on the values of the JES or JER and it is implemented in the FastFrames software library [87]. The method relies on matching the detector-level jets to the corresponding particle-level jets and changing the momenta of reconstructed jets using the formula

$$p_{\mathrm{T}}^{\mathrm{folded}} = s \cdot p_{\mathrm{T}}^{\mathrm{reco}} + (p_{\mathrm{T}}^{\mathrm{reco}} - \mathcal{R} \cdot p_{\mathrm{T}}^{\mathrm{gen}}) \cdot (r - s), \tag{1}$$

where $p_{\mathrm{T}}^{\mathrm{gen}}$ is the momentum of the generated particle-level jet matched to the reconstructed jet with transverse momentum $p_{\mathrm{T}}^{\mathrm{reco}}$ and s (r) is the parameter representing the flavour-inclusive correction factor to the simulated JES (JER). The correction factors from Eq. (1) are consistently applied to the jet's p_{T} and its energy. The jet energy response and resolution is averaged over η in the relevant analysis region with jet $|\eta| < 0.8$ as the detector is approximately homogeneous in this narrow central region. The forward-folding formula is used to generate templates, i.e. distributions representing various JES and JER correction factors with values ranging from 0.95 to 1.05 and 0.60 to 1.40, respectively, to cover the range of the expected corrections. The parameter $\mathcal{R}$ represents the mode of the jet response distribution

$$\mathcal{R} = \mathrm{argmax} \left\{ \frac{p_{\mathrm{T}}^{\mathrm{reco}}}{p_{\mathrm{T}}^{\mathrm{gen}}} \right\},$$

estimated in simulation by fitting a Gaussian function around the peak position separately in several jet p_{T} and $|\eta|$ bins, for different jet flavours and for LHC Run 2 and Run 3 simulations. The following jet flavours are identified for the parameter $\mathcal{R}$ using the MC particle-level record: b-jet, c-jet, light-flavour (u, d, s)-jet and gluon-jet. The $\mathcal{R}$ parameter is found to be close to unity in most of the kinematic regions and for most jet flavours. The JES variations are generated while keeping the nominal JER assumption, i.e. setting the parameter r in Eq. (1) to unity and vice-versa for the JER variations. All further procedures are applied after a specific set of r and s parameters are applied.

For each reconstructed jet, the closest particle-level jet in angular distance is identified. The reconstructed and particle-level jets are matched if the angular distance ΔR is smaller than 0.2 and there is only one particle-level jet satisfying the requirement for a given reconstructed jet. Additionally, isolation is imposed on the matched particle-level jet by requiring that no other particle-level jet is found within $\Delta R = 0.5$. Furthermore, to ensure the measured energy for a given reconstructed jet represents only the jet energy, no particle-level electrons or muons originating from on-shell W or Z bosons are allowed within $\Delta R = 0.5$ of the reconstructed jet. In simulation, under these criteria, more than 90% of the selected jets with $p_{\mathrm{T}} < 150$ GeV can be matched to the corresponding particle-level jets, while the fraction significantly drops for jets with $p_{\mathrm{T}} > 150$ GeV to about 25% in the most extreme case, where most of the jets fail to match due to the isolation requirements of the particle-level jets. Detector-level jets failing either the matching to the truth jet or truth-isolation requirements are not included in forward-folding, and they appear unmodified in the W-boson mass distributions. All other jets, including jets with p_{T} above 200 GeV and $|\eta| > 0.8$ (but below $|\eta| = 2.5$) and jets that are not identified to come from the W-boson decay are forward-folded. Changing the angular distance for the matching from $\Delta R < 0.2$ to $\Delta R < 0.3$ has no significant impact on the final results.

5 Event selection and W-boson mass reconstruction

Events are required to have at least four jets with $p_{\mathrm{T}} > 20$ GeV and at least two jets need to be b-tagged and have $p_{\mathrm{T}} > 30$ GeV. Only events with exactly one

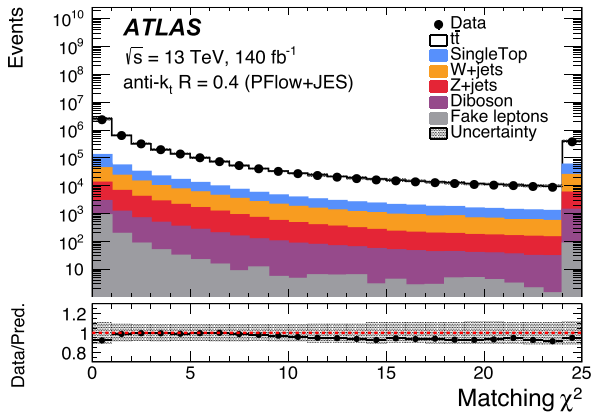


Fig. 1 The distribution of the best χ^2 value for the considered permutations for matching reconstructed jets to jets from the top-quark decay in the Run 2 data. Data without the JES *in situ* calibration (PFlow+JES) are shown as markers and compared to simulation from the signal and background processes. The uncertainty band includes all systematic uncertainties as described in Sect. 6. The bottom panel shows the ratio of the data to the prediction. The dashed line represents the ratio of one. The last bin contains the overflow events

electron or one muon with $p_{\mathrm{T}} > 27$ GeV are selected. The lepton p_{T} requirement is imposed to ensure the trigger efficiency is high. Additionally, the events are required to have $E_{\mathrm{T}}^{\mathrm{miss}} > 30$ GeV. These criteria are imposed on all events *after* the application of the forward-folding procedure described in Sect. 4 for each folded set of jets, as the results of the folding can change the event selection decision. To achieve this, the forward-folding technique is firstly applied to all jets in simulation for a looser selection of events with no $E_{\mathrm{T}}^{\mathrm{miss}}$ requirements and with the jet p_{T} selection lowered to 15 GeV.

The impact of the folding on $E_{\mathrm{T}}^{\mathrm{miss}}$ is estimated by propagating the difference between the folded and original jet four-momenta using the following equation

$$\vec{p}_{\mathrm{T}}^{\,\mathrm{miss,\,folded}} = \vec{p}_{\mathrm{T}}^{\,\mathrm{miss,\,original}} - \sum_i \left(\vec{p}_{\mathrm{T}}^{\,\mathrm{jet\,folded,i}} - \vec{p}_{\mathrm{T}}^{\,\mathrm{jet\,original,i}} \right),$$

with the missing transverse momentum vector $\vec{p}_{\mathrm{T}}^{\,\mathrm{miss}}$ and jet transverse momentum vector $\vec{p}_{\mathrm{T}}^{\,\mathrm{jet}}$ of jet i.

A simple permutational algorithm is used to identify the two jets from the hadronically decaying W boson. From all permutations of reconstructed jets, those that give the best agreement with the expected top-quark and W-boson masses—quantified by the χ^2 value defined below—are selected

$$\chi^2 = \frac{(m_t^{\mathrm{reco}} - m_t^{\mathrm{gen}})^2}{\Sigma_t^2} + \frac{(m_W^{\mathrm{reco}} - m_W^{\mathrm{gen}})^2}{\Sigma_W^2}. \quad (2)$$

Here m_t^{reco} represents the invariant mass of the three jet system from the top-quark decay, m_t^{gen} represents a fixed constant for the top-quark mass set to 172.5 GeV and the constant Σ_t represents the decay width of the top quark as well as the approximate experimental resolution and is set to 35 GeV. A systematic uncertainty varying the top-quark mass is considered as described in Sect. 6. Similarly, m_W^{reco} represents the invariant mass of the two jet system from the W-boson decay, m_W^{gen} represents the W-boson mass set to 80.38 GeV and Σ_W represents the decay width and resolution of the W boson and is set to 25 GeV. The χ^2 value is evaluated for permutations of up to six jets. If there are more than six jets in an event, at least two b-tagged jets (ordered in p_{T}) are always considered and then up to four other jets (ordered in p_{T}) are considered. For the permutations, within each top-quark combination, the jet not included in the W boson must be b-tagged and permutations corresponding to the same top-quark or W-boson combinations are only considered once. The permutation with the best (lowest) χ^2 value is chosen. Figure 1 shows the distribution of the χ^2 value for the best permutations in the Run 2 data sample without the JES *in situ* corrections applied. Good agreement between the prediction and data can be seen within the uncertainties. To improve the matching purity, only events for which the best permutation has $\chi^2 < 1$ are considered. This requirement removes about half of the pre-selected events satisfying all the previous criteria except the χ^2 requirement. Changing the parameters Σ_t and Σ_W in Eq. (2) to 15 and 10 GeV, respectively, and changing the χ^2 selection to keep the same selection efficiency, does not impact the matching purity significantly.

Additionally, the reconstructed jets identified as coming from the hadronically decaying W boson are required to be well isolated. For the reconstructed jets, a different isolation procedure compared to the particle-level jets is employed. A jet isolation variable f_{iso} is defined by

$$f_{\mathrm{iso}} = \frac{p_{\mathrm{T}}^{\mathrm{iso}} - \rho A_{\mathrm{iso}}}{p_{\mathrm{T}}^{\mathrm{jet}} - \rho A_{\mathrm{jet}}},$$

where $p_{\mathrm{T}}^{\mathrm{iso}}$ represents the scalar sum of the p_{T} of all inputs to the jet algorithm within an isolation annulus with inner and outer radii of 0.4 and 0.5. The ratio of momenta is calculated after subtracting the pile-up contribution, which is obtained by multiplying the jet active area A_{jet} and the area of the isolation annulus $A_{\mathrm{iso}} = \pi \cdot 0.5^2 - A_{\mathrm{jet}}$ by the pile-up density ρ [88]. The jets from the W-boson decay are required to have $f_{\mathrm{iso}} < 0.3$ to select well isolated jets. An alternative isolation requirement based on the angular distance between the closest reconstructed jets is found to give consistent results with the isolation variable requirement.

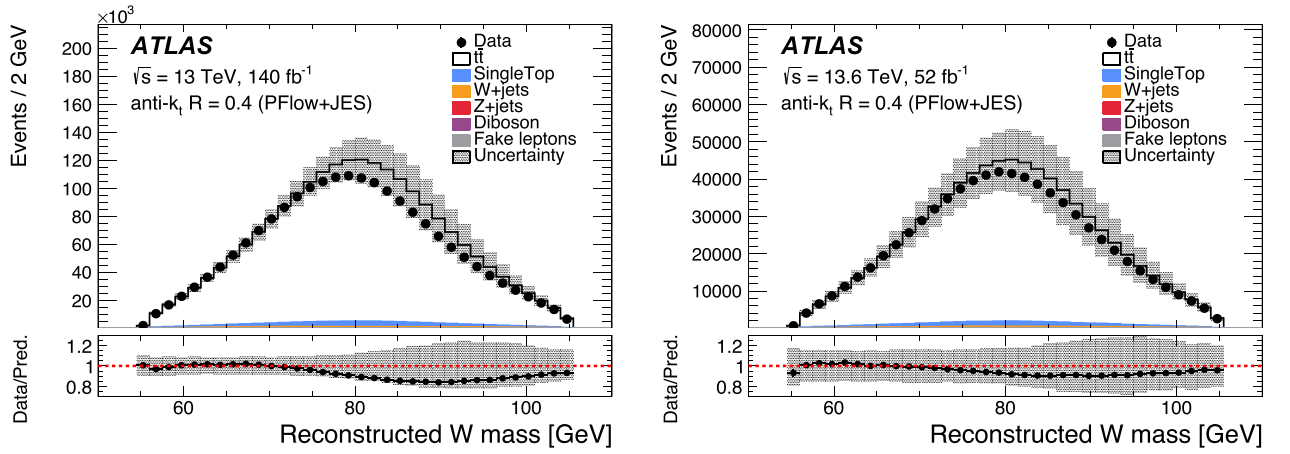


Fig. 2 Reconstructed hadronically decaying W-boson mass after applying all selection criteria in the **a** Run 2 data and **b** Run 3 data without the JES *in situ* corrections applied (PFlow+JES). The uncertainty band includes all systematic uncertainties. The bottom panels show the ratio of the data to the prediction. The dashed line represents the ratio of one

Figure 2 illustrates the reconstructed W-boson mass distribution in Run 2 and Run 3 after applying all the selection criteria including the $\chi^2 < 1$ requirement in data without the *in situ* jet calibration corrections applied. There is good agreement between the prediction and data within the uncertainties.

Only events where both of the jets from the W-boson decay have a p_{T} value in the range of 20–200 GeV, and $|\eta| < 0.8$ are analysed further. As the JES and JER corrections are determined as a function of the jet p_{T}, the distribution of the invariant mass of the two jets from the W-boson decay is analysed in multiple regions corresponding to bins in jet p_{T} for the leading and subleading jets. The *diagonal* regions refer to events where jets fall into the same jet p_{T} bin, while the remainder are referred to as *off-diagonal* regions. Figure 3 illustrates the definition of the regions used for the measurement and the selected events in each of the regions in Run 2 data without *in situ* corrections. Due to the kinematic restrictions of the W-boson decay, the diagonal region for the jet p_{T} range of 20–35 GeV is not considered further in the analysis. Figure 4 displays the reconstructed W-boson mass for various JES and JER assumptions in the diagonal region with jet p_{T} between 50 and 70 GeV in the Run 2 data. It can be seen that the JES assumptions mostly shift the distribution, while the JER assumptions mostly affect the width of the distribution.

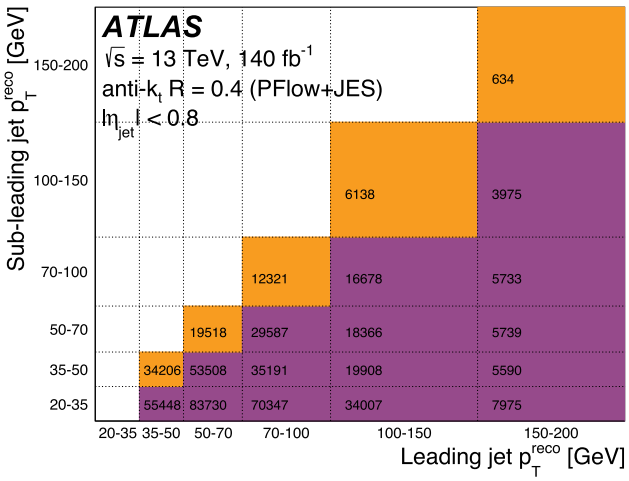
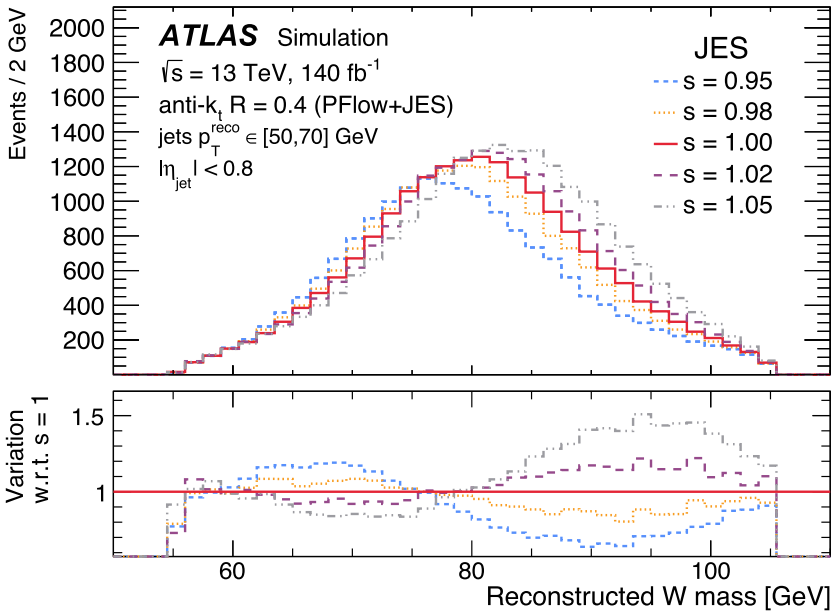


Fig. 3 Definition of the analysis regions based on reconstructed p_{T} and η of the two jets identified to originate from the W-boson decay. The two jets from W boson are required to have $|\eta| < 0.8$. The regions shown on the diagonal are the regions where both jets from the W boson fall into the same reconstructed p_{T} bin, off-diagonal are the regions where the two jets fall into different reconstructed p_{T} bins. The diagonal region with jets having a reconstructed p_{T} between 20 and 35 GeV is not used due to kinematic restrictions. The numbers in the bins represent the number of selected events in Run 2 data without *in situ* corrections

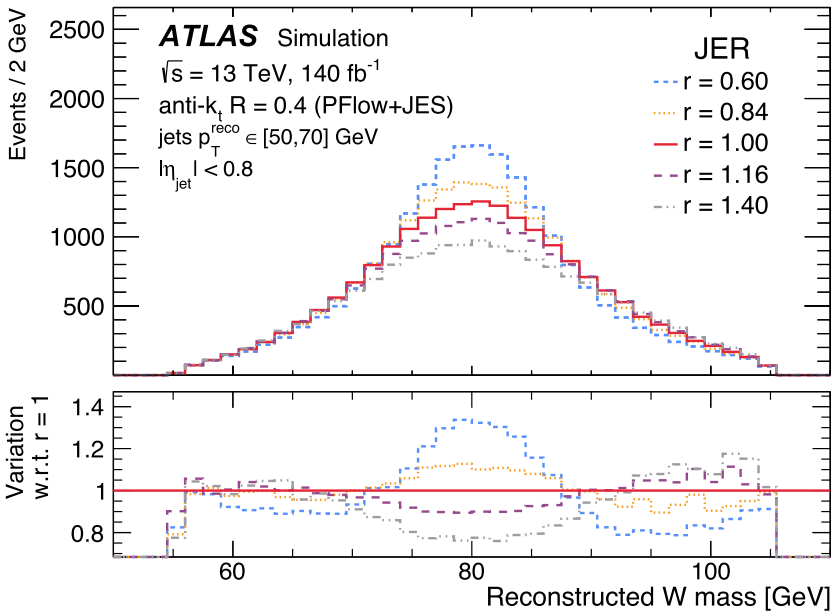
6 Systematic uncertainties

Several systematic uncertainties can affect the measurement of the JES and JER parameters. Uncertainties affecting leptons, $E_{\mathrm{T}}^{\mathrm{miss}}$ and b-tagged jets can impact the measurement due to the acceptance effects, while the uncertainties in the modelling can also affect the W-boson lineshape.

The uncertainties in the electron and muon identification, isolation, reconstruction, track-to-vertex association and trigger scale factors measured using $Z \to \mu^+\mu^-$ and $Z \to e^+e^-$ [29,30,74,76] are evaluated. Uncertainties related to the electron (muon) energy (momentum) scale and



(a)



(b)

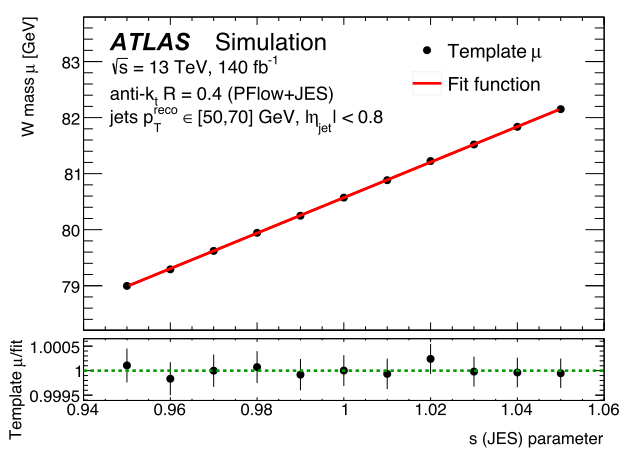
Fig. 4 Reconstructed W-boson mass in the region with the two jets from the W-boson decay with reconstructed p_{T} between 50 and 70 GeV in the Run 2 simulation. Templates with different **a** JES and **b** JER assumptions represented by the parameters of the forward-folding formula are shown. For the JES (JER) variations shown, the JER (JES) correction is set to one. The differences between the total yields for each distribution come from the acceptance effects due to the changes in the reconstructed jet p_{T}. The bottom panels show the ratios to the template with nominal **a** JES or **b** JER assumption. The solid line in the bottom panels represents the ratio of one

resolution are also evaluated as estimated by using resonance decays [74,75].

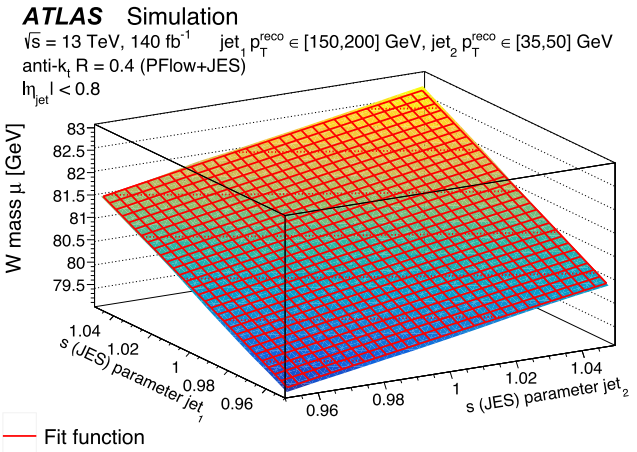
The uncertainty in the efficiency of the jet-vertex tagger algorithm is evaluated via the variation of the corrections applied to the simulation. The JES and JER uncertainties from the best available calibration are estimated by using the Run 2 data sample [79]. The same uncertainties are applied to the Run 3 based simulation, and are validated using Run 3 data. Additional uncertainties are considered for the Run 3 simulation to cover the residual differences between data and simulation.

The impact of the JER uncertainties is evaluated for the JES correction and the impact of the JES uncertainties is evaluated for the JER correction. The uncertainties in the efficiency of b-tagging are evaluated via the variation of the scale factors affecting the b-/c-/light-flavour (in)efficiencies, using measurements similar to Refs. [81–83].

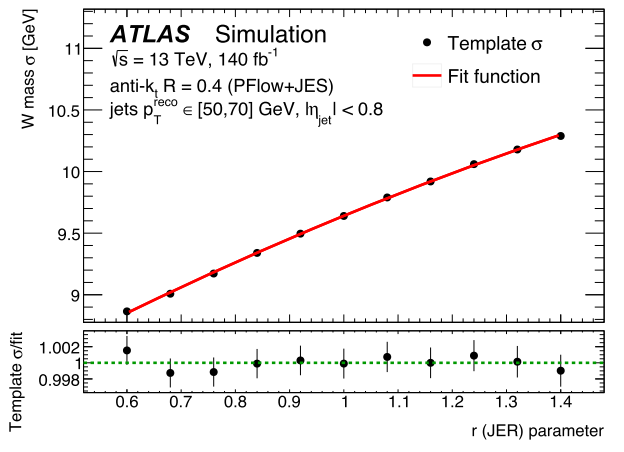
The uncertainty from the leptons and jets is propagated to the $E_{\mathrm{T}}^{\mathrm{miss}}$. Additionally, a dedicated set of uncertainties



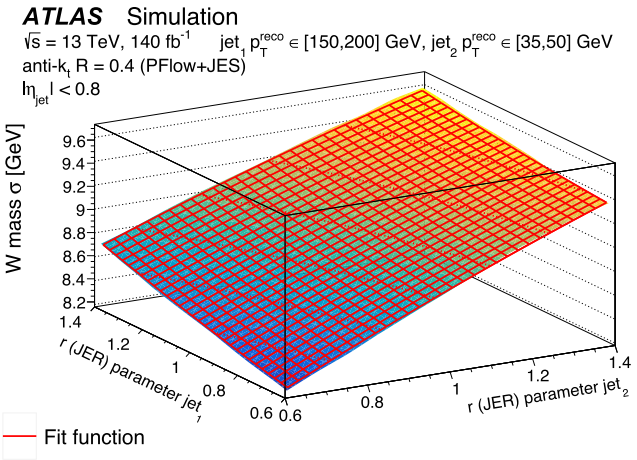
(a)



(b)



(c)

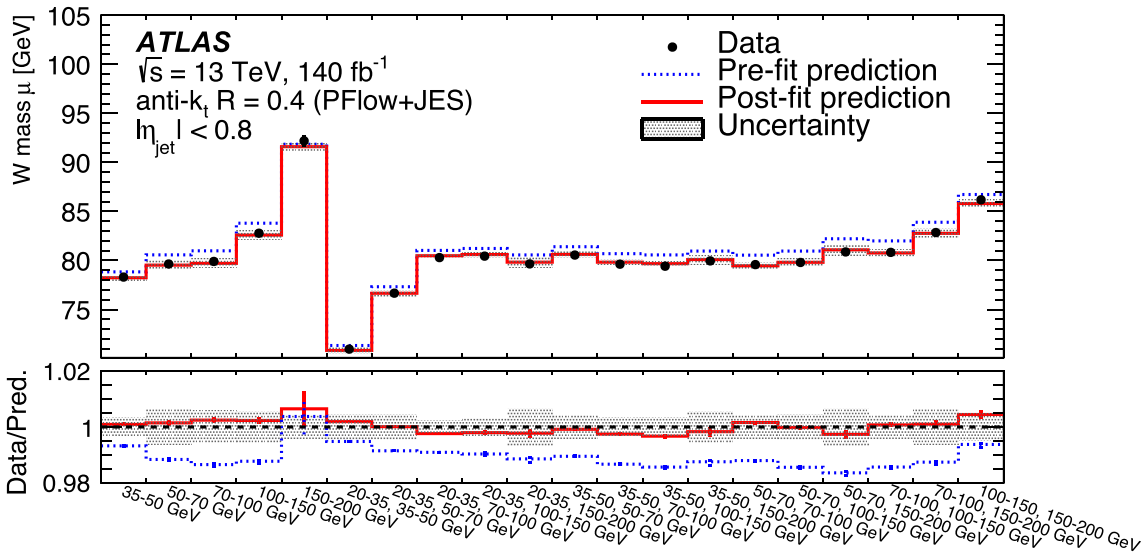


(d)

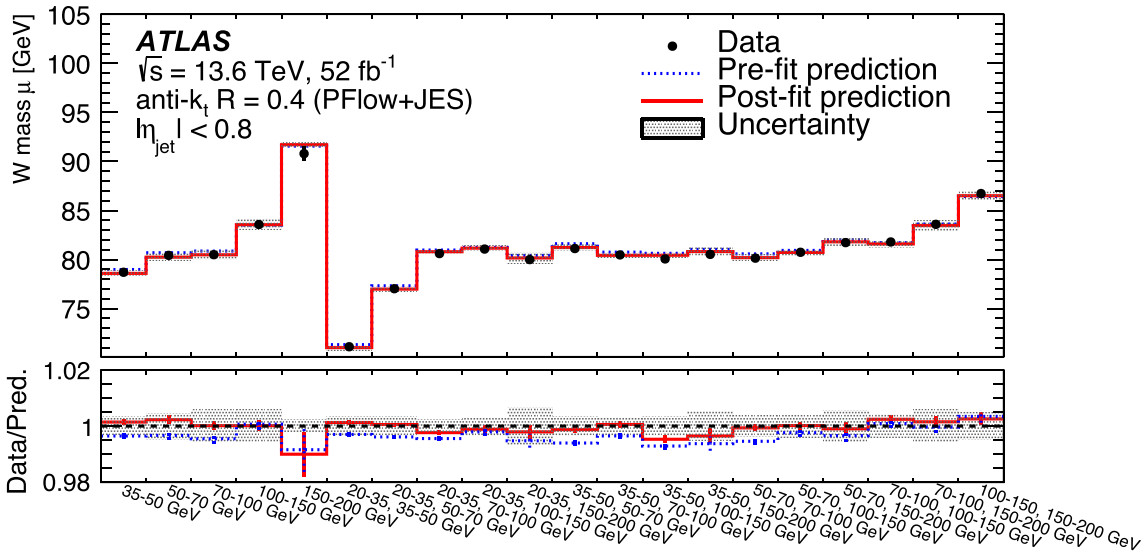
Fig. 5 The mean (top plots) and standard deviation (bottom plots) of the W-boson mass distribution in a representative reconstructed jet p_{T} region as a function of the JES (JER) parameter in the Run 2 simulation. **a** and **c** show the diagonal region with reconstructed jet p_{T} between 50 and 70 GeV, while **b** and **d** show the off-diagonal region with the leading jet (jet_1) with reconstructed p_{T} between 150 and 200 GeV and the sub-leading jet (jet_2) with reconstructed p_{T} between 35 and 50 GeV. The fitted function is shown by the solid line. For the diagonal regions, the bottom panels show the ratio of the mean (standard deviation) value to the fitted function. The dashed line in the bottom panels represents the ratio of one. For the off-diagonal regions, the colour gradient shows the mean (standard deviation) of the W-boson mass distribution for the JES (JER) templates

from the soft term is evaluated, varying the magnitude and the direction of the missing transverse momentum vector.

Several sources affecting the modelling of the $t\bar{t}$ process are evaluated, affecting the production or decay of the top quarks. Variations of the renormalisation and factorisation scale in the ME by factors of 0.5 and 2 are evaluated separately. Uncertainty in the initial-state radiation (ISR) is estimated by using the *Var3c* variation of the PYTHIA8 A14 tune [52]. Variations of the renormalisation scale in the strong coupling constant in the final-state radiation ($\alpha_{\mathrm{s}}^{\mathrm{FSR}}$) by factors of 0.5 and 2 of the A14 tune are evaluated. The uncertainty related to the POWHEG to PYTHIA matching is estimated by comparing with a dedicated POWHEG+PYTHIA 8 sample with the $p_{\mathrm{T}}^{\mathrm{hard}}$ parameter set to one instead of the default value of zero. The uncertainty in the choice of the h_{damp} parameter is estimated by comparing with a dedicated POWHEG+PYTHIA 8 sample produced with twice the nominal h_{damp} value ($h_{\mathrm{damp}} = 3m_{\mathrm{t}}$). Due to a known mismodelling of the top-quark p_{T} distribution, an uncertainty estimated from reweighting the top-quark p_{T} to NNLO QCD predictions [89] is evaluated as a proxy for missing higher order predictions in the kinematics. This uncertainty is found to have a negligible impact on the JES or JER estimate in the Run 2 analysis and is thus not considered further. The impact of using



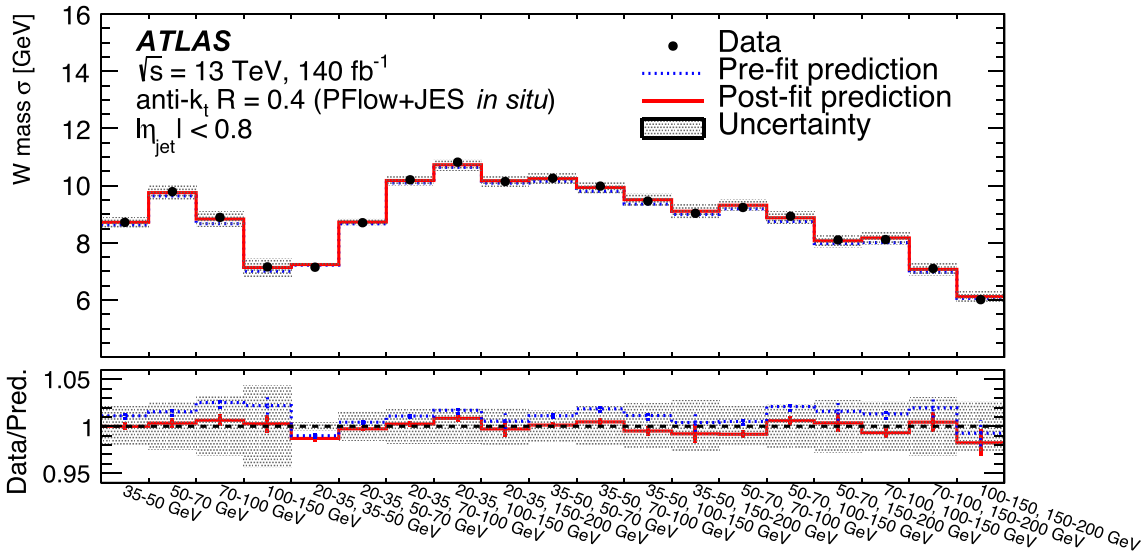
(a)



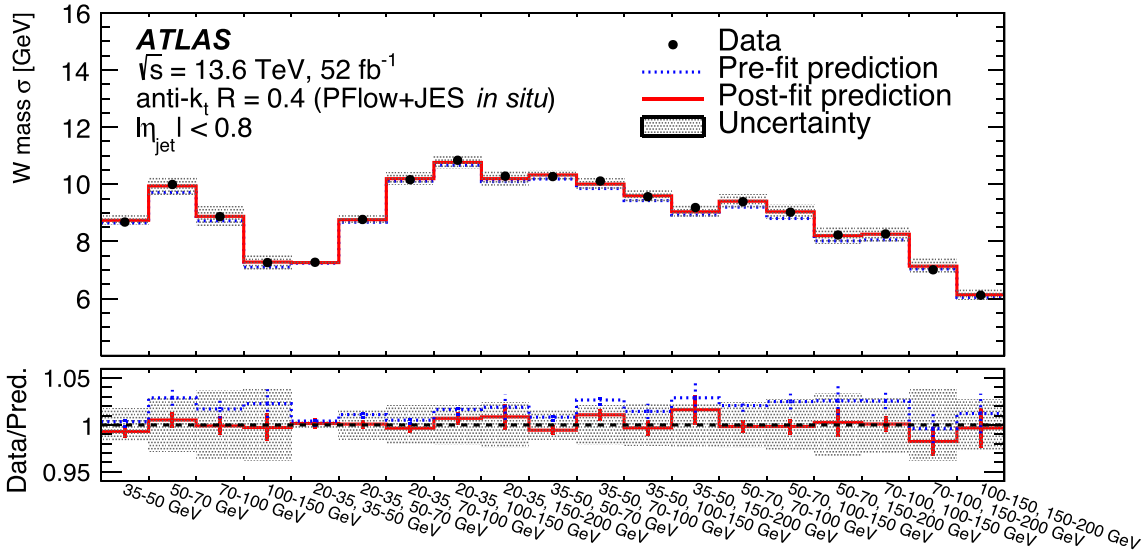
(b)

Fig. 6 Mean of the W mass distributions shown for the analysis regions defined in Sect. 5 in the JES fit in the **a** Run 2 and **b** Run 3 measurement. The values obtained in data are compared with those in simulations before and after the forward-folding correction. The uncertainties are obtained from pseudo-experiments taking into account the statistical and systematic uncertainties. The non-forward-folded (pre-fit) distribution is shown with a dotted line and the forward-folded (post-fit) distribution with a solid line. The first five bins show the diagonal regions, while the other bins show the off-diagonal regions. The bottom panels show the ratios of the data without the JES *in situ* calibration (PFlow+JES) to the pre-fit (dotted line) and post-fit (solid line) predictions, with the dashed line representing the ratio of one

a different parton shower and hadronisation model on the Run 2 (Run 3) analysis is evaluated by comparing the nominal $t\bar{t}$ sample with another sample generated with POWHEG interfaced to HERWIG 7.2.1 [90–92] (HERWIG 7.2.3), using the HERWIG 7.2 default set of tuned parameters [92] and the MMHT2014LO PDF set [93]. The POWHEG settings are the same as for the nominal sample. To estimate the uncertainty in the colour reconnection (CR), samples were generated with three models: CR0 — a multiple-parton-interactions (MPI) based model, CR1 — a QCD-based model and CR2 — a gluon-move based model [94]. The uncertainty is estimated by comparing the CR1 and CR2 models with the prediction of CR0 and taking the larger uncertainty. Variations in the top-quark mass of 0.5 GeV are evaluated by using dedicated samples with $m_{\text{top}} = 172.0$ GeV and $m_{\text{top}} = 173.0$ GeV. Variation in the MPI and underlying



(a)

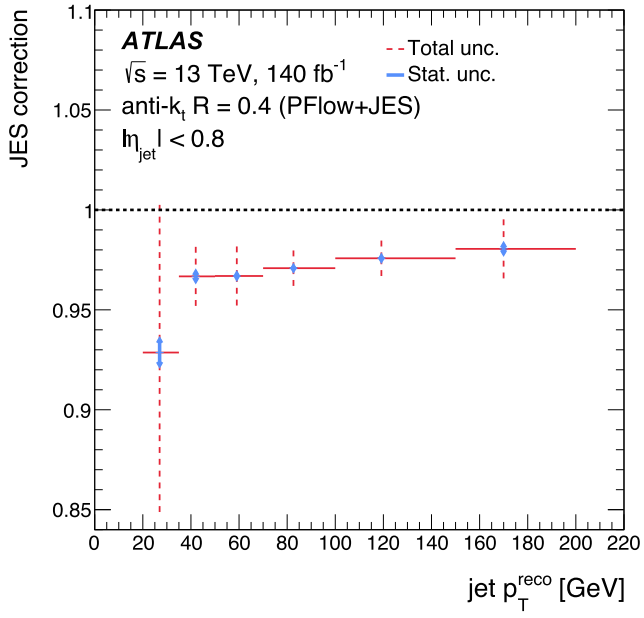


(b)

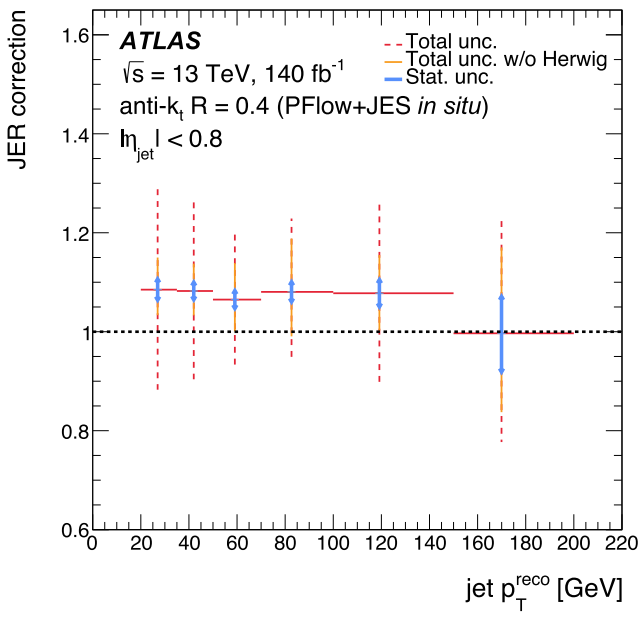
Fig. 7 The standard deviation of the W mass distributions shown for the analysis regions defined in Sect. 5 in the JER fit in the **a** Run 2 and **b** Run 3 measurement. The values obtained in data are compared with those in simulations before and after the forward-folding correction. The uncertainties are obtained from pseudo-experiments taking into account the statistical and systematic uncertainties. The non-forward-folded (pre-fit) distribution is shown with a dotted line and the forward-folded (post-fit) distribution with a solid line. The first four bins show the diagonal regions, while the other bins show the off-diagonal regions. The bottom panels show the ratios of the data with the JES *in situ* calibration (PFlow+JES *in situ*) to the pre-fit (dotted line) and post-fit (solid line) predictions, with the dashed line representing the ratio of one

event (UE) modelling (*Var1* variation in the A14 tune) is estimated with samples with UE variations in PYTHIA. The modelling of secondary gluon emissions from quarks originating from coloured resonance decays can affect both the b-quark and W-boson kinematics as well as the b-jet fragmentation. To assess the impact of this choice on the measurement, an alternative sample with the recoil model within PYTHIA 8 changed to *recoilToTop* was produced. The uncertainty in the PDF estimate for the $t\bar{t}$ process is assessed by evaluating the impact of the PDF4LHC [95,96] variations. Since the W bosons decay into an s-quark and a c-quark in about half of the hadronic decays, a variation of the Lund–Bowler c-fragmentation function [97,98] is tested, but it is found to have a negligible impact.

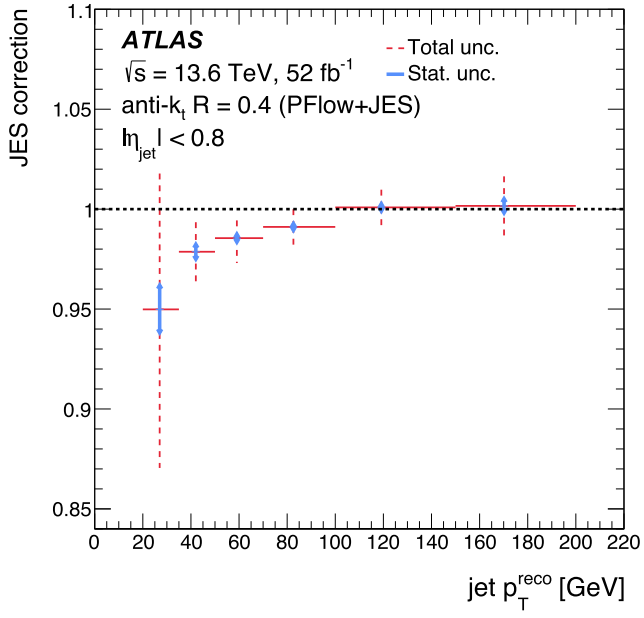
The uncertainty due to the choice of the parton shower generator for the tW process is estimated by comparing the



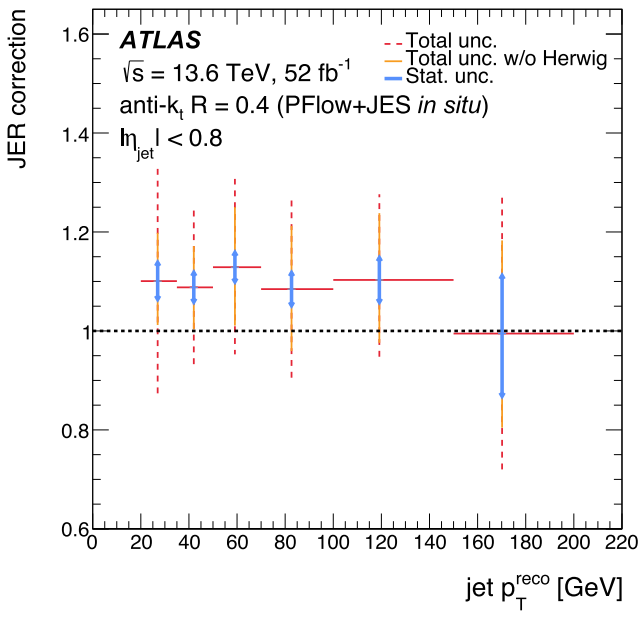
(a)



(b)



(c)



(d)

Fig. 8 The central values and the corresponding uncertainties for the **a** Run 2 JES and **b** JER and **c** Run 3 JES and **d** JER correction factors as a function of reconstructed jet p_{T}. The statistical uncertainty is shown with a thick solid bar with arrows on both ends, while the total uncertainty is shown with a thin dashed line. The thin solid line in the JER results **b**, **d** shows the total uncertainty without the PYTHIA versus HERWIG component. The horizontal values are taken from the mean of the reconstructed jet p_{T} distribution of the jets from the W-boson decay in each p_{T} bin. The dashed horizontal line represents no correction

nominal POWHEG+PYTHIA 8 sample with POWHEG interfaced to the HERWIG sample. The variations in the ME, *Var3c* and $\alpha_{\mathrm{s}}^{\mathrm{FSR}}$ are evaluated analogously to the $t\bar{t}$ case. The uncertainty in the overlap between the $t\bar{t}$ and tW diagrams is assessed by comparing the nominal prediction using the diagram-removal approach to the diagram-subtraction approach [46] in an alternative sample.

Uncertainties in the prediction of the cross-section of the various processes are taken into account although these are expected to have only a small impact on the measured W-boson line shape. A 5% uncertainty is considered for the $t\bar{t}$ and single-top processes following the uncertainty in the predicted cross-section [38–44,99]. A conservative 50% uncertainty is assigned to the V+jets and VV+jets, and 100% uncertainty is applied to the fake-lepton estimate. These uncertainties in the predicted cross-section have a negligible impact on the measured corrections for the JES and JER.

7 Results

The mean values μ of the W-boson mass distributions in the p_{T} regions defined in Sect. 5 are used to extract the JES parameters from a fit to data. Similarly, the standard deviation σ of the W-boson mass distribution is used for the JER measurement. The μ (σ) of each forward-folded W-boson mass distribution is extracted for each value of the s (r) parameters from the forward-folding Eq. (1) and in the case of the off-diagonal regions, for each combination of the s_1 and s_2 (r_1 and r_2) parameters of the JES (JER) estimate. Due to the $\chi^2 < 1$ selection, the minimum and the maximum of the reconstructed W-boson mass distribution is bounded to the range $m_W^{\mathrm{gen}} \pm 25$ GeV, thus the σ extraction does not suffer from outliers. In the diagonal regions the obtained μ (σ) are fitted with a linear (quadratic) function $\mathcal{F}(s)$ ($\mathcal{F}(r)$). In the off-diagonal regions, the μ (σ) are fitted with a quadratic function $\mathcal{F}(s_1, s_2)$ ($\mathcal{F}(r_1, r_2)$) where s_1 and s_2 (r_1 and r_2) are the forward-folding formula parameters for the leading and sub-leading jet identified to originate from the W-boson decay. The diagonal parameterisation function $\mathcal{F}(s)$ and off-diagonal parameterisation function $\mathcal{F}(s_1, s_2)$ share a set of six parameters s_i, one for each reconstructed jet p_{T} bin, and analogously for the JER parameterisation. For the JES parameterisation, most fitted points are within one standard deviation from the fitted function with only one point slightly above two standard deviation, with the standard deviation representing the uncertainty due to the finite number of simulated events. For the JER parameterisation, most fitted points are within one standard deviation with one point around 1.5 standard deviations away from the fitted function. Additionally, a dedicated uncertainty is assigned for the imperfect parameterisation and for neglecting possible correlations between the parameters in the $\mathcal{F}$ functions due to region migrations of simulated events when varying the JES and JER corrections and it is referred to as 'non-closure' uncertainty. Due to the low statistical power of the separation of the various JER smeared templates in the diagonal region with jet p_{T} between 150 and 200 GeV, this region is not included in the JER correction measurement. Figure 5 shows an example of the parameterisation for the JES and JER parameters in the Run 2 data. The larger impact on σ for the lower p_{T} jet compared to the higher p_{T} jet originates from the naturally lower resolution for the lower p_{T} jets due to the detector's calorimeter response.

Once the parameterisations $\mathcal{F}$ are obtained, a maximum-likelihood fit to μ (σ) in data is performed to extract the values of the JES (JER) parameters for all the regions simultaneously. The likelihood is defined as

$$\mathcal{L}(\vec{\mu}|\vec{s}) = \prod_{i \in \mathrm{reg}} G\left[\mu_i | \mathcal{F}_i(\vec{s}), \sigma_{\mu_i}\right],$$

where $\vec{\mu}$ is the vector of μ (σ) values measured in data, $\vec{s}$ is the vector of the scale (resolution) parameters to be estimated, G represents the Gaussian function, $\mathcal{F}$ is the parameterisation of μ (σ) values as described above and σ_{μ_i} is the data statistical uncertainty in the μ (σ) values in region i for the JES (JER) estimate.

The systematic uncertainties in the measurement of the JES and JER correction factors are estimated by shifting the expected distributions as summarised in Sect. 6, fitting the expected distributions with the nominal model and evaluating the impact on the best-fit parameters. The parameterisation 'non-closure' uncertainty is estimated by fitting the distributions representing a variation of up to 5% in JES and up to 25% in JER, and comparing the best-fit values with the s and r values used to generate the given varied distribution. The final 'non-closure' uncertainty in each p_{T} bin is estimated as the maximal deviation from the input value for all variations and is symmetrised.

Figures 6 and 7 show the μ or σ of the W mass distribution as obtained without forward-folding (pre-fit) and with forward-folding using the fitted JES or JER (post-fit) correction factors. Because each region has different selections applied, the μ and σ values vary accordingly, however the calibration procedure takes these differences into account. Due to the non-Gaussian nature of the uncertainties, stemming from the non-linear parameterisation, pseudo-experiments are used to obtain the uncertainty band. In the pseudo-experiments, random Gaussian distributed numbers are generated for the JES (JER) parameters with the standard deviation representing the total measured uncertainty, and the variations are then propagated to μ (σ) of the W-boson mass distribution using the obtained parameterisation. The diagonal region with jets between 150 and 200 GeV has a large statistical uncertainty due to the relatively low number of selected events compared to the other regions.

The fitted central values for the JES and JER parameters with their uncertainties are shown in Figure 8 for both Run 2 and Run 3 data. Bin-centre corrections are applied to the horizontal values by taking the mean of the jet p_{T} distribution of the jets from the W-boson decay in each p_{T} bin. Tables 1, 2,

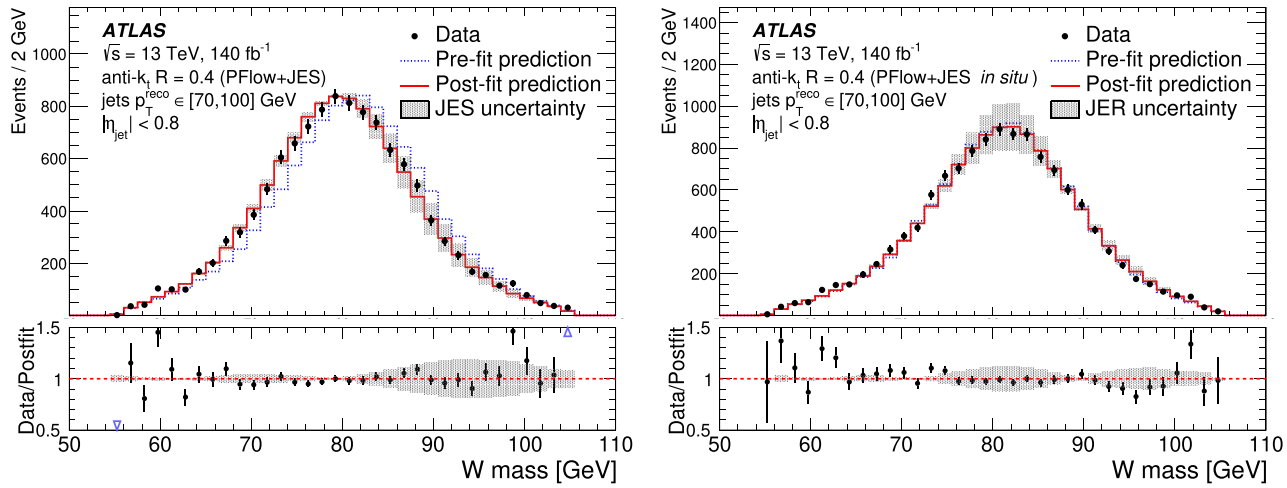


Fig. 9 The pre-fit (dotted line) and post-fit (solid line) predictions for the W-boson mass distribution in the diagonal region with reconstructed jet p_{T} between 70 and 100 GeV in the **a** JES and **b** JER fit to the Run 2 data. The hatched uncertainty band is estimated by propagating the total uncertainty in the **a** JES or **b** JER to the bin yield predictions. The predictions are normalised to the same total yield as data. The bottom panels show the ratio of the data **a** without the JES *in situ* calibration (PFlow+JES) or **b** with the JES *in situ* calibration (PFlow+JES *in situ*) to the post-fit prediction, with the dashed horizontal line representing the ratio of one. The arrows indicate a data value outside of the displayed range

3, 4 show the breakdown of the sources of systematic uncertainties for the JES and JER measurement for all jet p_{T} bins, separately for the Run 2 and Run 3 data. The central values for the JES measurement are below unity in the Run 2 data and in most jet p_{T} bins in the Run 3 data, indicating that the energy scale in the simulation needs to be decreased to match the scale observed in data. The measured JES correction factors in Run 2 are compatible with the previously measured corrections by ATLAS using the standard calibration techniques [10]. The measured JES correction factors in Run 2 are consistently about 2% lower than the Run 3 correction factors, which are closer to unity, suggesting the MC simulation in Run 3 models the experimental data better than the Run 2 simulation.

The measured JER correction factors are consistent with unity in all jet p_{T} bins.

Overall, the uncertainties are compatible between the Run 2 and Run 3 data. For the JES measurement, the first jet p_{T} bin suffers from large uncertainties due to low sensitivity because of the small separation in templates between the different JES correction factors for the lowest p_{T} bin. Apart from the first jet p_{T} bin, the JES uncertainties range from about 0.93% (0.98%) to about 1.7% (1.6%) in Run 2 (Run 3). The uncertainties in the JER measurement range from about 14% (16%) to about 22% (28%) in Run 2 (Run 3). The dominant uncertainties affecting the JES measurement stem from the variation of the $\alpha_{\mathrm{s}}^{\mathrm{FSR}}$ in the $t\bar{t}$ samples, the comparison between PYTHIA and HERWIG generators and the JER uncertainties. A shift in the $\alpha_{\mathrm{s}}^{\mathrm{FSR}}$ parameter shifts the peak of the reconstructed W-boson mass distribution mimicking the effects of the JES variation, and the impact decreases with higher jet p_{T}.

The JER uncertainties are dominated by the difference between PYTHIA and HERWIG that accounts for most of the total uncertainty. The difference can be traced to the large difference between the predictions of the W-boson lineshape in the generator output before the detector simulation and only part of the difference comes from the difference between the jet responses. The difference between the generators resembles resolution effects, thus the difference is highly correlated with the JER effects, resulting in a large uncertainty from the comparison of the two parton-shower generators.

Figure 9 compares the pre-fit and post-fit predictions and the observed data in the W-boson mass distribution for jets between 70 and 100 GeV in the Run 2 data. The post-fit prediction is obtained by propagating the fitted JES values to the predicted yield in each bin. The post-fit prediction agrees with data for all jet p_{T} regions.

8 Conclusion

A data-based calibration of the small-radius jet energy scale and resolution using $t\bar{t}$ events with the ATLAS detector is presented. The forward-folding technique is used to gener-

Table 1 Uncertainties in the JES estimate grouped into categories for the Run 2 data. Uncertainties for the different reconstructed jet p_{T} regions are presented

Category	JES uncertainty [%], Run 2					
Region [GeV]	$20 < p_{\mathrm{T}}^{\mathrm{reco}} < 35$	$35 < p_{\mathrm{T}}^{\mathrm{reco}} < 50$	$50 < p_{\mathrm{T}}^{\mathrm{reco}} < 70$	$70 < p_{\mathrm{T}}^{\mathrm{reco}} < 100$	$100 < p_{\mathrm{T}}^{\mathrm{reco}} < 150$	$150 < p_{\mathrm{T}}^{\mathrm{reco}} < 200$
JER	6.5	0.86	1.0	0.57	0.23	0.37
b-tagging	0.09	0.04	0.03	0.02	< 0.01	< 0.01
Electron	0.01	< 0.01	< 0.01	< 0.01	< 0.01	< 0.01
$E_{\mathrm{T}}^{\mathrm{miss}}$	0.07	0.01	< 0.01	< 0.01	< 0.01	0.01
Muon	0.02	< 0.01	< 0.01	< 0.01	< 0.01	< 0.01
$t\bar{t}$ PYTHIA versus HERWIG	2.8	0.63	1.0	0.71	0.83	1.6
$t\bar{t}$ $\alpha_{\mathrm{s}}^{\mathrm{FSR}}$	2.9	0.88	0.60	0.50	0.19	0.24
$t\bar{t}$ CR variation	0.98	0.21	0.05	0.17	0.15	0.10
$t\bar{t}$ UE variation	0.04	0.34	0.05	0.07	0.06	0.18
$t\bar{t}$ other	0.80	0.40	0.17	0.20	0.18	0.40
Single-top tW modelling	0.26	0.02	0.02	0.03	0.07	0.07
Non-closure	0.37	0.12	0.04	0.06	0.04	0.06
Normalisation	0.09	< 0.01	0.02	< 0.01	< 0.01	< 0.01
Other	0.13	0.03	0.04	0.06	0.07	0.09
Statistical	0.64	0.23	0.13	0.11	0.12	0.23
Total systematic	7.8	1.5	1.6	1.1	0.92	1.7
Total uncertainty	7.8	1.5	1.6	1.1	0.93	1.7

Table 2 Uncertainties in the JER estimate grouped into categories for the Run 2 data. Uncertainties for the different reconstructed jet p_{T} regions are presented

Category	JER uncertainty [%], Run 2					
Region [GeV]	$20 < p_{\mathrm{T}}^{\mathrm{reco}} < 35$	$35 < p_{\mathrm{T}}^{\mathrm{reco}} < 50$	$50 < p_{\mathrm{T}}^{\mathrm{reco}} < 70$	$70 < p_{\mathrm{T}}^{\mathrm{reco}} < 100$	$100 < p_{\mathrm{T}}^{\mathrm{reco}} < 150$	$150 < p_{\mathrm{T}}^{\mathrm{reco}} < 200$
JES	3.1	1.6	5.8	8.2	6.1	6.1
b-tagging	0.6	0.6	0.5	0.3	0.3	0.4
Electron	< 0.1	< 0.1	< 0.1	< 0.1	< 0.1	< 0.1
$E_{\mathrm{T}}^{\mathrm{miss}}$	0.1	< 0.1	< 0.1	< 0.1	0.1	0.3
Muon	< 0.1	< 0.1	< 0.1	< 0.1	< 0.1	0.2
$t\bar{t}$ PYTHIA versus HERWIG	20	17	12	10	17	15
$t\bar{t}$ $\alpha_{\mathrm{s}}^{\mathrm{FSR}}$	3.3	3.1	1.6	1.6	1.3	< 0.1
$t\bar{t}$ CR variation	1.2	1.0	1.0	1.0	0.6	11
$t\bar{t}$ UE variation	0.8	< 0.1	0.7	1.4	1.1	5.9
$t\bar{t}$ other	1.8	2.4	2.2	4.3	3.1	4.7
Single-top tW modelling	0.2	0.2	< 0.1	0.3	0.2	< 0.1
Non-closure	0.6	0.6	0.7	0.4	0.6	1.6
Normalisation	0.9	0.7	0.5	0.3	0.3	0.4
Other	0.8	0.7	0.7	0.4	0.4	0.2
Statistical	2.1	1.8	1.8	2.0	2.8	7.6
Total systematic	20	18	14	14	18	21
Total uncertainty	20	18	14	14	19	22

Table 3 Uncertainties in the JES estimate grouped into categories for the Run 3 data. Uncertainties for the different reconstructed jet p_{T} regions are presented

Category	JES uncertainty [%], Run 3					
Region [GeV]	$20 < p_{\mathrm{T}}^{\mathrm{reco}} < 35$	$35 < p_{\mathrm{T}}^{\mathrm{reco}} < 50$	$50 < p_{\mathrm{T}}^{\mathrm{reco}} < 70$	$70 < p_{\mathrm{T}}^{\mathrm{reco}} < 100$	$100 < p_{\mathrm{T}}^{\mathrm{reco}} < 150$	$150 < p_{\mathrm{T}}^{\mathrm{reco}} < 200$
JER	6.0	0.72	0.78	0.61	0.23	0.33
b-tagging	0.10	0.05	0.04	0.03	0.02	0.01
Electron	0.03	< 0.01	< 0.01	< 0.01	< 0.01	< 0.01
$E_{\mathrm{T}}^{\mathrm{miss}}$	0.04	0.01	0.01	< 0.01	< 0.01	0.01
Muon	0.03	< 0.01	< 0.01	< 0.01	< 0.01	0.01
$t\bar{t}$ PYTHIA versus HERWIG	2.0	0.20	0.64	0.71	0.83	1.4
$t\bar{t}$ $\alpha_{\mathrm{s}}^{\mathrm{FSR}}$	3.0	0.96	0.56	0.36	0.23	< 0.01
$t\bar{t}$ CR variation	0.40	0.38	0.09	0.04	0.09	0.12
$t\bar{t}$ UE variation	0.08	0.46	0.27	0.24	0.16	0.41
$t\bar{t}$ other	1.7	0.59	0.09	0.17	0.33	0.48
Single-top tW modelling	0.22	< 0.01	0.01	0.03	< 0.01	0.01
Non-closure	0.43	0.18	0.07	0.03	0.06	0.10
Normalisation	0.14	0.03	0.02	< 0.01	< 0.01	< 0.01
Other	0.21	0.02	0.05	0.04	0.05	0.07
Statistical	1.2	0.37	0.20	0.17	0.18	0.36
Total systematic	7.3	1.5	1.2	1.1	0.97	1.6
Total uncertainty	7.4	1.5	1.2	1.1	0.98	1.6

Table 4 Uncertainties in the JER estimate grouped into categories for the Run 3 data. Uncertainties for the different reconstructed jet p_{T} regions are presented

Category	JER uncertainty [%], Run 3					
Region [GeV]	$20 < p_{\mathrm{T}}^{\mathrm{reco}} < 35$	$35 < p_{\mathrm{T}}^{\mathrm{reco}} < 50$	$50 < p_{\mathrm{T}}^{\mathrm{reco}} < 70$	$70 < p_{\mathrm{T}}^{\mathrm{reco}} < 100$	$100 < p_{\mathrm{T}}^{\mathrm{reco}} < 150$	$150 < p_{\mathrm{T}}^{\mathrm{reco}} < 200$
JES	3.3	5.0	9.5	11	11	11
b-tagging	0.7	0.7	0.6	0.3	0.4	0.8
Electron	< 0.1	< 0.1	< 0.1	< 0.1	< 0.1	0.1
$E_{\mathrm{T}}^{\mathrm{miss}}$	0.1	0.3	0.2	< 0.1	0.2	0.4
Muon	< 0.1	< 0.1	< 0.1	< 0.1	< 0.1	0.1
$t\bar{t}$ PYTHIA versus HERWIG	22	14	13	13	11	21
$t\bar{t}$ $\alpha_{\mathrm{s}}^{\mathrm{FSR}}$	4.5	4.0	2.7	1.2	1.3	1.7
$t\bar{t}$ CR variation	2.6	2.5	3.8	2.3	3.6	7.0
$t\bar{t}$ UE variation	4.1	1.0	0.1	1.1	2.7	0.4
$t\bar{t}$ other	3.8	2.6	4.1	5.2	3.8	4.9
Single-top tW modelling	0.2	0.2	0.3	0.1	0.3	0.9
Non-closure	1.1	0.7	0.8	0.3	1.0	2.2
Normalisation	0.7	0.6	0.6	0.2	0.3	0.4
Other	0.9	0.7	0.8	0.5	0.5	1.4
Statistical	3.7	3.0	3.0	3.3	4.5	12
Total systematic	23	16	17	18	16	25
Total uncertainty	24	16	18	18	17	28

ate templates for the invariant mass of hadronically decaying W bosons that are then compared with the distribution in data. Two separate measurements are made, one for the full Run 2 data sample of the LHC at $\sqrt{s} = 13$ TeV corresponding to an integrated luminosity of 140 fb^{-1} and the other for the LHC Run 3 data sample collected in years 2022 and 2023, corresponding to an integrated luminosity of 52 fb^{-1}. The extracted values for correction of the energy scale and resolution are binned in the jet transverse momentum ranging from 20 to 200 GeV. This technique provides a precision that is competitive with the established calibration techniques for jet $p_{\mathrm{T}} > 35$ GeV. However, analyses with a similar final state, especially those using observables correlated with the W mass distribution as presented here, such as top-quark mass measurements, need to carefully evaluate whether this calibration can be applied to their measurements. The dominant uncertainties for the JES and JER calibration originate from the modelling of the final-state radiation and parton shower in the $t\bar{t}$ process. If the dominant $t\bar{t}$ modelling uncertainties are reduced in the future, a precision of about 0.5% for the jet energy scale and about 10% for the jet energy resolution could be reached using this $t\bar{t}$ calibration technique on its own. The results will be combined with the standard ATLAS calibration techniques.

Acknowledgements We thank CERN for the very successful operation of the LHC and its injectors, as well as the support staff at CERN and at our institutions worldwide without whom ATLAS could not be operated efficiently. The crucial computing support from all WLCG partners is acknowledged gratefully, in particular from CERN, the ATLAS Tier-1 facilities at TRIUMF/SFU (Canada), NDGF (Denmark, Norway, Sweden), CC-IN2P3 (France), KIT/GridKA (Germany), INFN-CNAF (Italy), NL-T1 (Netherlands), PIC (Spain), RAL (UK) and BNL (USA), the Tier-2 facilities worldwide and large non-WLCG resource providers. Major contributors of computing resources are listed in Ref. [100]. We gratefully acknowledge the support of ANPCyT, Argentina; YerPhI, Armenia; ARC, Australia; BMWFW and FWF, Austria; ANAS, Azerbaijan; CNPq and FAPESP, Brazil; NSERC, NRC and CFI, Canada; CERN; ANID, Chile; CAS, MOST and NSFC, China; Minciencias, Colombia; MEYS CR, Czech Republic; DNRF and DNSRC, Denmark; IN2P3-CNRS and CEA-DRF/IRFU, France; SRNSFG, Georgia; BMFTR, HGF and MPG, Germany; GSRI, Greece; RGC and Hong Kong SAR, China; ICHEP and Academy of Sciences and Humanities, Israel; INFN, Italy; MEXT and JSPS, Japan; CNRST, Morocco; NWO, Netherlands; RCN, Norway; MNiSW, Poland; FCT, Portugal; MNE/IFA, Romania; MSTDI, Serbia; MSSR, Slovakia; ARIS and MVZI, Slovenia; DSI/NRF, South Africa; MICIU/AEI, Spain; SRC and Wallenberg Foundation, Sweden; SERI, SNSF and Cantons of Bern and Geneva, Switzerland; NSTC, Taipei; TENMAK, Türkiye; STFC/UKRI, United Kingdom; DOE and NSF, United States of America. Individual groups and members have received support from BCKDF, CANARIE, CRC and DRAC, Canada; CERN-CZ, FORTE and PRIMUS, Czech Republic; COST, ERC, ERDF, Horizon 2020 and Marie Skłodowska-Curie Actions, European Union; Investissements d'Avenir Labex, Investissements d'Avenir Idex and ANR, France; DFG and AvH Foundation, Germany; Herakleitos, Thales and Aristeia programmes co-financed by EU-ESF and the Greek NSRF, Greece; BSF-NSF and MINERVA, Israel; NCN and NAWA, Poland; La Caixa Banking Foundation, CERCA Programme Generalitat de Catalunya and PROMETEO and GenT Programmes Generalitat Valenciana, Spain; Göran Gustafssons Stiftelse, Sweden; The Royal Society and Leverhulme Trust, United Kingdom; United States of America. In addition, individual members wish to acknowledge support from Chile: Agencia Nacional de Investigación y Desarrollo (ANID FONDECYT reg. 1230987, FONDECYT 1230812, FONDECYT 1240864, Fondecyt 3240661, Fondecyt Regular 1240721); China: Chinese Ministry of Science and Technology (MOST-2023YFA1605700, MOST-2023YFA1609300), National Natural Science Foundation of China (NSFC - 12175119, NSFC 12275265); Czech Republic: Czech Science Foundation (GACR - 24-11373S), Ministry of Education Youth and Sports (ERC-CZ-LL2327, FORTE CZ.02.01.01/00/22_008/0004632), PRIMUS Research Programme (PRIMUS/21/SCI/017); EU: H2020 European Research Council (ERC - 101002463); European Union: European Research Council (BARD No. 101116429, ERC - 948254, ERC 101089007), European Regional Development Fund (HE COFUND GA No.101081355, ERDF), European Union, Future Artificial Intelligence Research (FAIR-NextGenerationEU PE00000013), Marie Sklodowska-Curie Actions (GAP-101168829); France: Agence Nationale de la Recherche (ANR-21-CE31-0013, ANR-21-CE31-0022, ANR-22-EDIR-0002, ANR-24-CE31-0504-01); Germany: Deutsche Forschungsgemeinschaft (DFG - 469666862, DFG - CR 312/5-2); China: Research Grants Council (GRF); Italy: Ministero dell'Università e della Ricerca (NextGenEU 153D23001490006 M4C2.1.1, NextGenEU I53D23000820006 M4C2.1.1, NextGenEU I53D23001490006 M4C2.1.1, SOE2024_0000023); Japan: Japan Society for the Promotion of Science (JSPS KAKENHI JP22H01227, JSPS KAKENHI JP22H04944, JSPS KAKENHI JP22KK0227, JSPS KAKENHI JP24K23939, JSPS KAKENHI JP24KK0251, JSPS KAKENHI JP25H00650, JSPS KAKENHI JP25H01291, JSPS KAKENHI JP25K01023); Norway: Research Council of Norway (RCN-314472); Poland: Ministry of Science and Higher Education (IDUB AGH, POB8, D4 no 9722), Polish National Science Centre (NCN 2021/42/E/ST2/00350, NCN OPUS 2023/51/B/ST2/02507, NCN OPUS nr 2022/47/B/ST2/03059, NCN UMO-2019/34/E/ST2/00393, UMO-2022/47/O/ST2/00148, UMO-2023/49/B/ST2/04085, UMO-2023/51/B/ST2/00920, UMO-2024/53/N/ST2/00869); Portugal: Foundation for Science and Technology (FCT); Spain: Agencia de Gestión de Ayudas Universitarias y de Investigación (AGAUR - 2023 BP 00141), Generalitat Valenciana (ASFAE/2022/008), Ministry of Science and Innovation (RYC2019-028510-I, RYC2020-030254-I, RYC2021-031273-I, RYC2022-038164-I), Ministerio de Ciencia, Innovación y Universidades/Agencia Estatal de Investigación (PID2022-142604OB-C22); Sweden: Carl Trygger Foundation (Carl Trygger Foundation CTS 22:2312), Swedish Research Council (Swedish Research Council 2023-04654, VR 2021-03651, VR 2022-03845, VR 2022-04683, VR 2023-03403, VR 2024-05451), Knut and Alice Wallenberg Foundation (KAW 2018.0458, KAW 2022.0358, KAW 2023.0366); Switzerland: Swiss National Science Foundation (SNSF - PCEFP2_194658); United Kingdom: The Binks Trust, Royal Society (NIF-R1-231091); United States of America: U.S. Department of Energy (ECA DE-AC02-76SF00515), John Templeton Foundation (John Templeton Foundation 63206), Neubauer Family Foundation.

Data Availability Statement Data will be made available on reasonable request. [Authors' comment: The public release of data supporting the findings of this article will follow the CERN Open Data Policy CERN-OPEN-2020-013. Inquiries about plots and tables associated with this article can be addressed to atlas.publications@cern.ch.]

Code Availability Statement This manuscript has associated code/software in a data repository. [Authors' comment: The ATLAS Collaboration's Athena software, including the configuration of the event generators, is open source (http://gitlab.cern.ch/atlas/athena).]

Open Access This article is licensed under a Creative Commons Attribution 4.0 International License, which permits use, sharing, adaptation, distribution and reproduction in any medium or format, as long as you

give appropriate credit to the original author(s) and the source, provide a link to the Creative Commons licence, and indicate if changes were made. The images or other third party material in this article are included in the article's Creative Commons licence, unless indicated otherwise in a credit line to the material. If material is not included in the article's Creative Commons licence and your intended use is not permitted by statutory regulation or exceeds the permitted use, you will need to obtain permission directly from the copyright holder. To view a copy of this licence, visit http://creativecommons.org/licenses/by/4.0/.
Funded by SCOAP[3].

References

1. L. Evans, P. Bryant, L.H.C. Machine, JINST **3**, S08001 (2008). https://doi.org/10.1088/1748-0221/3/08/S08001
2. ATLAS Collaboration, Measurements of jet cross-section ratios in 13 TeV proton–proton collisions with ATLAS, Phys. Rev. D 110 (2024) 072019, arXiv:2405.20206 [hep-ex]. https://doi.org/10.1103/PhysRevD.110.072019
3. ATLAS Collaboration, Measurement of hadronic event shapes in high-p_{T} mult.et final states at $\sqrt{s}$ = 13 TeV with the ATLAS detector. JHEP **01**, 188 (2021). https://doi.org/10.1007/JHEP01(2021)188. arXiv:2007.12600 [hep-ex]. [Erratum: JHEP 12 (2021) 053 https://doi.org/10.1007/JHEP12(2021)053]
4. ATLAS Collaboration, Measurement of single top-quark production in association with a W boson in pp collisions at $\sqrt{s}$ = 13 TeV with the ATLAS detector. Phys. Rev. D **110**, 072010 (2024). https://doi.org/10.1103/PhysRevD.110.072010. arXiv:2407.15594 [hep-ex]
5. ATLAS Collaboration, Measurement of the top quark mass with the ATLAS detector using $t\bar{t}$ events with a high transverse momentum top quark. Phys. Lett. B **867**, 139608 (2025). https://doi.org/10.1016/j.physletb.2025.139608. arXiv:2502.18216 [hep-ex]
6. ATLAS Collaboration, Measurement of the top-quark pole mass in dileptonic $t\bar{t}$ + 1-jet events at $\sqrt{s}$ = 13 TeV with the ATLAS experiment. JHEP **12**, 023 (2025). https://doi.org/10.1007/JHEP12(2025)023. arXiv:2507.02632 [hep-ex]
7. ATLAS Collaboration, Determination of jet calibration and energy resolution in proton–proton collisions at $\sqrt{s}$ = 8 TeV using the ATLAS detector. Eur. Phys. J. C **80**, 1104 (2020). https://doi.org/10.1140/epjc/s10052-020-08477-8. arXiv:1910.04482 [hep-ex]
8. ATLAS Collaboration, Jet reconstruction and performance using particle flow with the ATLAS detector. Eur. Phys. J. C **77**, 466 (2017). https://doi.org/10.1140/epjc/s10052-017-5031-2. arXiv:1703.10485 [hep-ex]
9. ATLAS Collaboration, Jet energy scale measurements and their systematic uncertainties in proton–proton collisions at $\sqrt{s}$ = 13 TeV with the ATLAS detector. Phys. Rev. D **96**, 072002 (2017). https://doi.org/10.1103/PhysRevD.96.072002. arXiv:1703.09665 [hep-ex]
10. ATLAS Collaboration, Jet energy scale and resolution measured in proton–proton collisions at $\sqrt{s}$ = 13TeV with the ATLAS detector. Eur. Phys. J. C **81**, 689 (2021). https://doi.org/10.1140/epjc/s10052-021-09402-3. arXiv:2007.02645 [hep-ex]
11. ATLAS Collaboration, New techniques for jet calibration with the ATLAS detector. Eur. Phys. J. C **83**, 761 (2023). https://doi.org/10.1140/epjc/s10052-023-11837-9. arXiv:2303.17312 [hep-ex]
12. M. Cacciari, G.P. Salam, G. Soyez, The anti-k_t jet clustering algorithm. JHEP **04**, 063 (2008). https://doi.org/10.1088/1126-6708/2008/04/063. arXiv:0802.1189 [hep-ph]
13. ATLAS Collaboration, Jet energy measurement and its systematic uncertainty in proton–proton collisions at $\sqrt{s}$ = 7 TeV with the ATLAS detector. Eur. Phys. J. C **75**, 17 (2015). https://doi.org/10.1140/epjc/s10052-014-3190-y. arXiv:1406.0076 [hep-ex]
14. V.M. Abazov et al., Combination of D0 measurements of the top quark mass. Phys. Rev. D **95**, 112004 (2017). https://doi.org/10.1103/PhysRevD.95.112004. arXiv:1703.06994 [hep-ex]
15. ATLAS and CMS Collaborations, Combination of measurements of the top quark mass from data collected by the ATLAS and CMS Experiments at $\sqrt{s}$ = 7 and 8TeV. Phys. Rev. Lett. **132**, 261902 (2024). https://doi.org/10.1103/PhysRevLett.132.261902. arXiv:2402.08713 [hep-ex]
16. The ATLAS and CDF and CMS and D0 Collaborations, First combination of Tevatron and LHC measurements of the top-quark mass. 2014. arXiv:1403.4427 [hep-ex]
17. ATLAS Collaboration, Measurement of the top quark mass in the $t\bar{t} \to$ lepton+jets and $t\bar{t} \to$ dilepton channels using $\sqrt{s} = 7$TeV ATLAS data. Eur. Phys. J. C **75**, 330 (2015). https://doi.org/10.1140/epjc/s10052-015-3544-0. arXiv:1503.05427 [hep-ex]
18. ATLAS Collaboration, Measurement of the top quark mass in the $t\bar{t} \to lepton + jets\, channel from \sqrt{s}$ = 8 TeV ATLAS data and combination with previous results. Eur. Phys. J. C **79**, 290 (2019). https://doi.org/10.1140/epjc/s10052-019-6757-9. arXiv:1810.01772 [hep-ex]
19. ATLAS Collaboration, Measurement of large radius jet mass reconstruction performance at $\sqrt{s}$ = 8 TeV using the ATLAS detector. ATLAS-CONF-2016-008, 2016. https://cds.cern.ch/record/2139642
20. ATLAS Collaboration, The ATLAS Experiment at the CERN Large Hadron Collider. JINST **3**, S08003 (2008). https://doi.org/10.1088/1748-0221/3/08/S08003
21. ATLAS Collaboration, The ATLAS experiment at the CERN Large Hadron Collider: a description of the detector configuration for Run 3. JINST **19**, P05063 (2024). https://doi.org/10.1088/1748-0221/19/05/P05063. arXiv:2305.16623 [physics.ins-det]
22. G. Avoni et al., The new LUCID-2 detector for luminosity measurement and monitoring in ATLAS. JINST **13**, P07017 (2018). https://doi.org/10.1088/1748-0221/13/07/P07017
23. ATLAS Collaboration, Performance of the ATLAS trigger system in 2015. Eur. Phys. J. C **77**, 317 (2017). https://doi.org/10.1140/epjc/s10052-017-4852-3. arXiv:1611.09661 [hep-ex]
24. ATLAS Collaboration, The ATLAS trigger system for LHC Run 3 and trigger performance in 2022. JINST **19**, P06029 (2024). https://doi.org/10.1088/1748-0221/19/06/P06029. arXiv:2401.06630 [hep-ex]
25. ATLAS Collaboration, Software and computing for Run 3 of the ATLAS experiment at the LHC. Eur. Phys. J. C **85**, 234 (2025). https://doi.org/10.1140/epjc/s10052-024-13701-w. arXiv:2404.06335 [hep-ex]. [Erratum: Eur. Phys. J. C 85 (2025) 907 https://doi.org/10.1140/epjc/s10052-025-14572-5]
26. ATLAS Collaboration, ATLAS data quality operations and performance for 2015–2018 data-taking. JINST **15**, P04003 (2020). https://doi.org/10.1088/1748-0221/15/04/P04003. arXiv:1911.04632 [physics.ins-det]
27. ATLAS Collaboration, Luminosity determination in pp collisions at $\sqrt{s}$ = 13 TeV using the ATLAS detector at the LHC. Eur. Phys. J. C **83**, 982 (2023). https://doi.org/10.1140/epjc/s10052-023-11747-w. arXiv:2212.09379 [hep-ex]
28. ATLAS Collaboration, Preliminary analysis of the luminosity calibration for the ATLAS 13.6 TeV data recorded in 2023. ATL-DAPR-PUB-2024-001, 2024. https://cds.cern.ch/record/2900949
29. ATLAS Collaboration, Performance of the ATLAS muon triggers in Run 2. JINST **15**, P09015 (2020). https://doi.org/10.1088/1748-0221/15/09/p09015. arXiv:2004.13447 [physics.ins-det]
30. ATLAS Collaboration, Performance of electron and photon triggers in ATLAS during LHC Run 2. Eur. Phys. J. C

80, 47 (2020). https://doi.org/10.1140/epjc/s10052-019-7500-2. arXiv:1909.00761 [hep-ex]
31. D.J. Lange, The EvtGen particle decay simulation package. Nucl. Instrum. Methods A **462**, 152 (2001). https://doi.org/10.1016/S0168-9002(01)00089-4
32. S. Frixione, G. Ridolfi, P. Nason, A positive-weight next-to-leading-order Monte Carlo for heavy flavour hadroproduction. JHEP **09**, 126 (2007). https://doi.org/10.1088/1126-6708/2007/09/126. arXiv:0707.3088 [hep-ph]
33. P. Nason, A new method for combining NLO QCD with shower Monte Carlo algorithms. JHEP **11**, 040 (2004). https://doi.org/10.1088/1126-6708/2004/11/040. arXiv:hep-ph/0409146
34. S. Frixione, P. Nason, C. Oleari, Matching NLO QCD computations with parton shower simulations: the POWHEG method. JHEP **11**, 070 (2007). https://doi.org/10.1088/1126-6708/2007/11/070. arXiv:0709.2092 [hep-ph]
35. S. Alioli, P. Nason, C. Oleari, E. Re, A general framework for implementing NLO calculations in shower Monte Carlo programs: the POWHEG BOX. JHEP **06**, 043 (2010). https://doi.org/10.1007/JHEP06(2010)043. arXiv:1002.2581 [hep-ph]
36. NNPDF Collaboration, R.D. Ball et al., Parton distributions for the LHC run II. JHEP **04**, 040 (2015). https://doi.org/10.1007/JHEP04(2015)040. arXiv:1410.8849 [hep-ph]
37. ATLAS Collaboration, Studies on top-quark Monte Carlo modelling for Top2016. ATL-PHYS-PUB-2016-020, 2016. https://cds.cern.ch/record/2216168
38. M. Beneke, P. Falgari, S. Klein, C. Schwinn, Hadronic top-quark pair production with NNLL threshold resummation. Nucl. Phys. B **855**, 695 (2012). https://doi.org/10.1016/j.nuclphysb.2011.10.021. arXiv:1109.1536 [hep-ph]
39. M. Cacciari, M. Czakon, M. Mangano, A. Mitov, P. Nason, Top-pair production at hadron colliders with next-to-next-to-leading logarithmic soft-gluon resummation. Phys. Lett. B **710**, 612 (2012). https://doi.org/10.1016/j.physletb.2012.03.013. arXiv:1111.5869 [hep-ph]
40. P. Bärnreuther, M. Czakon, A. Mitov, Percent-level-precision physics at the Tevatron: next-to-next-to-leading order QCD corrections to $q\bar{q} \to t\bar{t} + X$. Phys. Rev. Lett. **109**, 132001 (2012). https://doi.org/10.1103/PhysRevLett.109.132001. arXiv:1204.5201 [hep-ph]
41. M. Czakon, A. Mitov, NNLO corrections to top-pair production at hadron colliders: the all-fermionic scattering channels. JHEP **12**, 054 (2012). https://doi.org/10.1007/JHEP12(2012)054. arXiv:1207.0236 [hep-ph]
42. M. Czakon, A. Mitov, NNLO corrections to top pair production at hadron colliders: the quark-gluon reaction. JHEP **01**, 080 (2013). https://doi.org/10.1007/JHEP01(2013)080. arXiv:1210.6832 [hep-ph]
43. M. Czakon, P. Fiedler, A. Mitov, Total top-quark pair-production cross section at hadron colliders through $\mathcal{O}(\alpha_S^4)$. Phys. Rev. Lett. **110**, 252004 (2013). https://doi.org/10.1103/PhysRevLett.110.252004. arXiv:1303.6254 [hep-ph]
44. M. Czakon, A. Mitov, Top++: a program for the calculation of the top-pair cross-section at hadron colliders. Comput. Phys. Commun. **185**, 2930 (2014). https://doi.org/10.1016/j.cpc.2014.06.021. arXiv:1112.5675 [hep-ph]
45. E. Re, Single-top Wt-channel production matched with parton showers using the POWHEG method. Eur. Phys. J. C **71**, 1547 (2011). https://doi.org/10.1140/epjc/s10052-011-1547-z. arXiv:1009.2450 [hep-ph]
46. S. Frixione, E. Laenen, P. Motylinski, C. White, B.R. Webber, Single-top hadroproduction in association with a W boson. JHEP **07**, 029 (2008). https://doi.org/10.1088/1126-6708/2008/07/029. arXiv:0805.3067 [hep-ph]
47. N. Kidonakis, Two-loop soft anomalous dimensions for single top quark associated production with a W^- or H^-. Phys. Rev. D **82**, 054018 (2010). https://doi.org/10.1103/PhysRevD.82.054018. arXiv:1005.4451 [hep-ph]
48. N. Kidonakis, Top quark production. in Proceedings, Helmholtz International Summer School on Physics of Heavy Quarks and Hadrons (HQ2013) (JINR, Dubna, Russia, 15th–28th July 2013), p. 139. arXiv:1311.0283 [hep-ph]
49. R. Frederix, E. Re, P. Torrielli, Single-top t-channel hadroproduction in the four-flavour scheme with POWHEG and aMC@NLO. JHEP **09**, 130 (2012). https://doi.org/10.1007/JHEP09(2012)130. arXiv:1207.5391 [hep-ph]
50. S. Alioli, P. Nason, C. Oleari, E. Re, NLO single-top production matched with shower in POWHEG: s- and t-channel contributions. JHEP **09**, 111 (2009). https://doi.org/10.1088/1126-6708/2009/09/111. arXiv:0907.4076 [hep-ph]. [Erratum: JHEP 02 (2010) 011 https://doi.org/10.1007/JHEP02(2010)011]
51. T. Sjöstrand et al., An introduction to PYTHIA 8.2. Comput. Phys. Commun. **191**, 159 (2015). https://doi.org/10.1016/j.cpc.2015.01.024. arXiv:1410.3012 [hep-ph]
52. ATLAS Collaboration, ATLAS Pythia 8 tunes to 7TeV data. ATL-PHYS-PUB-2014-021, 2014. https://cds.cern.ch/record/1966419
53. NNPDF Collaboration, R.D. Ball et al., Parton distributions with LHC data. Nucl. Phys. B **867**, 244 (2013). https://doi.org/10.1016/j.nuclphysb.2012.10.003. arXiv:1207.1303 [hep-ph]
54. E. Bothmann et al., Event generation with Sherpa 2.2. SciPost Phys. **7**, 034 (2019). https://doi.org/10.21468/SciPostPhys.7.3.034. arXiv:1905.09127 [hep-ph]
55. T. Gleisberg, S. Höche, Comix, a new matrix element generator. JHEP **12**, 039 (2008). https://doi.org/10.1088/1126-6708/2008/12/039. arXiv:0808.3674 [hep-ph]
56. F. Buccioni et al., OpenLoops 2. Eur. Phys. J. C **79**, 866 (2019). https://doi.org/10.1140/epjc/s10052-019-7306-2. arXiv:1907.13071 [hep-ph]
57. F. Cascioli, P. Maierhöfer, S. Pozzorini, Scattering amplitudes with open loops. Phys. Rev. Lett. **108**, 111601 (2012). https://doi.org/10.1103/PhysRevLett.108.111601. arXiv:1111.5206 [hep-ph]
58. A. Denner, S. Dittmaier, L. Hofer, Collier: a fortran-based complex one-loop library in extended regularizations. Comput. Phys. Commun. **212**, 220 (2017). https://doi.org/10.1016/j.cpc.2016.10.013. arXiv:1604.06792 [hep-ph]
59. S. Schumann, F. Krauss, A parton shower algorithm based on Catani–Seymour dipole factorisation. JHEP **03**, 038 (2008). https://doi.org/10.1088/1126-6708/2008/03/038. arXiv:0709.1027 [hep-ph]
60. S. Höche, F. Krauss, M. Schönherr, F. Siegert, A critical appraisal of NLO+PS matching methods. JHEP **09**, 049 (2012). https://doi.org/10.1007/JHEP09(2012)049. arXiv:1111.1220 [hep-ph]
61. S. Höche, F. Krauss, M. Schönherr, F. Siegert, QCD matrix elements + parton showers. The NLO case. JHEP **04**, 027 (2013). https://doi.org/10.1007/JHEP04(2013)027. arXiv:1207.5030 [hep-ph]
62. S. Catani, F. Krauss, B.R. Webber, R. Kuhn, QCD matrix elements + parton showers. JHEP **11**, 063 (2001). https://doi.org/10.1088/1126-6708/2001/11/063. arXiv:hep-ph/0109231
63. S. Höche, F. Krauss, S. Schumann, F. Siegert, QCD matrix elements and truncated showers. JHEP **05**, 053 (2009). https://doi.org/10.1088/1126-6708/2009/05/053. arXiv:0903.1219 [hep-ph]
64. C. Anastasiou, L. Dixon, K. Melnikov, F. Petriello, High-precision QCD at hadron colliders: electroweak gauge boson rapidity distributions at next-to-next-to leading order. Phys. Rev. D **69**, 094008 (2004). https://doi.org/10.1103/PhysRevD.69.094008. arXiv:hep-ph/0312266
65. ATLAS Collaboration, Emulating the impact of additional proton–proton interactions in the ATLAS simulation by presampling sets of inelastic Monte Carlo events. Comput. Softw. Big

Sci. **6**, 3 (2022). https://doi.org/10.1007/s41781-021-00062-2. arXiv:2102.09495 [hep-ex]
66. K. Werner, F.-M. Liu, T. Pierog, Parton ladder splitting and the rapidity dependence of transverse momentum spectra in deuteron-gold collisions at the BNL Relativistic Heavy Ion Collider. Phys. Rev. C **74**, 044902 (2006). https://doi.org/10.1103/PhysRevC.74.044902. arXiv:hep-ph/0506232
67. C. Bierlich et al., A comprehensive guide to the physics and usage of PYTHIA 8.3. SciPost Phys. Codebases **8** (2022). https://doi.org/10.21468/SciPostPhysCodeb.8. arXiv:2203.11601 [hep-ph]
68. T. Pierog, I. Karpenko, J.M. Katzy, E. Yatsenko, K. Werner, EPOS LHC: test of collective hadronization with data measured at the CERN Large Hadron Collider. Phys. Rev. C **92**, 034906 (2015). https://doi.org/10.1103/PhysRevC.92.034906. arXiv:1306.0121 [hep-ph]
69. ATLAS Collaboration, The Pythia 8 A3 tune description of ATLAS minimum bias and inelastic measurements incorporating the Donnachie–Landshoff diffractive model. ATL-PHYS-PUB-2016-017, 2016. https://cds.cern.ch/record/2206965
70. S. Agostinelli et al., Geant4 – a simulation toolkit. Nucl. Instrum. Methods A **506**, 250 (2003). https://doi.org/10.1016/S0168-9002(03)01368-8
71. ATLAS Collaboration, The ATLAS Simulation Infrastructure. Eur. Phys. J. C **70**, 823 (2010). https://doi.org/10.1140/epjc/s10052-010-1429-9. arXiv:1005.4568 [physics.ins-det]
72. ATLAS Collaboration, AtlFast3: the next generation of fast simulation in ATLAS. Comput. Softw. Big Sci. **6**, 7 (2022). https://doi.org/10.1007/s41781-021-00079-7. arXiv:2109.02551 [hep-ex]
73. ATLAS Collaboration, Electron reconstruction and identification in the ATLAS experiment using the 2015 and 2016 LHC proton–proton collision data at $\sqrt{s} = 13$ TeV. Eur. Phys. J. C **79**, 639 (2019). https://doi.org/10.1140/epjc/s10052-019-7140-6. arXiv:1902.04655 [physics.ins-det]
74. ATLAS Collaboration, Electron and photon performance measurements with the ATLAS detector using the 2015–2017 LHC proton–proton collision data. JINST **14**, P12006 (2019). https://doi.org/10.1088/1748-0221/14/12/P12006. arXiv:1908.00005 [hep-ex]
75. ATLAS Collaboration, Studies of the muon momentum calibration and performance of the ATLAS detector with pp collisions at $\sqrt{s} = 13$ TeV. Eur. Phys. J. C **83**, 686 (2023). https://doi.org/10.1140/epjc/s10052-023-11584-x. arXiv:2212.07338 [hep-ex]
76. ATLAS Collaboration, Muon reconstruction and identification efficiency in ATLAS using the full Run 2 pp collision data set at $\sqrt{s} = 13$ TeV. Eur. Phys. J. C **81**, 578 (2021). https://doi.org/10.1140/epjc/s10052-021-09233-2. arXiv: 2012.00578 [hep-ex]
77. ATLAS Collaboration, Vertex reconstruction performance of the ATLAS detector at $\sqrt{s} = 13$ TeV. ATL-PHYS-PUB-2015-026, 2015. https://cds.cern.ch/record/2037717
78. M. Cacciari, G.P. Salam, G. Soyez, FastJet user manual. Eur. Phys. J. C **72**, 1896 (2012). https://doi.org/10.1140/epjc/s10052-012-1896-2. arXiv: 1111.6097 [hep-ph]
79. ATLAS Collaboration, Performance of pile-up mitigation techniques for jets in pp collisions at $\sqrt{s} = 8$TeV using the ATLAS detector. Eur. Phys. J. C **76**, 581 (2016). https://doi.org/10.1140/epjc/s10052-016-4395-z. arXiv:1510.03823 [hep-ex]
80. ATLAS Collaboration, Transforming jet flavour tagging at ATLAS. (2025). arXiv:2505.19689 [hep-ex]
81. ATLAS Collaboration, ATLAS $b-jet$ identification performance and efficiency measurement with $t\bar{t}$ events in pp collisions at $\sqrt{s} = 13$ TeV. Eur. Phys. J. C **79**, 970 (2019). https://doi.org/10.1140/epjc/s10052-019-7450-8. arXiv:1907.05120 [hep-ex]
82. , ATLAS Collaboration, Calibration of the light-flavour jet mistagging efficiency of the b-tagging algorithms with Z+jets events using 139fb^{-1} of ATLAS proton–proton collision data at $\sqrt{s} =$ 13 TeV. Eur. Phys. J. C **83**, 728 (2023). https://doi.org/10.1140/epjc/s10052-023-11736-z. arXiv:2301.06319 [hep-ex]
83. ATLAS Collaboration, Measurement of the c-jet mistagging efficiency in $t\bar{t}$ events using pp collision data at $\sqrt{s} =$ 13 TeV collected with the ATLAS detector. Eur. Phys. J. C **82**, 95 (2022). https://doi.org/10.1140/epjc/s10052-021-09843-w. arXiv:2109.10627 [hep-ex]
84. ATLAS Collaboration, The performance of missing transverse momentum reconstruction and its significance with the ATLAS detector using 140 fb^{-1} of $\sqrt{s} =$ 13TeV pp collisions. Eur. Phys. J. C **85**, 606 (2025). https://doi.org/10.1140/epjc/s10052-025-14062-8. arXiv:2402.05858 [hep-ex]
85. ATLAS Collaboration, Jet mass reconstruction with the ATLAS detector in early Run 2 data. ATLAS-CONF-2016-035, 2016. https://cds.cern.ch/record/2200211
86. ATLAS Collaboration, In-situ measurements of the ATLAS large-radius jet response in 13 TeV (pp) collisions. ATLAS-CONF-2017-063, 2017. https://cds.cern.ch/record/2275655
87. T. Dado et al., FastFrames, Zenodo, version 6.1.0, 2024. https://doi.org/10.5281/zenodo.17233309
88. M. Cacciari, G.P. Salam, Pileup subtraction using jet areas. Phys. Lett. B **659**, 119 (2008). https://doi.org/10.1016/j.physletb.2007.09.077. arXiv:0707.1378 [hep-ph]
89. M. Czakon et al., Top-pair production at the LHC through NNLO QCD and NLO EW. JHEP **10**, 186 (2017). https://doi.org/10.1007/JHEP10(2017)186. arXiv:1705.04105 [hep-ph]
90. M. Bähr et al., Herwig++ physics and manual. Eur. Phys. J. C **58**, 639 (2008). https://doi.org/10.1140/epjc/s10052-008-0798-9. arXiv:0803.0883 [hep-ph]
91. J. Bellm et al., Herwig 7.0/Herwig++ 3.0 release note. Eur. Phys. J. C **76**, 196 (2016). https://doi.org/10.1140/epjc/s10052-016-4018-8. arXiv:1512.01178 [hep-ph]
92. J. Bellm et al., Herwig 7.2 release note. Eur. Phys. J. C 80, 452 (2020). https://doi.org/10.1140/epjc/s10052-020-8011-x. arXiv:1912.06509 [hep-ph]
93. L.A. Harland-Lang, A.D. Martin, P. Motylinski, R.S. Thorne, Parton distributions in the LHC era: MMHT 2014 PDFs. Eur. Phys. J. C **75**, 204 (2015). https://doi.org/10.1140/epjc/s10052-015-3397-6. arXiv:1412.3989 [hep-ph]
94. ATLAS Collaboration, A study of different colour reconnection settings for Pythia8 generator using underlying event observables. ATL-PHYS-PUB-2017-008, 2017. https://cds.cern.ch/record/2262253
95. J. Butterworth et al., PDF4LHC recommendations for LHC Run II. J. Phys. G **43**, 023001 (2016). https://doi.org/10.1088/0954-3899/43/2/023001. arXiv:1510.03865 [hep-ph]
96. R.D. Ball et al., The PDF4LHC21 combination of global PDF fits for the LHC Run III. J. Phys. G **49**, 080501 (2022). https://doi.org/10.1088/1361-6471/ac7216. arXiv:2203.05506 [hep-ph]
97. B. Andersson, G. Gustafson, B. Söderberg, A general model for jet fragmentation. Z. Phys. C **20**, 317 (1983). https://doi.org/10.1007/BF01407824
98. M.G. Bowler, e^+e^- production of heavy quarks in the string model. Z. Phys. C **11**, 169 (1981). https://doi.org/10.1007/BF01574001
99. N. Kidonakis, N. Yamanaka, Higher-order corrections for tW production at high-energy hadron colliders. JHEP **05**, 278 (2021). https://doi.org/10.1007/JHEP05(2021)278. arXiv:2102.11300 [hep-ph]
100. ATLAS Collaboration, ATLAS computing acknowledgements. ATL-SOFT-PUB-2026-001, 2026. https://cds.cern.ch/record/2952666

ATLAS Collaboration[★]

G. Aad[103], E. Aakvaag[17], B. Abbott[122], S. Abdelhameed[118a], K. Abeling[55], N. J. Abicht[49], S. H. Abidi[30], M. Aboelela[45], A. Aboulhorma[36e], H. Abramowicz[156], B. S. Acharya[69a,69b,m], A. Ackermann[63a], C. Adam Bourdarios[4], L. Adamczyk[86a], S. V. Addepalli[148], M. J. Addison[102], J. Adelman[117], A. Adiguzel[22c], T. Adye[136], A. A. Affolder[138], Y. Afik[40], M. N. Agaras[13], A. Aggarwal[101], C. Agheorghiesei[28c], F. Ahmadov[39,ad], S. Ahuja[96], S. Ahuja[168], X. Ai[142b], G. Aielli[76a,76b], A. Aikot[168], M. Ait Tamlihat[36e], B. Aitbenchikh[36a], T. P. A. Åkesson[99], D. Akiyama[173], N. N. Akolkar[25], S. Aktas[171], G. L. Alberghi[24b], J. Albert[170], U. Alberti[20], P. Albicocco[53], G. L. Albouy[60], S. Alderweireldt[52], Z. L. Alegria[123], M. Aleksa[37], I. N. Aleksandrov[39], C. Alexa[28b], T. Alexopoulos[10], F. Alfonsi[24b], M. Algren[56], M. Alhroob[172], B. Ali[134], H. M. J. Ali[92,v], S. Ali[32], S. W. Alibocus[93], M. Aliev[34c], G. Alimonti[71a], W. Alkakhi[55], C. Allaire[66], B. M. M. Allbrooke[151], D. R. Allen[123], J. S. Allen[102], J. F. Allen[52], C. S. Alley[1], A. Aloisio[72a,72b], F. Alonso[91], C. Alpigiani[141], Z. M. K. Alsolami[92], A. Alvarez Fernandez[101], M. Alves Cardoso[56], M. G. Alviggi[72a,72b], M. Aly[102], Y. Amaral Coutinho[82b], A. Ambler[105], C. Amelung[37], M. Amerl[102], T. Amezza[129], B. Amini[54], K. Amirie[160], A. Amirkhanov[39], S. P. Amor Dos Santos[132a], D. Amperiadou[157], S. An[83], C. Anastopoulos[144], T. Andeen[11], J. K. Anders[93], A. C. Anderson[59], A. Andreazza[71a,71b], S. Angelidakis[9], A. Angerami[42], A. V. Anisenkov[39], A. Annovi[74a], C. Antel[37], E. Antipov[150], M. Antonelli[53], F. Anulli[75a], M. Aoki[83], T. Aoki[158], M. A. Aparo[13], L. Aperio Bella[48], M. Apicella[31], C. Appelt[156], A. Apyan[27], M. Arampatzi[10], S. J. Arbiol Val[87], C. Arcangeletti[53], A. T. H. Arce[51], J-F. Arguin[109], S. Argyropoulos[157], J. -H. Arling[48], O. Arnaez[4], H. Arnold[150], G. Artoni[75a,75b], H. Asada[112], S. Asatryan[178], N. A. Asbah[37], R. A. Ashby Pickering[172], A. M. Aslam[96], K. Assamagan[30], R. Astalos[29a], K. S. V. Astrand[99], S. Atashi[164], R. J. Atkin[34a], H. Atmani[36f], P. A. Atmasiddha[130], K. Augsten[134], A. D. Auriol[41], V. A. Austrup[102], A. S. Avad[95], G. Avolio[37], K. Axiotis[56], A. Azzam[13], D. Babal[29b], H. Bachacou[137], K. Bachas[157,p], A. Bachiu[35], E. Bachmann[50], M. J. Backes[63a], A. Badea[40], T. M. Baer[107], M. Bahmani[19], D. Bahner[54], K. Bai[125], L. Baines[95], O. K. Baker[177], D. Bakshi Gupta[8], L. E. Balabram Filho[82b], V. Balakrishnan[122], R. Balasubramanian[4], E. M. Baldin[38], P. Balek[86a], E. Ballabene[24a,24b], F. Balli[137], L. M. Baltes[63a], W. K. Balunas[128], J. Balz[101], I. Bamwidhi[118b], E. Banas[87], M. Bandieramonte[131], A. Bandyopadhyay[25], S. Bansal[25], L. Barak[156], M. Barakat[48], E. L. Barberio[106], D. Barberis[18b], M. Barbero[103], M. Z. Barel[116], T. Barillari[111], M-S. Barisits[37], T. Barklow[148], P. Baron[135], D. A. Baron Moreno[102], A. Baroncelli[62], A. J. Barr[128], J. D. Barr[97], F. Barreiro[100], J. Barreiro Guimarães da Costa[14], M. G. Barros Teixeira[132a], S. Barsov[38], F. Bartels[63a], R. Bartoldus[148], A. E. Barton[92], P. Bartos[29a], M. Baselga[49], S. Bashiri[87], A. Bassalat[66,b], M. J. Basso[161a], S. Bataju[45], R. Bate[169], R. L. Bates[59], S. Batlamous[100], M. Battaglia[138], D. Battulga[19], M. Bauce[75a,75b], L. Bauckhage[48], P. Bauer[25], L. T. Bayer[48], L. T. Bazzano Hurrell[31], J. B. Beacham[111], T. Beau[129], J. Y. Beaucamp[91], P. H. Beauchemin[163], P. Bechtle[25], H. P. Beck[20,o], K. Becker[172], A. J. Beddall[81], V. A. Bednyakov[39], C. P. Bee[150], L. J. Beemster[16], M. Begalli[82d], M. Begel[30], J. K. Behr[48], J. F. Beirer[37], F. Beisiegel[25], M. Belfkir[118b], G. Bella[156], L. Bellagamba[24b], A. Bellerive[35], C. D. Bellgraph[68], P. Bellos[21], K. Beloborodov[38], I. Benaoumeur[21], D. Benchekroun[36a], F. Bendebba[36a], Y. Benhammou[156], K. C. Benkendorfer[61], L. Beresford[48], M. Beretta[53], E. Bergeaas Kuutmann[166], N. Berger[4], B. Bergmann[134], J. Beringer[18a], G. Bernardi[5], C. Bernius[148], F. U. Bernlochner[25], A. Berrocal Guardia[13], T. Berry[96], P. Berta[135], A. Berti[132a], R. Bertrand[103], S. Bethke[111], A. Betti[75a,75b], A. J. Bevan[95], L. Bezio[56], N. K. Bhalla[54], S. Bharthuar[111], S. Bhatta[150], P. Bhattarai[148], Z. M. Bhatti[119], K. D. Bhide[54], V. S. Bhopatkar[123], R. M. Bianchi[131], G. Bianco[24a,24b], O. Biebel[110], M. Biglietti[77a], P. Bijl[54], C. S. Billingsley[45], Y. Bimgdi[36f], M. Bindi[55], A. Bingham[176], A. Bingul[22b], C. Bini[75a,75b], G. A. Bird[33], M. Birman[174], M. Biros[135], S. Biryukov[151], T. Bisanz[49], E. Bisceglie[24a,24b], J. P. Biswal[136], D. Biswas[146], I. Bloch[48], A. Blue[59], U. Blumenschein[95], V. S. Bobrovnikov[39], L. Boccardo[57a,57b], M. Boehler[54], B. Boehm[171], D. Bogavac[13], A. G. Bogdanchikov[38], L. S. Boggia[129], V. Boisvert[96], P. Bokan[166], T. Bold[86a], M. Bomben[5], M. Bona[95], M. Boonekamp[137], A. G. Borbély[59], I. S. Bordulev[38], G. Borissov[92], D. Bortoletto[128], D. Boscherini[24b], M. Bosman[13], K. Bouaouda[36a], L. Boudet[4], J. Boudreau[131], E. V. Bouhova-Thacker[92], D. Boumediene[41], R. Bouquet[57a,57b], A. Boveia[121], J. Boyd[37], D. Boye[30], I. R. Boyko[39], L. Bozianu[56], J. Bracinik[21], N. Brahimi[4], G. Brandt[176], O. Brandt[33], B. Brau[104], R. Brener[174], L. Brenner[116], R. Brenner[166], S. Bressler[174], G. Brianti[116], D. Britton[59], D. Britzger[111], I. Brock[25], R. Brock[108], H. Bronson[130], G. Brooijmans[42], A. J. Brooks[68], E. M. Brooks[161b],

E. Brost[30], L. M. Brown[161a,170], L. E. Bruce[61], T. L. Bruckler[128], P. A. Bruckman de Renstrom[87], B. Brüers[48], A. Bruni[24b], G. Bruni[24b], D. Brunner[47a,47b], M. Bruschi[24b], N. Bruscino[75a,75b], T. Buanes[17], Q. Buat[141], D. Buchin[111], A. G. Buckley[59], J. Bucko[135], M. Buhring[50], O. Bulekov[81], B. A. Bullard[148], S. Burdin[93], C. D. Burgard[49], A. M. Burger[90], B. Burghgrave[8], O. Burlayenko[54], J. Burleson[167], J. C. Burzynski[147], V. Büscher[101], P.J. Bussey[59], O. But[25], J. M. Butler[26], C. M. Buttar[59], J. M. Butterworth[97], P. Butti[37], W. Buttinger[136], C. J. Buxo Vazquez[108], A. R. Buzykaev[39], S. Cabrera Urbán[168], L. Cadamuro[66], H. Cai[37], Y. Cai[24a,24b,113c], Y. Cai[113a], V. M. M. Cairo[37], O. Cakir[3a], N. Calace[37], P. Calafiura[18a], G. Calderini[129], P. Calfayan[35], L. Calic[99], G. Callea[59], L. P. Caloba[82b], D. Calvet[41], S. Calvet[41], R. Camacho Toro[129], S. Camarda[37], D. Camarero Munoz[27], P. Camarri[76a,76b], C. Camincher[37], M. Campanelli[97], A. Camplani[43], V. Canale[72a,72b], A. C. Canbay[3a], E. Canonero[96], J. Cantero[168], Y. Cao[167], F. Capocasa[27], M. Capua[44a,44b], A. Carbone[71a,71b], R. Cardarelli[76a], J. C. J. Cardenas[8], M. P. Cardiff[27], G. Carducci[44a,44b], T. Carli[37], G. Carlino[72a], J. I. Carlotto[13], B. T. Carlson[131,q], E. M. Carlson[170], L. Carminati[71a,71b], A. Carnelli[4], M. Carnesale[37], S. Caron[115], E. Carquin[139g], I. B. Carr[106], S. Carrá[73a,73b], G. Carratta[24a,24b], C. Carrion Martinez[168], A. M. Carroll[125], M. P. Casado[13,h], P. Casolaro[72a,72b], M. Caspar[48], W. R. Castiglioni[40], F. L. Castillo[4], L. Castillo Garcia[13], V. Castillo Gimenez[168], N. F. Castro[132a,132e], A. Catinaccio[37], J. R. Catmore[127], T. Cavaliere[4], V. Cavaliere[30], L. J. Caviedes Betancourt[23b], E. Celebi[81], S. Cella[156], V. Cepaitis[56], K. Cerny[124], A. S. Cerqueira[82a], A. Cerri[74a,am], L. Cerrito[76a,76b], F. Cerutti[18a], B. Cervato[71a,71b], A. Cervelli[24b], G. Cesarini[53], S. A. Cetin[81], P. M. Chabrillat[129], R. Chakkappai[66], S. Chakraborty[172], A. Chambers[61], J. Chan[18a], W. Y. Chan[158], J. D. Chapman[33], E. Chapon[137], B. Chargeishvili[154b], D. G. Charlton[21], C. Chauhan[133], Y. Che[113a], S. Chekanov[6], G. A. Chelkov[39,a], B. Chen[170], H. Chen[30], J. Chen[143a], J. Chen[147], M. Chen[128], S. Chen[88], S. J. Chen[113a], X. Chen[143a], X. Chen[15,ah], Z. Chen[62], C. L. Cheng[175], H. C. Cheng[64a], S. Cheong[148], A. Cheplakov[39], E. Cherepanova[116], E. Cheu[7], K. Cheung[65], L. Chevalier[137], G. Chiarelli[74a], G. Chiodini[70a], A. S. Chisholm[21], A. Chitan[28b], M. Chitishvili[168], M. V. Chizhov[39,r], K. Choi[11], Y. Chou[141], E. Y. S. Chow[115], K. L. Chu[174], M. C. Chu[64a], Z. Chubinidze[53], J. Chudoba[133], J. J. Chwastowski[87], D. Cieri[111], K. M. Ciesla[86a], V. Cindro[94], A. Ciocio[18a], F. Cirotto[72a,72b], Z. H. Citron[174], M. Citterio[71a], D. A. Ciubotaru[28b], A. Clark[56], P. J. Clark[52], N. Clarke Hall[97], C. Clarry[160], S. E. Clawson[48], C. Clement[47a,47b], L. Clissa[24a,24b], Y. Coadou[103], M. Cobal[69a,69c], A. Coccaro[57b], R. F. Coelho Barrue[132a], R. Coelho Lopes De Sa[104], S. Coelli[71a], M. M. Cohen[130], L. S. Colangeli[160], B. Cole[42], P. Collado Soto[100], J. Collot[60], M. R. Coluccia[70a], P. Conde Muiño[132a,132g], M. P. Connell[34c], S. H. Connell[34c], E. I. Conroy[128], M. Contreras Cossio[11], F. Conventi[72a,aj], A. M. Cooper-Sarkar[128], L. Corazzina[75a,75b], F. A. Corchia[24a,24b], A. Cordeiro Oudot Choi[141], L. D. Corpe[41], M. Corradi[75a,75b], F. Corriveau[105,ab], A. Cortes-Gonzalez[158], M. J. Costa[168], F. Costanza[4], D. Costanzo[144], J. Couthures[4], G. Cowan[96], K. Cranmer[175], L. Cremer[49], D. Cremonini[24a,24b], S. Crépé-Renaudin[60], F. Crescioli[129], T. Cresta[73a,73b], M. Cristinziani[146], M. Cristoforetti[78a,78b], E. Critelli[97], G. Crosetti[44a,44b], A. Cueto[100], H. Cui[97], Z. Cui[7], B. M. Cunnett[151], W. R. Cunningham[59], F. Curcio[168], J. R. Curran[52], M. J. Da Cunha Sargedas De Sousa[57a,57b], J. V. Da Fonseca Pinto[82b], C. Da Via[102], W. Dabrowski[86a], T. Dado[37], S. Dahbi[153], T. Dai[107], D. Dal Santo[20], C. Dallapiccola[104], M. Dam[43], G. D'amen[30], V. D'Amico[110], J. R. Dandoy[35], M. D'Andrea[57a,57b], D. Dannheim[37], G. D'anniballe[74a,74b], M. Danninger[147], V. Dao[150], G. Darbo[57b], S. J. Das[30], F. Dattola[48], S. D'Auria[71a,71b], A. D'Avanzo[72a,72b], T. Davidek[135], J. Davidson[172], I. Dawson[95], K. De[8], C. De Almeida Rossi[160], R. De Asmundis[72a], N. De Biase[48], S. De Castro[24a,24b], N. De Groot[115], P. de Jong[116], H. De la Torre[117], A. De Maria[113a], A. De Salvo[75a], U. De Sanctis[76a,76b], F. De Santis[70a,70b], A. De Santo[151], J. B. De Vivie De Regie[60], J. Debevc[94], D. V. Dedovich[39], J. Degens[93], A. M. Deiana[45], J. Del Peso[100], L. Delagrange[129], F. Deliot[137], C. M. Delitzsch[49], M. Della Pietra[72a,72b], D. Della Volpe[56], A. Dell'Acqua[37], L. Dell'Asta[71a,71b], M. Delmastro[4], C. C. Delogu[57a,57b], P. A. Delsart[60], S. Demers[177], M. Demichev[39], S. P. Denisov[38], H. Denizli[22a,l], M. G. Depala[93], L. D'Eramo[41], D. Derendarz[87], F. Derue[129], P. Dervan[93,*], A. M. Desai[1], K. Desch[25], F. A. Di Bello[74a,74b], A. Di Ciaccio[76a,76b], L. Di Ciaccio[4], C. Di Donato[72a,72b], A. Di Girolamo[37], G. Di Gregorio[66], A. Di Luca[78a,78b], B. Di Micco[77a,77b], R. Di Nardo[77a,77b], K. F. Di Petrillo[40], M. Diamantopoulou[35], F. A. Dias[116], M. A. Diaz[139a,139b], A. R. Didenko[39], M. Didenko[168], S. D. Diefenbacher[18a], E. B. Diehl[107], S. Díez Cornell[48], C. Diez Pardos[146], C. Dimitriadi[149], A. Dimitrievska[21], A. Dimri[150], Y. Ding[62], J. Dingfelder[25], T. Dingley[128], I-M. Dinu[28b], S. J. Dittmeier[63b], F. Dittus[37], M. Divisek[135], B. Dixit[93], F. Djama[103], T. Djobava[154b], C. Doglioni[99,102], A. Dohnalova[29a], Z. Dolezal[135], K. Domijan[86a],

K. M. Dona[40], M. Donadelli[82d], B. Dong[108], J. Donini[41], A. D'Onofrio[72a,72b], M. D'Onofrio[93], J. Dopke[136], A. Doria[72a], N. Dos Santos Fernandes[132a], I. A. Dos Santos Luz[82e], P. Dougan[45], M. T. Dova[91], A. T. Doyle[59], M. P. Drescher[55], E. Dreyer[174], I. Drivas-koulouris[10], M. Drnevich[119], D. Du[62], T. A. du Pree[116], Z. Duan[113a], M. Dubau[4], F. Dubinin[39], M. Dubovsky[29a], E. Duchovni[174], G. Duckeck[110], P. K. Duckett[97], O. A. Ducu[28b], D. Duda[52], A. Dudarev[37], M. M. Dudek[87], E. R. Duden[27], M. D'uffizi[102], L. Duflot[66], M. Dührssen[37], I. Duminica[28g], A. E. Dumitriu[28b], M. Dunford[63a], A. Duperrin[103], H. Duran Yildiz[3a], A. Durglishvili[154b], G. I. Dyckes[18a], M. Dyndal[86a], B. S. Dziedzic[37], Z. O. Earnshaw[151], G. H. Eberwein[128], B. Eckerova[29a], S. Eggebrecht[55], E. Egidio Purcino De Souza[82e], G. Eigen[17], K. Einsweiler[18a], T. Ekelof[166], P. A. Ekman[99], S. El Farkh[36b], Y. El Ghazali[62], H. El Jarrari[105], A. El Moussaouy[36a], I. Elbaz[156], D. Elitez[37], M. Ellert[166], F. Ellinghaus[176], T. A. Elliot[96], J. Elmsheuser[30], M. Elsawy[118a], M. Elsing[37], D. Emeliyanov[136], Y. Enari[83], S. Epari[109], D. Ernani Martins Neto[87], F. Ernst[37], M. Escalier[66], C. Escobar[168], R. Estevam De Paula[82c], E. Etzion[156], G. Evans[132a,132b], H. Evans[68], L. S. Evans[48], A. Ezhilov[38], S. Ezzarqtouni[36a], F. Fabbri[24a,24b], L. Fabbri[24a,24b], G. Facini[97], V. Fadeyev[138], R. M. Fakhrutdinov[38], D. Fakoudis[101], S. Falciano[75a], L. F. Falda Ulhoa Coelho[27], F. Fallavollita[111], G. Falsetti[44a,44b], J. Faltova[135], C. Fan[167], K. Y. Fan[64b], Y. Fan[14], Y. Fang[14,113c], M. Fanti[71a,71b], M. Faraj[69a,69c], Z. Farazpay[98], A. Farbin[8], A. Farilla[77a], K. Farman[153], J. N. Farr[177], M. S. Farrington[61], S. M. Farrington[52,136], F. Fassi[36e], D. Fassouliotis[9], L. Fayard[66], P. Federic[135], P. Federicova[133], O. L. Fedin[38,a], M. Feickert[175], L. Feligioni[103], D. E. Fellers[18a], C. Feng[142a], Y. Feng[14], Z. Feng[66], B. Fernandez Barbadillo[92], P. Fernandez Martinez[67], M. J. V. Fernoux[103], J. Ferrando[92], A. Ferrari[166], P. Ferrari[115,116], R. Ferrari[73a], D. Ferrere[56], C. Ferretti[107], M. P. Fewell[1], D. Fiacco[75a,75b], F. Fiedler[101], P. Fiedler[134], S. Filimonov[39], M. S. Filip[28b,s], A. Filipčič[94], E. K. Filmer[161a], F. Filthaut[115], M. C. N. Fiolhais[132a,132c,c], L. Fiorini[168], W. C. Fisher[108], T. Fitschen[102], P. M. Fitzhugh[137], I. Fleck[146], P. Fleischmann[107], T. Flick[176], M. Flores[34d,ag], L. R. Flores Castillo[64a], M. Foll[127], F. M. Follega[78a,78b], N. Fomin[33], J. H. Foo[160], A. Formica[137], A. C. Forti[102], E. Fortin[150], A. W. Fortman[18a], L. Foster[18a], L. Fountas[9], H. Fox[92], P. Francavilla[74a,74b], S. Francescato[61], S. Franchellucci[56], M. Franchini[24a,24b], S. Franchino[63a], D. Francis[37], L. Franco[48], L. Franconi[48], M. Franklin[61], G. Frattari[27], Y. Y. Frid[156], J. Friend[59], N. Fritzsche[37], A. Froch[56], D. Froidevaux[37], J. A. Frost[136], Y. Fu[108], S. Fuenzalida Garrido[139g], M. Fujimoto[150], K. Y. Fung[64a], E. Furtado De Simas Filho[82e], M. Furukawa[158], M. Fuste Costa[48], J. Fuster[168], A. Gaa[55], A. Gabrielli[24a,24b], A. Gabrielli[160], P. Gadow[37], G. Gagliardi[57a,57b], L. G. Gagnon[18a], S. Gaid[84b], S. Galantzan[156], J. Gallagher[1], E. J. Gallas[128], A. L. Gallen[166], B. J. Gallop[136], K. K. Gan[121], Y. Gao[52], Z. Gao[113a], A. Garabaglu[141], F. M. Garay Walls[139a,139b], C. García[168], A. Garcia Alonso[116], A. G. Garcia Caffaro[177], J. E. García Navarro[168], M. A. Garcia Ruiz[23b], M. Garcia-Sciveres[18a], G. L. Gardner[130], R. W. Gardner[40], N. Garelli[163], R. B. Garg[148], J. M. Gargan[33], C. A. Garner[160], C. M. Garvey[34a], V. K. Gassmann[163], G. Gaudio[73a], V. Gautam[13], J. Gavranovic[94], I. L. Gavrilenko[132a], A. Gavrilyuk[38], C. Gay[169], G. Gaycken[125], A. Gekow[121], C. Gemme[57b], M. H. Genest[60], A. D. Gentry[114], S. George[96], T. Geralis[46], A. A. Gerwin[122], P. Gessinger-Befurt[37], M. Ghani[172], K. Ghorbanian[95], A. Ghosal[146], A. Ghosh[164], A. Ghosh[7], B. Giacobbe[24b], S. Giagu[75a,75b], A. Giannini[62], S. M. Gibson[96], D. T. Gil[86b], A. K. Gilbert[86a], B. J. Gilbert[42], D. Gillberg[35], G. Gilles[116], D. M. Gingrich[2,ai], M. P. Giordani[69a,69c], P. F. Giraud[137], G. Giugliarelli[69a,69c], D. Giugni[71a], F. Giuli[76a,76b], I. Gkialas[9,i], L. K. Gladilin[38], C. Glasman[100], M. Glazewska[20], R. M. Gleason[164], G. Glemža[48], M. Glisic[125], I. Gnesi[44b], Y. Go[30], M. Goblirsch-Kolb[37], B. Gocke[49], D. Godin[109], B. Gokturk[22a], S. Goldfarb[106], T. Golling[56], M. G. D. Gololo[34c], A. Golub[141], D. Golubkov[38], J. P. Gombas[108], A. Gomes[132a,132b], G. Gomes Da Silva[146], A. J. Gomez Delegido[37], R. Gonçalo[132a], A. Gongadze[154c], F. Gonnella[21], J. L. Gonski[148], R. Y. González Andana[52], S. González de la Hoz[168], M. V. Gonzalez Rodrigues[48], R. Gonzalez Suarez[166], S. Gonzalez-Sevilla[56], L. Goossens[37], B. Gorini[37], E. Gorini[70a,70b], A. Gorišek[94], T. C. Gosart[130], A. T. Goshaw[51], M. I. Gostkin[39], S. Goswami[123], C. A. Gottardo[37], S. A. Gotz[110], M. Gouighri[36b], A. G. Goussiou[141], N. Govender[34c], R. P. Grabarczyk[128], I. Grabowska-Bold[86a], K. Graham[35], E. Gramstad[127], S. Grancagnolo[70a,70b], C. M. Grant[1], P. M. Gravila[28f], F. G. Gravili[70a,70b], H. M. Gray[18a], M. Greco[111], M. J. Green[1], C. Grefe[25], A. S. Grefsrud[17], I. M. Gregor[48], K. T. Greif[164], P. Grenier[148], S. G. Grewe[111], K. Grimm[32], S. Grinstein[13,x], E. Gross[174], J. Grosse-Knetter[55], L. H. Grossman[18b], L. Guan[107], G. Guerrieri[37], R. Guevara[127], R. Gugel[101], J. A. M. Guhit[107], A. Guida[19], E. Guilloton[172], S. Guindon[37], F. Guo[14,113c], J. Guo[143a], L. Guo[48], L. Guo[113b,u], Y. Guo[107], Y. Guo[42], A. Gupta[49], R. Gupta[131], S. Gupta[27], S. Gurbuz[25], S. S. Gurdasani[48], G. Gustavino[75a,75b], P. Gutierrez[122], L. F. Gutierrez Zagazeta[130], M. Gutsche[50], C. Gutschow[97], C. Gwenlan[128], C. B. Gwilliam[93],

E. S. Haaland[127], A. Haas[119], M. Habedank[59], C. Haber[18a], H. K. Hadavand[8], A. Haddad[41], A. Hadef[50], A. I. Hagan[92], J. J. Hahn[146], M. Haleem[171], J. Haley[123], G. D. Hallewell[103], J. A. Hallford[48], K. Hamano[170], H. Hamdaoui[166], M. Hamer[25], S. E. D. Hammoud[66], E. J. Hampshire[96], L. Han[113a], L. Han[62], S. Han[14], K. Hanagaki[83], M. Hance[138], D. A. Hangal[42], H. Hanif[147], M. D. Hank[130], J. B. Hansen[43], P. H. Hansen[43], T. Harenberg[176], S. Harkusha[178], M. L. Harris[104], Y. T. Harris[25], J. Harrison[13], P. F. Harrison[172], M. L. E. Hart[97], N. M. Hartman[111], N. M. Hartmann[110], R. Z. Hasan[96,136], Y. Hasegawa[145], D. Hashimoto[112], F. Haslbeck[37], S. Hassan[17], R. Hauser[108], M. Haviernik[135], C. M. Hawkes[21], R. J. Hawkings[37], Y. Hayashi[158], D. Hayden[108], R. L. Hayes[116], C. P. Hays[128], J. M. Hays[95], H. S. Hayward[93], M. He[14,113c], Y. He[48], Y. He[97], N. B. Heatley[95], V. Hedberg[99], J. Heilman[35], S. Heim[48], T. Heim[18a], J. J. Heinrich[125], L. Heinrich[111], J. Hejbal[133], M. Helbig[50], A. Held[175], S. Hellesund[17], C. M. Helling[169], H. Herde[99], Y. Hernández Jiménez[150], L. M. Herrmann[25], G. Herten[54], R. Hertenberger[110], L. Hervas[37], M. E. Hesping[101], N. P. Hessey[161a], J. Hessler[111], M. Hidaoui[36b], N. Hidic[135], E. Hill[160], T. S. Hillersoy[17], S. J. Hillier[21], J. R. Hinds[108], F. Hinterkeuser[25], M. Hirose[126], S. Hirose[162], D. Hirschbuehl[176], T. G. Hitchings[102], B. Hiti[94], J. Hobbs[150], R. Hobincu[28e], N. Hod[174], A. M. Hodges[167], M. C. Hodgkinson[144], B. H. Hodkinson[128], A. Hoecker[37], D. D. Hofer[107], J. Hofer[168], J. Hofner[101], M. Holzbock[37], L. B. A. H. Hommels[33], V. Homsak[128], J. J. Hong[68], T. M. Hong[131], B. H. Hooberman[167], W. H. Hopkins[6], M. C. Hoppesch[167], Y. Horii[112], M. E. Horstmann[111], S. Hou[153], M. R. Housenga[167], J. Howarth[59], J. Hoya[6], M. Hrabovsky[124], T. Hryn'ova[4], P. J. Hsu[65], S. -C. Hsu[141], T. Hsu[66], M. Hu[18a], Q. Hu[62], S. Huang[33], X. Huang[14,113c], Y. Huang[135], Y. Huang[113b], Y. Huang[14], Z. Huang[66], Z. Hubacek[134], F. Huegging[25], T. B. Huffman[128], M. Hufnagel Maranha De Faria[82a], C. A. Hugli[48], M. Huhtinen[37], S. K. Huiberts[127], R. Hulsken[105], C. E. Hultquist[18a], D. L. Humphreys[104], N. Huseynov[12], J. Huston[108], B. Huth[37], J. Huth[61], L. Huth[48], R. Hyneman[7], G. Iacobucci[56], G. Iakovidis[30], L. Iconomidou-Fayard[66], J. P. Iddon[37], P. Iengo[72a,72b], Y. Iiyama[158], T. Iizawa[158], Y. Ikegami[83], D. Iliadis[157], N. Ilic[160], H. Imam[36a], G. Inacio Goncalves[82d], S. A. Infante Cabanas[139c], T. Ingebretsen Carlson[47a,47b], J. M. Inglis[95], G. Introzzi[73a,73b], M. Iodice[77a], V. Ippolito[75a,75b], R. K. Irwin[93], M. Ishino[158], W. Islam[175], C. Issever[19], S. Istin[22a,ao], K. Itabashi[126], H. Ito[173], R. Iuppa[78a,78b], A. Ivina[174], S. Izumiyama[112], V. Izzo[72a], P. Jacka[134], P. Jackson[1], P. R. Jacobson[51], P. Jain[48], K. Jakobs[54], T. Jakoubek[174], J. Jamieson[59], W. Jang[158], S. Jankovych[116], M. Javurkova[104], P. Jawahar[102], L. Jeanty[125], J. Jejelava[154a,ae], P. Jenni[54,f], C. E. Jessiman[35], H. Jia[169], J. Jia[150], X. Jia[111,113c], Z. Jia[113a], C. Jiang[52], Q. Jiang[64b], S. Jiggins[48], M. Jimenez Ortega[168], J. Jimenez Pena[13], S. Jin[113a], A. Jinaru[28b], O. Jinnouchi[140], P. Johansson[144], K. A. Johns[7], J. W. Johnson[138], F. A. Jolly[48], D. M. Jones[151], E. Jones[48], K. S. Jones[8], P. Jones[33], R. W. L. Jones[92], T. J. Jones[93], H. L. Joos[55], R. Joshi[121], J. Jovicevic[16], X. Ju[18a], J. J. Junggeburth[37], T. Junkermann[63a], A. Juste Rozas[13,x], M. K. Juzek[87], S. Kabana[139f], A. Kaczmarska[87], S. A. Kadir[148], M. Kado[111], H. Kagan[121], M. Kagan[148], A. Kahn[130], C. Kahra[101], T. Kaji[158], E. Kajomovitz[155], N. Kakati[174], N. Kakoty[13], S. Kandel[8], N. Kanellos[10], N. J. Kang[138], D. Kar[34j,*], E. Karentzos[25], K. Karki[8], O. Karkout[116], S. N. Karpov[39], Z. M. Karpova[39], V. Kartvelishvili[92,154b], A. N. Karyukhin[38], E. Kasimi[157], J. Katzy[48], S. Kaur[35], K. Kawade[145], M. P. Kawale[122], C. Kawamoto[88], E. F. Kay[37], S. Kazakos[108], K. Kazakova[103], V. F. Kazanin[38], J. M. Keaveney[34a], R. Keeler[170], G. V. Kehris[61], J. S. Keller[35], J. M. Kelly[170], J. J. Kempster[151], O. Kepka[133], J. Kerr[161b], B. P. Kerridge[136], B. P. Kerševan[94], L. Keszeghova[29a], R. A. Khan[131], A. Khanov[123], A. G. Kharlamov[38], T. Kharlamova[38], M. Kholodenko[132a], T. J. Khoo[19], G. Khoriauli[171], Y. Khoulaki[36a], Y. A. R. Khwaira[129], D. Kim[6], D. W. Kim[18b], Y. K. Kim[40], N. Kimura[97], M. K. Kingston[55], C. Kirfel[25], F. Kirfel[25], J. Kirk[136], A. E. Kiryunin[111], S. Kita[162], O. Kivernyk[25], M. Klassen[163], C. Klein[35], L. Klein[171], M. H. Klein[45], S. B. Klein[56], U. Klein[93], A. Klimentov[30], P. Kluit[116], S. Kluth[111], E. Kneringer[79], T. M. Knight[160], A. Knue[49], M. Kobel[50], D. Kobylianskii[174], S. F. Koch[37], M. Kocian[148], P. Kodyš[135], D. M. Koeck[125], T. Koffas[35], O. Kolay[50], I. Koletsou[4], T. Komarek[87], K. Köneke[55], A. X. Y. Kong[1], T. Kono[120], N. Konstantinidis[97], P. Kontaxakis[56], B. Konya[99], R. Kopeliansky[42], S. Koperny[86a], R. Koppenhofer[54], K. Korcyl[87], K. Kordas[157,d], A. Korn[97], S. Korn[55], I. Korolkov[13], N. Korotkova[38], B. Kortman[116], O. Kortner[111], S. Kortner[111], W. H. Kostecka[117], M. Kostov[29a], V. V. Kostyukhin[146], A. Kotsokechagia[37], A. Kotwal[51], A. Koulouris[37], A. Kourkoumeli-Charalampidi[73a,73b], E. Kourlitis[111], O. Kovanda[125], R. Kowalewski[170], W. Kozanecki[125], A. S. Kozhin[38], V. A. Kramarenko[38], G. Kramberger[94], P. Kramer[25], A. Krasznahorkay[104], A. C. Kraus[117], J. W. Kraus[176], J. A. Kremer[48], N. B. Krengel[146], T. Kresse[50], L. Kretschmann[176], J. Kretzschmar[93], P. Krieger[160], K. Krizka[21], K. Kroeninger[49], H. Kroha[111],

J. Kroll[133], J. Kroll[130], K. S. Krowpman[108], U. Kruchonak[39], H. Krüger[25], N. Krumnack[80], M. C. Kruse[51], O. Kuchinskaia[39], S. Kuday[3a], S. Kuehn[37], R. Kuesters[54], T. Kuhl[48], V. Kukhtin[39], Y. Kulchitsky[39], S. Kuleshov[139b,139d], J. Kull[1], E. V. Kumar[110], M. Kumar[34j], N. Kumari[48], P. Kumari[161b], A. Kupco[133], A. Kupich[38], O. Kuprash[54], H. Kurashige[85], L. L. Kurchaninov[161a], O. Kurdysh[4], A. Kurova[38], M. Kuze[140], A. K. Kvam[104], J. Kvita[124], N. G. Kyriacou[141], M. Laassiri[30], C. Lacasta[168], H. Lacker[19], D. Lacour[129], E. Ladygin[39], A. Lafarge[41], B. Laforge[129], T. Lagouri[177], F. Z. Lahbabi[36a], S. Lai[55], W. S. Lai[97], I. K. Lakomiec[55], J. E. Lambert[170], S. Lammers[68], W. Lampl[7], C. Lampoudis[157], G. Lamprinoudis[171], A. N. Lancaster[117], U. Landgraf[54], M. P. J. Landon[95], V. S. Lang[54], A. J. Lankford[164], F. Lanni[37], C. S. Lantz[167], K. Lantzsch[25], A. Lanza[73a], M. Lanzac Berrocal[168], T. Lari[71a], D. Larsen[17], L. Larson[11], F. Lasagni Manghi[24b], M. Lassnig[37], S. D. Lawlor[144], R. Lazaridou[164], M. Lazzaroni[71a,71b], E. T. T. Le[164], H. D. M. Le[108], E. M. Le Boulicaut[177], L. T. Le Pottier[18a], B. Leban[24a,24b], F. Ledroit-Guillon[60], T. F. Lee[161b], L. L. Leeuw[34h], M. Lefebvre[170], C. Leggett[18a], G. Lehmann Miotto[37], M. Leigh[56], W. A. Leight[104], W. Leinonen[115], A. Leisos[157,t], M. A. L. Leite[82c], C. E. Leitgeb[19], R. Leitner[135], K. J. C. Leney[45], T. Lenz[25], S. Leone[74a], C. Leonidopoulos[52], A. Leopold[149], J. LePage-Bourbonnais[35], R. Les[108], C. G. Lester[33], M. Levchenko[38], J. Levêque[4], L. J. Levinson[174], G. Levrini[24a,24b], M.P. Lewicki[87], C. Lewis[141], D. J. Lewis[4], L. Lewitt[144], A. Li[30], B. Li[142a], C. Li[107], C-Q. Li[111], H. Li[142a], H. Li[102], H. Li[15], H. Li[62], H. Li[142a], J. Li[143a], L. Li[143a], R. Li[177], S. Li[143a,143b], T. Li[5], Y. Li[14], Z. Li[14,113c], Z. Li[62], S. Liang[14,113c], Z. Liang[14], M. Liberatore[137], B. Liberti[76a], G. B. Libotte[82d], K. Lie[64c], J. Lieber Marin[82e], H. Lien[68], H. Lin[107], S. F. Lin[150], L. Linden[110], R. E. Lindley[7], J. H. Lindon[37], J. Ling[61], E. Lipeles[130], A. Lipniacka[17], A. Lister[169], J. D. Little[68], B. Liu[14], B. X. Liu[113b], D. Liu[155], D. Liu[138], E. H. L. Liu[21], H. Liu[113b], J. K. K. Liu[119], K. Liu[143b], K. Liu[143b], M. Liu[62], M. Y. Liu[62], P. Liu[142a], Q. Liu[148], S. Liu[150], X. Liu[142a], Y. Liu[113b,113c], Y. Liu[167], Y. L. Liu[142a], Y. W. Liu[62], Z. Liu[66,j], S. L. Lloyd[95], E. M. Lobodzinska[48], P. Loch[7], E. Lodhi[160], K. Lohwasser[144], E. Loiacono[48], J. D. Lomas[21], I. Longarini[164], R. Longo[167], A. Lopez Solis[13], N. A. Lopez-canelas[7], N. Lorenzo Martinez[4], A. M. Lory[110], M. Losada[118a], G. Löschcke Centeno[4], X. Lou[14,113c], P. A. Love[92], M. Lu[66], S. Lu[130], Y. J. Lu[153], H. J. Lubatti[141], C. Luci[75a,75b], F. L. Lucio Alves[113a], F. Luehring[68], B. S. Lunday[130], O. Lundberg[149], J. Lunde[37], N. A. Luongo[6], M. S. Lutz[170], A. B. Lux[26], D. Lynn[30], R. Lysak[133], V. Lysenko[134], E. Lytken[99], V. Lyubushkin[39], T. Lyubushkina[39], M. M. Lyukova[150], H. Ma[30], K. Ma[62], L. L. Ma[142a], W. Ma[62], Y. Ma[123], J. C. MacDonald[101], P. C. Machado De Abreu Farias[82e], D. Macina[37], R. Madar[41], T. Madula[97], J. Maeda[85], T. Maeno[30], P. T. Mafa[34f], H. Maguire[144], M. Maheshwari[33], V. Maiboroda[66], A. Maio[132a,132b,132d], K. Maj[86a], O. Majersky[48], S. Majewski[125], R. Makhmanazarov[38], N. Makovec[66], V. Maksimovic[16], B. Malaescu[129], J. Malamant[127], Pa. Malecki[87], V. P. Maleev[38], F. Malek[60,n], M. Mali[94], D. Malito[96], A. Maloizel[5], A. Malvezzi Lopes[82d], S. Malyukov[39], J. Mamuzic[94], G. Mancini[53], M. N. Mancini[27], G. Manco[73a,73b], S. S. Mandarry[151], I. Mandić[94], L. Manhaes de Andrade Filho[82a], I. M. Maniatis[174], J. Manjarres Ramos[90], D. C. Mankad[174], A. Mann[110], T. Manoussos[37], M. N. Mantinan[40], S. Manzoni[37], L. Mao[143a], X. Mapekula[34c], A. Marantis[157], R. R. Marcelo Gregorio[1], G. Marchiori[5], C. Marcon[71a], E. Maricic[16], M. Marinescu[48], S. Marium[48], M. Marjanovic[122], A. Markhoos[54], M. Markovitch[66], M. K. Maroun[104], M. C. Marr[147], G. T. Marsden[102], E. J. Marshall[92], Z. Marshall[18a], S. Marti-Garcia[168], J. Martin[97], T. A. Martin[136], V. J. Martin[52], B. Martin dit Latour[17], L. Martinelli[75a,75b], P. Martinez Agullo[168], V. I. Martinez Outschoorn[104], P. Martinez Suarez[37], S. Martin-Haugh[136], G. Martinovicova[135], V. S. Martoiu[28b], A. C. Martyniuk[97], A. Marzin[37], D. Mascione[78a,78b], L. Masetti[101], J. Masik[102], A. L. Maslennikov[39], S. L. Mason[42], P. Massarotti[72a,72b], P. Mastrandrea[74a,74b], A. Mastroberardino[44a,44b], T. Masubuchi[126], T. T. Mathew[125], J. Matousek[135], D. M. Mattern[49], K. Mauer[48], J. Maurer[28b], T. Maurin[59], A. J. Maury[66], B. Maček[94], C. Mavungu Tsava[103], D. A. Maximov[38], A. E. May[102], E. Mayer[41], R. Mazini[34j], S. M. Mazza[138], E. Mazzeo[37], J. P. Mc Gowan[170], S. P. Mc Kee[107], C. A. Mc Lean[6], C. C. McCracken[169], E. F. McDonald[106], L. F. Mcelhinney[92], J. A. Mcfayden[151], R. P. McGovern[130], R. P. Mckenzie[34j], D. J. Mclaughlin[97], S. J. McMahon[136], C. M. Mcpartland[93], R. A. McPherson[170,ab], S. Mehlhase[110], A. Mehta[93], D. Melini[168], B. R. Mellado Garcia[34j], A. H. Melo[55], F. Meloni[48], A. M. Mendes Jacques Da Costa[102], L. Meng[92], S. Menke[111], M. Mentink[37], E. Meoni[44a,44b], G. Mercado[117], S. Merianos[157], C. Merlassino[69a,69c], C. Meroni[71a,71b], J. Metcalfe[6], A. S. Mete[6], E. Meuser[101], C. Meyer[68], J-P. Meyer[137], Y. Miao[113a], R. P. Middleton[136], M. Mihovilovic[66], L. Mijović[52], G. Mikenberg[174], M. Mikestikova[133], M. Mikuž[94], H. Mildner[101], A. Milic[37], D. W. Miller[40], E. H. Miller[148], A. Milov[174],

D. A. Milstead[47a,47b], T. Min[113a], A. A. Minaenko[38], I. A. Minashvili[154b], A. I. Mincer[119], B. Mindur[86a], M. Mineev[39], Y. Mino[88], L. M. Mir[13], M. Miralles Lopez[59], M. Mironova[18a], M. Missio[41], A. Mitra[172], V. A. Mitsou[168], Y. Mitsumori[112], P. S. Miyagawa[95], T. Mkrtchyan[37], M. Mlinarevic[97], T. Mlinarevic[97], M. Mlynarikova[135], L. Mlynarska[86a], C. Mo[143a], S. Mobius[20], M. H. Mohamed Farook[114], S. Mohapatra[42], M. F. Mohd Soberi[52], S. Mohiuddin[123], G. Mokgatitswane[34j], L. Moleri[174], U. Molinatti[128], L. G. Mollier[20], B. Mondal[133], S. Mondal[135], K. Mönig[48], E. Monnier[103], L. Monsonis Romero[168], A. Montella[47a,47b], M. Montella[121], F. Montereali[77a,77b], F. Monticelli[91], S. Monzani[69a,69c], A. Morancho Tarda[43], N. Morange[66], M. Moreno Llácer[168], C. Moreno Martinez[56], J. M. Moreno Perez[23b], P. Morettini[57b], S. Morgenstern[63a], M. Morii[61], M. Morinaga[158], F. Morodei[75a,75b], P. Moschovakos[37], B. Moser[54], M. Mosidze[154b], T. Moskalets[45], P. Moskvitina[115], J. Moss[32], T. Motta Quirino[82d], A. Moussa[36d], Y. Moyal[174,k], H. Moyano Gomez[13], E. J. W. Moyse[104], T. G. Mroz[87], S. Muanza[103], M. Mucha[25], J. Mueller[131], G. A. Mullier[166], A. J. Mullin[33], J. J. Mullin[51], A. C. Mullins[45], A. E. Mulski[61], D. P. Mungo[160], D. Munoz Perez[168], F. J. Munoz Sanchez[102], W. J. Murray[136,172], E. Musajan[62], M. Muškinja[94], C. Mwewa[48], A. G. Myagkov[38,a], A. J. Myers[8], G. Myers[107], M. Myska[134], B. P. Nachman[148], K. Nagai[128], K. Nagano[83], R. Nagasaka[158], J. L. Nagle[30,al], E. Nagy[103], A. M. Nairz[37], Y. Nakahama[83], K. Nakamura[83], K. Nakkalil[5], A. Nandi[63b], H. Nanjo[126], E. A. Narayanan[45], Y. Narukawa[158], I. Naryshkin[38], L. Nasella[71a,71b], S. Nasri[118b], C. Nass[25], G. Navarro[23a], A. Nayaz[19], P. Y. Nechaeva[38], S. Nechaeva[24a,24b], F. Nechansky[133], L. Nedic[128], A. Negri[73a,73b], M. Negrini[24b], C. Nellist[116], C. Nelson[105], K. Nelson[107], S. Nemecek[133], M. Nessi[37,g], M. S. Neubauer[167], J. Newell[93], P. R. Newman[21], Y. W. Y. Ng[167], B. Ngair[118a], H. D. N. Nguyen[109], J. D. Nichols[122], R. Nicolaidou[137], J. Nielsen[138], M. Niemeyer[55], J. Niermann[37], N. Nikiforou[37], V. Nikolaenko[38,a], I. Nikolic-Audit[129], P. Nilsson[30], G. Ninio[156], A. Nisati[75a], R. Nisius[111], N. Nitika[174], E. K. Nkadimeng[34b], T. Nobe[158], D. Noll[148], T. Nommensen[152], M. B. Norfolk[144], B. J. Norman[35], L. C. Nosler[18a], M. Noury[36a], J. Novak[94], T. Novak[94], P. Novotny[174], R. Novotny[134], L. Nozka[124], K. Ntekas[37], D. Ntounis[148], N. M. J. Nunes De Moura Junior[82b], J. Ocariz[129], I. Ochoa[132a], A. Odella Rodriguez[13], S. Oerdek[48], J. T. Offermann[40], A. Ogrodnik[87], A. Oh[102], C. C. Ohm[149], H. Oide[83], M. L. Ojeda[37], Y. Okumura[158], L. F. Oleiro Seabra[132a], I. Oleksiyuk[56], G. Oliveira Correa[13], D. Oliveira Damazio[30], J. L. Oliver[1], R. Omar[68], A. P. O'Neill[20], Y. Onoda[140], A. Onofre[132a,132e,e], P. U. E. Onyisi[11], M. J. Oreglia[40], D. Orestano[77a,77b], R. Orlandini[77a,77b], R. S. Orr[160], L. M. Osojnak[42], Y. Osumi[112], G. Otero y Garzón[31], H. Otono[89], M. Ouchrif[36d], F. Ould-Saada[127], T. Ovsiannikova[141], M. Owen[59], R. E. Owen[136], V. E. Ozcan[22a], F. Ozturk[87], N. Ozturk[8], S. Ozturk[81], H. A. Pacey[128], K. Pachal[161a], A. Pacheco Pages[13], C. Padilla Aranda[13], G. Padovano[75a,75b], S. Pagan Griso[18a], L. Pagani[76a,76b], J. Pampel[25], J. Pan[177], D. K. Panchal[11], C. E. Pandini[60], J. G. Panduro Vazquez[136], H. D. Pandya[1], H. Pang[137], P. Pani[48], G. Panizzo[69a,69c], L. Panwar[129,w], L. Paolozzi[56], S. Parajuli[167], A. Paramonov[6], C. Paraskevopoulos[53], D. Paredes Hernandez[64b], S. R. Paredes Saenz[52], A. Pareti[73a,73b], K. R. Park[42], T. H. Park[111], F. Parodi[57a,57b], J. A. Parsons[42], U. Parzefall[54], B. Pascual Dias[41], L. Pascual Dominguez[100], E. Pasqualucci[75a], S. Passaggio[57b], F. Pastore[96], P. Patel[87], U. M. Patel[51], J. R. Pater[102], T. Pauly[37], F. Pauwels[135], C. I. Pazos[163], M. Pedersen[127], R. Pedro[132a], S. V. Peleganchuk[38], O. Penc[133], S. Peng[15], G. D. Penn[177], K. E. Penski[110], M. Penzin[38], B. S. Peralva[82d], A. P. Pereira Peixoto[141], L. Pereira Sanchez[148], D. V. Perepelitsa[30,al], G. Perera[104], E. Perez Codina[37], M. Perganti[10], H. Pernegger[37], S. Perrella[75a,75b], K. Peters[48], R. F. Y. Peters[102], B. A. Petersen[37], T. C. Petersen[43], E. Petit[103], V. Petousis[134], A. R. Petri[71a,71b], T. Petru[135], M. Pettee[18a], A. Petukhov[81], K. Petukhova[37], R. Pezoa[139g], L. Pezzotti[24a,24b], G. Pezzullo[177], L. Pfaffenbichler[37], A. J. Pfleger[79], T. M. Pham[175], T. Pham[106], P. W. Phillips[136], G. Piacquadio[150], E. Pianori[18a], F. Piazza[125], R. Piegaia[31], D. Pietreanu[28b], A. D. Pilkington[102], M. Pinamonti[69a,69c], J. L. Pinfold[2], G. Pinheiro Matos[42], B. C. Pinheiro Pereira[132a], J. Pinol Bel[13], A. E. Pinto Pinoargote[129], L. Pintucci[69a,69c], A. Pirttikoski[56], D. A. Pizzi[35], L. Pizzimento[64b], A. Plebani[33], M. -A. Pleier[30], V. Pleskot[135], E. Plotnikova[39], G. Poddar[95], R. Poettgen[99], L. Poggioli[129], S. Polacek[135], G. Polesello[73a], A. Poley[147], A. Polini[24b], C. S. Pollard[172], Z. B. Pollock[121], E. Pompa Pacchi[122], N. I. Pond[97], D. Ponomarenko[68], L. Pontecorvo[37], S. Popa[28a], G. A. Popeneciu[28d], A. Poreba[63a], D. M. Portillo Quintero[161a], S. Pospisil[134], M. A. Postill[144], P. Postolache[28c], K. Potamianos[172], P. A. Potepa[86a], I. N. Potrap[39], C. J. Potter[33], H. Potti[152], J. Poveda[168], M. E. Pozo Astigarraga[37], R. Pozzi[37], A. Prades Ibanez[76a,76b], S. R. Pradhan[144], J. Pretel[170], D. Price[102], M. Primavera[70a], L. Primomo[69a,69c], M.A. Principe Martin[100], R. Privara[124], T. Procter[86b], M. L. Proffitt[141], N. Proklova[130], K. Prokofiev[64c], G. Proto[111], J. Proudfoot[6], M. Przybycien[86a],

W. W. Przygoda[86b], A. Psallidas[46], J. E. Puddefoot[144], D. Pudzha[53], H. I. Purnell[1], D. Pyatiizbyantseva[115], J. Qian[107], R. Qian[108], D. Qichen[128], Y. Qin[13], T. Qiu[52], A. Quadt[55], M. Queitsch-Maitland[102], G. Quetant[56], R. P. Quinn[169], G. Rabanal Bolanos[61], D. Rafanoharana[111], F. Raffaeli[76a,76b], J. L. Rainbolt[40], S. Rajagopalan[30], E. Ramakoti[39], L. Rambelli[57a,57b], I. A. Ramirez-Berend[35], K. Ran[107,113c], D. S. Rankin[130], N. P. Rapheeha[34j], H. Rasheed[28b], A. Rastogi[18a], S. Rave[101], S. Ravera[57a,57b], B. Ravina[37], I. Ravinovich[174], M. Raymond[37], A. L. Read[127], N. P. Readioff[144], D. M. Rebuzzi[73a,73b], A. S. Reed[59], K. Reeves[27], D. Reikher[37], A. Rej[49], C. Rembser[37], H. Ren[62], M. Renda[28b], F. Renner[48], A. G. Rennie[59], M. Repik[56], A. L. Rescia[57a,57b], S. Resconi[71a], M. Ressegotti[57b], S. Rettie[116], W. F. Rettie[35], M. M. Revering[33], O. L. Rezanova[39], P. Reznicek[135], H. Riani[36d], N. Ribaric[51], B. Ricci[69a,69c], E. Ricci[78a,78b], R. Richter[111], S. Richter[47a,47b], E. Richter-Was[86b], M. Ridel[129], S. Ridouani[36d], P. Rieck[119], P. Riedler[37], E. M. Riefel[47a,47b], J. O. Rieger[116], M. Rimoldi[34c], L. Rinaldi[24a,24b], P. Rincke[55,166], G. Ripellino[166], I. Riu[13], J. C. Rivera Vergara[170], F. Rizatdinova[123], E. Rizvi[95], B. R. Roberts[40], S. S. Roberts[138], D. Robinson[33], A. Robson[59], A. Rocchi[76a,76b], C. Roda[74a,74b], F. A. Rodriguez[117], S. Rodriguez Bosca[37], Y. Rodriguez Garcia[23a], A. M. Rodríguez Vera[117], S. Roe[37], J. T. Roemer[37], O. Røhne[127], R. A. Rojas[37], C. P. A. Roland[129], A. Romaniouk[79], E. Romano[73a,73b], M. Romano[24b], N. Rompotis[93], L. Roos[129], S. Rosati[75a], B. J. Rosser[40], E. Rossi[128], E. Rossi[72a,72b], L. P. Rossi[61], L. Rossini[54], R. Rosten[121], M. Rotaru[28b], R. Roth[37], D. Rousseau[66], D. Rousso[48], S. Roy-Garand[160], A. Rozanov[103], Z. M. A. Rozario[59], Y. Rozen[155], A. Rubio Jimenez[168], V. H. Ruelas Rivera[19], T. A. Ruggeri[1], A. Ruggiero[128], A. Ruiz-Martinez[168], A. Rummler[37], G. B. Rupnik Boero[37], Z. Rurikova[54], N. A. Rusakovich[39], S. Ruscelli[49], H. L. Russell[170], G. Russo[138], J. P. Rutherfoord[7], S. Rutherford Colmenares[119], M. Rybar[135], P. Rybczynski[86a], A. Ryzhov[45], F. Safai Tehrani[75a], S. Saha[1], B. Sahoo[174], A. Saibel[168], B. T. Saifuddin[122], M. Saimpert[137], G. T. Saito[82c], M. Saito[158], T. Saito[158], A. Sala[71a,71b], A. Salnikov[148], J. Salt[168], A. Salvador Salas[156], F. Salvatore[151], A. Salzburger[37], D. Sammel[54], E. Sampson[92], D. Sampsonidis[157,d], D. Sampsonidou[125], M. A. A. Samy[59], J. Sánchez[168], V. Sanchez Sebastian[168], H. Sandaker[127], C. O. Sander[48], J. A. Sandesara[175], M. Sandhoff[176], C. Sandoval[23b], L. Sanfilippo[63a], D. P. C. Sankey[136], T. Sano[88], A. Sansoni[53], M. Santana Queiroz[18b], L. Santi[37], C. Santoni[41], H. Santos[132a,132b], L. Santos Pereira Trigo[48], E. Sanzani[24a,24b], K. A. Saoucha[84b], J. G. Saraiva[132a,132d], J. Sardain[7], O. Sasaki[83], K. Sato[162], C. Sauer[37], E. Sauvan[4], P. Savard[160,ai], R. Sawada[158], C. Sawyer[136], L. Sawyer[98], A. M. Sayed[27], C. Sbarra[24b], A. Sbrizzi[24a,24b], T. Scanlon[97], J. Schaarschmidt[141], U. Schäfer[101], A. C. Schaffer[45,66], D. Schaile[110], R. D. Schamberger[150], C. Scharf[19], M. M. Schefer[20], V. A. Schegelsky[38], D. Scheirich[135], M. Schernau[139f], C. Scheulen[56], C. Schiavi[57a,57b], M. Schioppa[44a,44b], S. Schlenker[37], J. Schmeing[176], E. Schmidt[111], M. A. Schmidt[176], K. Schmieden[25], C. Schmitt[101], N. Schmitt[101], S. Schmitt[48], N. A. Schneider[110], L. Schoeffel[137], A. Schoening[63b], P. G. Scholer[35], E. Schopf[146], M. Schott[25], S. Schramm[56], T. Schroer[56], H-C. Schultz-Coulon[63a], M. Schumacher[54], B. A. Schumm[138], Ph. Schune[137], H. R. Schwartz[7], A. Schwartzman[148], T. A. Schwarz[107], Ph. Schwemling[137], R. Schwienhorst[108], F. G. Sciacca[20], A. Sciandra[30], G. Sciolla[27], S. A. Scoville[131], F. Scuri[74a], C. D. Sebastiani[37], K. Sedlaczek[117], S. C. Seidel[114], B. D. Seidlitz[42], C. Seitz[48], J. M. Seixas[82b], G. Sekhniaidze[72a], L. Selem[129], N. Semprini-Cesari[24a,24b], A. Semushin[178], D. Sengupta[56], V. Senthilkumar[116], L. Serin[66], M. Sessa[72a,72b], H. Severini[122], F. Sforza[57a,57b], A. Sfyrla[56], Q. Sha[14], H. Shaddix[117], A. H. Shah[33], R. Shaheen[149], J. D. Shahinian[130], M. Shamim[37], L. Y. Shan[14], M. Shapiro[18a], A. Sharma[37], A. S. Sharma[169], P. Sharma[30], P. B. Shatalov[38], K. Shaw[151], S. M. Shaw[102], Q. Shen[14], D. J. Sheppard[147], P. Sherwood[97], L. Shi[97], X. Shi[14], S. Shimizu[83], I. P. J. Shipsey[128,*], S. Shirabe[89], M. Shiyakova[39,z], M. J. Shochet[40], D. R. Shope[127], B. Shrestha[122], S. Shrestha[121,an], I. Shreyber[39], M. J. Shroff[105], P. Sicho[133], A. M. Sickles[167], E. Sideras Haddad[34j,165], A. C. Sidley[116], A. Sidoti[24b], F. Siegert[50], Dj. Sijacki[16], F. Sili[62], J. M. Silva[52], I. Silva Ferreira[82b], M. V. Silva Oliveira[30], S. B. Silverstein[47a], S. Simion[66], R. Simoniello[37], E. L. Simpson[102], H. Simpson[151], L. R. Simpson[6], S. Simsek[81], S. Sindhu[55], S. N. Singh[27], S. Singh[30], S. Sinha[48], S. Sinha[102], M. Sioli[24a,24b], K. Sioulas[9], I. Siral[37], E. Sitnikova[48], J. Sjölin[47a,47b], A. Skaf[55], E. Skorda[21], P. Skubic[122], M. Slawinska[87], I. Slazyk[17], I. Sliusar[127], V. Smakhtin[174], B. H. Smart[136], S. Yu. Smirnov[139b], Y. Smirnov[34c], L. N. Smirnova[38,a], O. Smirnova[99], A. C. Smith[42], J. L. Smith[102], M. B. Smith[35], R. Smith[148], H. Smitmanns[101], M. Smizanska[92], K. Smolek[134], P. Smolyanskiy[134], A. A. Snesarev[39], H. L. Snoek[116], R. M. Snyder[51], S. Snyder[30], R. Sobie[170,ab], A. Soffer[156], C. A. Solans Sanchez[37], E. Yu. Soldatov[39], U. Soldevila[168], A. A. Solodkov[34j], S. Solomon[27], A. Soloshenko[39], K. Solovieva[54], O. V. Solovyanov[41], P. Sommer[50], A. Sonay[13],

A. Sopczak[134], A. L. Sopio[52], F. Sopkova[29b], J. D. Sorenson[114], I. R. Sotarriva Alvarez[140], V. Sothilingam[63a], O. J. Soto Sandoval[139b,139c], S. Sottocornola[68], R. Soualah[84a], Z. Soumaimi[36e], D. South[48], N. Soybelman[174], S. Spagnolo[70a,70b], A. S. Spellman[125], D. Sperlich[54], B. Spisso[72a,72b], L. Splendori[103], M. Spousta[135], E. J. Staats[35], R. Stamen[63a], E. Stanecka[87], W. Stanek-Maslouska[48], M. V. Stange[50], B. Stanislaus[18a], M. M. Stanitzki[48], E. A. Starchenko[38], G. H. Stark[138], J. Stark[90], P. Staroba[133], P. Starovoitov[84b], R. Staszewski[87], C. Stauch[110], G. Stavropoulos[46], A. Stefl[37], A. Stein[101], P. Steinberg[30], B. Stelzer[147,161a], H. J. Stelzer[131], O. Stelzer[161a], H. Stenzel[58], T. J. Stevenson[151], G. A. Stewart[48], G. Stoicea[28b], M. Stolarski[132a], S. Stonjek[111], A. Straessner[50], J. Strandberg[149], S. Strandberg[47a,47b], M. Stratmann[176], M. Strauss[122], T. Strebler[103], P. Strizenec[29b], R. Ströhmer[171], D. M. Strom[125], R. Stroynowski[45], A. Strubig[47a,47b], S. A. Stucci[30], B. Stugu[17], J. Stupak[122], N. A. Styles[48], D. Su[148], S. Su[62], X. Su[62], D. Suchy[29a], A. D. Sudhakar Ponnu[55], L. Sudit[174], Y. Sue[83], K. Sugizaki[130], V. V. Sulin[38], D. M. S. Sultan[128], L. Sultanaliyeva[25], S. Sultansoy[3b], S. Sun[175], W. Sun[14], S. Sundar Raman[169], N. Sur[99], N. Suri Jr.[177], M. R. Sutton[151], M. Svatos[133], P. N. Swallow[33], M. Swiatlowski[161a], A. Swoboda[37], I. Sykora[29a], M. Sykora[135], T. Sykora[135], D. Ta[101], K. Tackmann[48,y], A. Taffard[164], R. Tafirout[161a], Y. Takubo[83], M. Talby[103], A. A. Talyshev[38], N. M. Tamir[156], A. Tanaka[158], J. Tanaka[158], R. Tanaka[66], M. Tanasini[150], Z. Tao[169], S. Tapia Araya[139g], S. Tapprogge[101], A. Tarek Abouelfadl Mohamed[37], S. Tarem[155], K. Tariq[14], G. Tarna[37], G. F. Tartarelli[71a], M. J. Tartarin[90], P. Tas[135], M. Tasevsky[133], E. Tassi[44a,44b], A. C. Tate[167], Y. Tayalati[36e,aa], G. N. Taylor[106], W. Taylor[161b], R. J. Taylor Vara[168], A. S. Tegetmeier[90], P. Teixeira-Dias[96], J. J. Teoh[160], K. Terashi[158], J. Terron[100], S. Terzo[13], M. Testa[53], R. J. Teuscher[160,ab], A. Thaler[79], O. Theiner[56], T. Theveneaux-Pelzer[103], J. P. Thomas[21], E. A. Thompson[18a], P. D. Thompson[21], E. Thomson[130], R. E. Thornberry[45], C. Tian[62], Y. Tian[56], V. Tikhomirov[81], Yu. A. Tikhonov[39], S. Timoshenko[38], D. Timoshyn[135], E. X.vL. Ting[1], P. Tipton[177], A. Tishelman-Charny[30], K. Todome[140], S. Todorova-Nova[135], L. Toffolin[69a,69c], M. Togawa[83], J. Tojo[89], S. Tokár[29a], O. Toldaiev[68], G. Tolkachev[103], M. Tomoto[83], L. Tompkins[148], E. Torrence[125], H. Torres[90], D. I. Torres Arza[139g], E. Torró Pastor[168], M. Toscani[31], C. Tosciri[40], M. Tost[11], D. R. Tovey[144], T. Trefzger[171], P. M. Tricarico[13], A. Tricoli[30], I. M. Trigger[161a], S. Trincaz-Duvoid[129], D. A. Trischuk[170], A. Tropina[39], D. Truncali[76a,76b], L. Truong[34c], M. Trzebinski[87], A. Trzupek[87], F. Tsai[150], M. Tsai[107], A. Tsiamis[157], P. V. Tsiareshka[39], S. Tsigaridas[161a], A. Tsirigotis[157,t], V. Tsiskaridze[154a], E. G. Tskhadadze[154a], Y. Tsujikawa[88], I. I. Tsukerman[38], V. Tsulaia[18a], K. Tsuri[120], D. Tsybychev[150], Y. Tu[64b], A. Tudorache[28b], V. Tudorache[28b], S. B. Tuncay[128], S. Turchikhin[57a,57b], I. Turk Cakir[3a], R. Turra[71a], T. Turtuvshin[39,ac], P. M. Tuts[42], Y. Uematsu[83], F. Ukegawa[162], P. A. Ulloa Poblete[139b,139c], G. Unal[37], A. Undrus[30], J. Urban[29b], P. Urrejola[139e], G. Usai[8], R. Ushioda[159], M. Usman[109], F. Ustuner[52], Z. Uysal[81], V. Vacek[134], B. Vachon[105], T. Vafeiadis[37], A. Vaitkus[97], C. Valderanis[110], E. Valdes Santurio[47a,47b], M. Valente[37], S. Valentinetti[24a,24b], A. Valero[168], E. Valiente Moreno[168], A. Vallier[90], J. A. Valls Ferrer[168], D. R. Van Arneman[116], R. Van Den Broucke[129], A. Van Der Graaf[49], H. Z. Van Der Schyf[34j], P. Van Gemmeren[6], M. Van Rijnbach[37], S. Van Stroud[97], I. Van Vulpen[116], P. Vana[135], M. Vanadia[76a,76b], U. M. Vande Voorde[149], W. Vandelli[37], E. R. Vandewall[148], D. Vannicola[156], L. Vannoli[53], R. Vari[75a], M. Varma[177], E. W. Varnes[7], C. Varni[79], D. Varouchas[66], L. Varriale[168], K. E. Varvell[152], M. E. Vasile[28b], L. Vaslin[83], M. D. Vassilev[148], A. Vasyukov[39], L. M. Vaughan[123], R. Vavricka[135], T. Vazquez Schroeder[13], J. Veatch[32], V. Vecchio[102], M. J. Veen[104], I. Veliscek[30], I. Velkovska[94], L. M. Veloce[160], F. Veloso[132a,132c], A. G. Veltman[52], S. H. Venetianer[163], S. Veneziano[75a], A. Ventura[70a,70b], A. Verbytskyi[111], M. Verducci[74a,74b], C. Vergis[95], M. Verissimo De Araujo[82b], W. Verkerke[116], J. C. Vermeulen[116], C. Vernieri[148], M. Vessella[164], M. C. Vetterli[147,ai], A. Vgenopoulos[101], N. Viaux Maira[139g,af], T. Vickey[144], O. E. Vickey Boeriu[144], G. H. A. Viehhauser[128], L. Vigani[63b], M. Vigl[111], M. Villa[24a,24b], M. Villaplana Perez[168], E. M. Villhauer[40], E. Vilucchi[53], M. Vincent[168], M. G. Vincter[35], A. Visibile[116], A. Visive[116], C. Vittori[37], I. Vivarelli[24a,24b], M. I. Vivas Albornoz[48], E. Voevodina[111], F. Vogel[110], J. C. Voigt[50], P. Vokac[134], Yu. Volkotrub[86b], L. Vomberg[25], E. Von Toerne[25], B. Vormwald[37], K. Vorobev[51], M. Vos[168], K. Voss[146], M. Vozak[37], L. Vozdecky[122], N. Vranjes[16], M. Vranjes Milosavljevic[16], M. Vreeswijk[116], N. K. Vu[143a,143b], R. Vuillermet[37], O. Vujinovic[101], I. Vukotic[40], I. K. Vyas[35], J. F. Wack[33], A. Wada[112], S. Wada[162], C. Wagner[148], J. M. Wagner[18a], W. Wagner[176], S. Wahdan[176], H. Wahlberg[91], C. H. Waits[122], J. Walder[136], R. Walker[110], K. Walkingshaw Pass[59], W. Walkowiak[146], A. Wall[130], E. J. Wallin[99], T. Wamorkar[148], K. Wandall-Christensen[168], A. Wang[62], A. Z. Wang[138], C. Wang[48], C. Wang[11], H. Wang[18a], J. Wang[64c], P. Wang[102], P. Wang[97], R. Wang[61], R. Wang[107], R. Wang[6], S. M. Wang[153], S. Wang[14], T. Wang[115],

T. Wang[62], W. T. Wang[128], X. Wang[167], X. Wang[143a], X. Wang[48], Y. Wang[150], Y. Wang[114], Z. Wang[107], Z. Wang[143b], Z. Wang[107], C. Wanotayaroj[83], A. Warburton[105], A. L. Warnerbring[146], S. Waterhouse[96], A. T. Watson[21], H. Watson[52], M. F. Watson[21], E. Watton[37], G. Watts[141], B. M. Waugh[97], J. M. Webb[54], C. Weber[30], M. S. Weber[20], C. Wei[62], Y. Wei[54], A. R. Weidberg[128], E. J. Weik[119], J. Weingarten[49], C. Weiser[54], C. J. Wells[48], T. Wenaus[30], T. Wengler[37], N. S. Wenke[111], N. Wermes[25], M. Wessels[63a], A. M. Wharton[92], A. S. White[37], A. White[8], M. J. White[1], D. Whiteson[164], L. Wickremasinghe[126], W. Wiedenmann[175], M. Wielers[136], R. Wierda[149], C. Wiglesworth[43], H. G. Wilkens[37], J. J. H. Wilkinson[33], S. Williams[33], S. Willocq[104], D. J. Wilson[102], P. J. Windischhofer[40], F. I. Winkel[31], F. Winklmeier[125], B. T. Winter[54], M. Wittgen[148], M. Wobisch[98], T. Wojtkowski[60], Z. Wolffs[116], J. Wollrath[37], M. W. Wolter[87], H. Wolters[132a,132c], M. C. Wong[138], E. L. Woodward[42], S. D. Worm[48], B. K. Wosiek[87], K. W. Woźniak[87], S. Wozniewski[55], K. Wraight[59], C. Wu[160], C. Wu[21], J. Wu[158], M. Wu[113b], M. Wu[115], S. L. Wu[175], S. Wu[14,ak], X. Wu[62], Y. Q. Wu[160], Y. Wu[62], Z. Wu[4], Z. Wu[113a], J. Wuerzinger[111], T. R. Wyatt[102], B. M. Wynne[52], S. Xella[43], L. Xia[113a], M. Xie[62], A. Xiong[125], D. Xu[14], H. Xu[62], L. Xu[62], R. Xu[130], T. Xu[107], W. Xu[113a], Y. Xu[141], Z. Xu[52], R. Xue[131], B. Yabsley[152], S. Yacoob[11], Y. Yamaguchi[83], E. Yamashita[158], H. Yamauchi[162], T. Yamazaki[18a], Y. Yamazaki[85], S. Yan[59], Z. Yan[104], H. J. Yang[143a], H. T. Yang[62], S. Yang[62], X. Yang[37], X. Yang[14], Y. Yang[158], Y. Yang[62], W-M. Yao[18a], C. L. Yardley[151], J. Ye[14], S. Ye[30], X. Ye[62], Y. Yeh[97], I. Yeletskikh[39], B. Yeo[18b], M. R. Yexley[97], T. P. Yildirim[128], K. Yorita[173], C. J. S. Young[37], C. Young[148], I. N. L. Young[59], N. D. Young[125], Y. Yu[62], J. Yuan[14,113c,ak], M. Yuan[107], R. Yuan[143b], L. Yue[97], M. Zaazoua[62], B. Zabinski[87], I. Zahir[36a], A. Zaio[57a,57b], Z. K. Zak[87], T. Zakareishvili[168], S. Zambito[56], J. A. Zamora Saa[139d], J. Zang[158], R. Zanzottera[71a,71b], O. Zaplatilek[134], C. Zeitnitz[176], H. Zeng[14], D. T. Zenger Jr.[27], O. Zenin[38], T. Ženiš[29a], S. Zenz[95], D. Zerwas[66], B. Zhang[172], D. F. Zhang[144], G. Zhang[14,ak], J. Zhang[142a], J. Zhang[6], L. Zhang[62], L. Zhang[113a], P. Zhang[14,113c], R. Zhang[113a], S. Zhang[90], Y. Zhang[141], Y. Zhang[97], Y. Zhang[62], Y. Zhang[113a], Z. Zhang[18a], Z. Zhang[142a], Z. Zhang[66], H. Zhao[141], T. Zhao[142a], Y. Zhao[35], Z. Zhao[62], Z. Zhao[62], A. Zhemchugov[39], J. Zheng[113a], K. Zheng[167], L. Zheng[142a], X. Zheng[62], Z. Zheng[148], D. Zhong[167], B. Zhou[107], B. Zhou[143a,143b], H. Zhou[7], N. Zhou[143a], Y. Zhou[15], Y. Zhou[113a], Y. Zhou[7], J. Zhu[107], X. Zhu[143b], Y. Zhu[143a], X. Zhuang[14], K. Zhukov[68], N. I. Zimine[39], J. Zinsser[63b], M. Ziolkowski[146], L. Živković[16], A. Zoccoli[24a,24b], K. Zoch[61], A. Zografos[37], T. G. Zorbas[144], O. Zormpa[46], L. Zwalinski[37]

[1] Department of Physics, University of Adelaide, Adelaide, Australia
[2] Department of Physics, University of Alberta, Edmonton, AB, Canada
[3] [(a)]Department of Physics, Ankara University, Ankara, Turkey; [(b)]Division of Physics, TOBB University of Economics and Technology, Ankara, Turkey
[4] LAPP, Université Savoie Mont Blanc, CNRS/IN2P3, Annecy, France
[5] APC, Université Paris Cité, CNRS/IN2P3, Paris, France
[6] High Energy Physics Division, Argonne National Laboratory, Argonne, IL, USA
[7] Department of Physics, University of Arizona, Tucson, AZ, USA
[8] Department of Physics, University of Texas at Arlington, Arlington, TX, USA
[9] Physics Department, National and Kapodistrian University of Athens, Athens, Greece
[10] Physics Department, National Technical University of Athens, Zografou, Greece
[11] Department of Physics, University of Texas at Austin, Austin, TX, USA
[12] Institute of Physics, Azerbaijan Academy of Sciences, Baku, Azerbaijan
[13] Institut de Física d'Altes Energies (IFAE), Barcelona Institute of Science and Technology, Barcelona, Spain
[14] Institute of High Energy Physics, Chinese Academy of Sciences, Beijing, China
[15] Physics Department, Tsinghua University, Beijing, China
[16] Institute of Physics, University of Belgrade, Belgrade, Serbia
[17] Department for Physics and Technology, University of Bergen, Bergen, Norway
[18] [(a)]Physics Division, Lawrence Berkeley National Laboratory, Berkeley, CA, USA; [(b)]University of California, Berkeley, CA, USA
[19] Institut für Physik, Humboldt Universität zu Berlin, Berlin, Germany
[20] Albert Einstein Center for Fundamental Physics and Laboratory for High Energy Physics, University of Bern, Bern, Switzerland
[21] School of Physics and Astronomy, University of Birmingham, Birmingham, UK

[22] [(a)]Department of Physics, Bogazici University, Istanbul, Turkey; [(b)]Department of Physics Engineering, Gaziantep University, Gaziantep, Turkey; [(c)]Department of Physics, Istanbul University, Istanbul, Turkey
[23] [(a)]Facultad de Ciencias y Centro de Investigaciónes, Universidad Antonio Nariño, Bogotá, Colombia; [(b)]Departamento de Física, Universidad Nacional de Colombia, Bogotá, Colombia
[24] [(a)]Dipartimento di Fisica e Astronomia A. Righi, Università di Bologna, Bologna, Italy; [(b)]INFN Sezione di Bologna, Bologna, Italy
[25] Physikalisches Institut, Universität Bonn, Bonn, Germany
[26] Department of Physics, Boston University, Boston, MA, USA
[27] Department of Physics, Brandeis University, Waltham, MA, USA
[28] [(a)]Transilvania University of Brasov, Brasov, Romania; [(b)]Horia Hulubei National Institute of Physics and Nuclear Engineering, Bucharest, Romania; [(c)]Department of Physics, Alexandru Ioan Cuza University of Iasi, Iasi, Romania; [(d)]National Institute for Research and Development of Isotopic and Molecular Technologies, Physics Department, Cluj-Napoca, Romania; [(e)]National University of Science and Technology Politechnica, Bucharest, Romania; [(f)]West University in Timisoara, Timisoara, Romania; [(g)]Faculty of Physics, University of Bucharest, Bucharest, Romania
[29] [(a)]Faculty of Mathematics, Physics and Informatics, Comenius University, Bratislava, Slovakia; [(b)]Department of Subnuclear Physics, Institute of Experimental Physics of the Slovak Academy of Sciences, Kosice, Slovak Republic
[30] Physics Department, Brookhaven National Laboratory, Upton, NY, USA
[31] Universidad de Buenos Aires, Facultad de Ciencias Exactas y Naturales, Departamento de Física, y CONICET, Instituto de Física de Buenos Aires (IFIBA), Buenos Aires, Argentina
[32] California State University, Long Beach, CA, USA
[33] Cavendish Laboratory, University of Cambridge, Cambridge, UK
[34] [(a)]Department of Physics, University of Cape Town, Cape Town, South Africa; [(b)]iThemba Labs, Western Cape, South Africa; [(c)]Department of Mechanical Engineering Science, University of Johannesburg, Johannesburg, South Africa; [(d)]National Institute of Physics, University of the Philippines Diliman (Philippines), Quezon City, Philippines; [(e)]Department of Physics, Stellenbosch University, Matieland, Western Cape, South Africa; [(f)]School of Agriculture and Science, Mathematics, University of KwaZulu-Natal, Westville, South Africa; [(g)]Department of Physics, University of South Africa, Pretoria, South Africa; [(h)]Department of Mechanical and Aeronautical Engineering, University of Pretoria, Pretoria, South Africa; [(i)]University of Zululand, KwaDlangezwa, South Africa; [(j)]School of Physics, University of the Witwatersrand, Johannesburg, South Africa
[35] Department of Physics, Carleton University, Ottawa, ON, Canada
[36] [(a)]Faculté des Sciences Ain Chock, Université Hassan II de Casablanca, Casablanca, Morocco; [(b)]Faculté des Sciences, Université Ibn-Tofail, Kénitra, Morocco; [(c)]Faculté des Sciences Semlalia, Université Cadi Ayyad, LPHEA-Marrakech, Marrakech, Morocco; [(d)]LPMR, Faculté des Sciences, Université Mohamed Premier, Oujda, Morocco; [(e)]Faculté des Sciences, Université Mohammed V, Rabat, Morocco; [(f)]Institute of Applied Physics, Mohammed VI Polytechnic University, Ben Guerir, Morocco
[37] CERN, Geneva, Switzerland
[38] Affiliated with an Institute Formerly Covered by a Cooperation Agreement with CERN, Geneva, Switzerland
[39] Affiliated with an International Laboratory Covered by a Cooperation Agreement with CERN, Switzerland, Switzerland
[40] Enrico Fermi Institute, University of Chicago, Chicago, IL, USA
[41] LPC, Université Clermont Auvergne, CNRS/IN2P3, Clermont-Ferrand, France
[42] Nevis Laboratory, Columbia University, Irvington, NY, USA
[43] Niels Bohr Institute, University of Copenhagen, Copenhagen, Denmark
[44] [(a)]Dipartimento di Fisica, Università della Calabria, Rende, Italy; [(b)]INFN Gruppo Collegato di Cosenza, Laboratori Nazionali di Frascati, Frascati, Italy
[45] Physics Department, Southern Methodist University, Dallas, TX, USA
[46] National Centre for Scientific Research "Demokritos", Agia Paraskevi, Greece
[47] [(a)]Department of Physics, Stockholm University, Stockholm, Sweden; [(b)]Oskar Klein Centre, Stockholm, Sweden
[48] Deutsches Elektronen-Synchrotron DESY, Hamburg and Zeuthen, Germany
[49] Fakultät Physik, Technische Universität Dortmund, Dortmund, Germany
[50] Institut für Kern-und Teilchenphysik, Technische Universität Dresden, Dresden, Germany
[51] Department of Physics, Duke University, Durham, NC, USA
[52] SUPA - School of Physics and Astronomy, University of Edinburgh, Edinburgh, UK

[53] INFN e Laboratori Nazionali di Frascati, Frascati, Italy
[54] Physikalisches Institut, Albert-Ludwigs-Universität Freiburg, Freiburg, Germany
[55] II. Physikalisches Institut, Georg-August-Universität Göttingen, Göttingen, Germany
[56] Département de Physique Nucléaire et Corpusculaire, Université de Genève, Geneva, Switzerland
[57] [(a)]Dipartimento di Fisica, Università di Genova, Genoa, Italy; [(b)]INFN Sezione di Genova, Genoa, Italy
[58] II. Physikalisches Institut, Justus-Liebig-Universität Giessen, Giessen, Germany
[59] SUPA - School of Physics and Astronomy, University of Glasgow, Glasgow, UK
[60] LPSC, Université Grenoble Alpes, CNRS/IN2P3, Grenoble INP, Grenoble, France
[61] Laboratory for Particle Physics and Cosmology, Harvard University, Cambridge, MA, USA
[62] Department of Modern Physics and State Key Laboratory of Particle Detection and Electronics, University of Science and Technology of China, Hefei, China
[63] [(a)]Kirchhoff-Institut für Physik, Ruprecht-Karls-Universität Heidelberg, Heidelberg, Germany; [(b)]Physikalisches Institut, Ruprecht-Karls-Universität Heidelberg, Heidelberg, Germany
[64] [(a)]Department of Physics, Chinese University of Hong Kong, Shatin N.T., Hong Kong; [(b)]Department of Physics, University of Hong Kong, Pok Fu Lam, Hong Kong; [(c)]Department of Physics and Institute for Advanced Study, Hong Kong University of Science and Technology, Clear Water Bay, Kowloon, Hong Kong, China
[65] Department of Physics, National Tsing Hua University, Hsinchu, Taiwan
[66] IJCLab, Université Paris-Saclay, CNRS/IN2P3, 91405 Orsay, France
[67] Centro Nacional de Microelectrónica (IMB-CNM-CSIC), Barcelona, Spain
[68] Department of Physics, Indiana University, Bloomington, IN, USA
[69] [(a)]INFN Gruppo Collegato di Udine, Sezione di Trieste, Udine, Italy; [(b)]ICTP, Trieste, Italy; [(c)]Dipartimento Politecnico di Ingegneria e Architettura, Università di Udine, Udine, Italy
[70] [(a)]INFN Sezione di Lecce, Lecce, Italy; [(b)]Dipartimento di Matematica e Fisica, Università del Salento, Lecce, Italy
[71] [(a)]INFN Sezione di Milano, Milan, Italy; [(b)]Dipartimento di Fisica, Università di Milano, Milan, Italy
[72] [(a)]INFN Sezione di Napoli, Naples, Italy; [(b)]Dipartimento di Fisica, Università di Napoli, Naples, Italy
[73] [(a)]INFN Sezione di Pavia, Pavia, Italy; [(b)]Dipartimento di Fisica, Università di Pavia, Pavia, Italy
[74] [(a)]INFN Sezione di Pisa, Pisa, Italy; [(b)]Dipartimento di Fisica E. Fermi, Università di Pisa, Pisa, Italy
[75] [(a)]INFN Sezione di Roma, Rome, Italy; [(b)]Dipartimento di Fisica, Sapienza Università di Roma, Rome, Italy
[76] [(a)]INFN Sezione di Roma Tor Vergata, Rome, Italy; [(b)]Dipartimento di Fisica, Università di Roma Tor Vergata, Rome, Italy
[77] [(a)]INFN Sezione di Roma Tre, Rome, Italy; [(b)]Dipartimento di Matematica e Fisica, Università Roma Tre, Rome, Italy
[78] [(a)]INFN-TIFPA, Povo, Italy; [(b)]Università degli Studi di Trento, Trento, Italy
[79] Universität Innsbruck, Department of Astro and Particle Physics, Innsbruck, Austria
[80] Department of Physics and Astronomy, Iowa State University, Ames, IA, USA
[81] Istinye University, Sariyer, Istanbul, Turkey
[82] [(a)]Departamento de Engenharia Elétrica, Universidade Federal de Juiz de Fora (UFJF), Juiz de Fora, Brazil; [(b)]Universidade Federal do Rio De Janeiro COPPE/EE/IF, Rio de Janeiro, Brazil; [(c)]Instituto de Física, Universidade de São Paulo, São Paulo, Brazil; [(d)]Rio de Janeiro State University, Rio de Janeiro, Brazil; [(e)]Federal University of Bahia, Bahia, Brazil
[83] KEK, High Energy Accelerator Research Organization, Tsukuba, Japan
[84] [(a)]Khalifa University of Science and Technology, Abu Dhabi, United Arab Emirates; [(b)]University of Sharjah, Sharjah, United Arab Emirates
[85] Graduate School of Science, Kobe University, Kobe, Japan
[86] [(a)]Faculty of Physics and Applied Computer Science, AGH University of Krakow, Krakow, Poland; [(b)]Marian Smoluchowski Institute of Physics, Jagiellonian University, Krakow, Poland
[87] Institute of Nuclear Physics Polish Academy of Sciences, Krakow, Poland
[88] Faculty of Science, Kyoto University, Kyoto, Japan
[89] Research Center for Advanced Particle Physics and Department of Physics, Kyushu University, Fukuoka , Japan
[90] L2IT, Université de Toulouse, CNRS/IN2P3, UPS, Toulouse, France
[91] Instituto de Física La Plata, Universidad Nacional de La Plata and CONICET, La Plata, Argentina
[92] Physics Department, Lancaster University, Lancaster, UK
[93] Oliver Lodge Laboratory, University of Liverpool, Liverpool, UK

[94] Department of Experimental Particle Physics, Jožef Stefan Institute and Department of Physics, University of Ljubljana, Ljubljana, Slovenia
[95] Department of Physics and Astronomy, Queen Mary University of London, London, UK
[96] Department of Physics, Royal Holloway University of London, Egham, UK
[97] Department of Physics and Astronomy, University College London, London, UK
[98] Louisiana Tech University, Ruston, LA, USA
[99] Fysiska institutionen, Lunds universitet, Lund, Sweden
[100] Departamento de Física Teorica C-15 and CIAFF, Universidad Autónoma de Madrid, Madrid, Spain
[101] Institut für Physik, Universität Mainz, Mainz, Germany
[102] School of Physics and Astronomy, University of Manchester, Manchester, UK
[103] CPPM, Aix-Marseille Université, CNRS/IN2P3, Marseille, France
[104] Department of Physics, University of Massachusetts, Amherst, MA, USA
[105] Department of Physics, McGill University, Montreal, QC, Canada
[106] School of Physics, University of Melbourne, Melbourne, VIC, Australia
[107] Department of Physics, University of Michigan, Ann Arbor, MI, USA
[108] Department of Physics and Astronomy, Michigan State University, East Lansing, MI, USA
[109] Group of Particle Physics, University of Montreal, Montreal, QC, Canada
[110] Fakultät für Physik, Ludwig-Maximilians-Universität München, München, Germany
[111] Max-Planck-Institut für Physik (Werner-Heisenberg-Institut), München, Germany
[112] Graduate School of Science and Kobayashi-Maskawa Institute, Nagoya University, Nagoya, Japan
[113] [(a)]Department of Physics, Nanjing University, Nanjing, China; [(b)]School of Science, Shenzhen Campus of Sun Yat-sen University, Guangzhou, China; [(c)]University of Chinese Academy of Science (UCAS), Beijing, China
[114] Department of Physics and Astronomy, University of New Mexico, Albuquerque, NM, USA
[115] Institute for Mathematics, Astrophysics and Particle Physics, Radboud University/Nikhef, Nijmegen, The Netherlands
[116] Nikhef National Institute for Subatomic Physics and University of Amsterdam, Amsterdam, The Netherlands
[117] Department of Physics, Northern Illinois University, DeKalb, IL, USA
[118] [(a)]New York University Abu Dhabi, Abu Dhabi, United Arab Emirates; [(b)]United Arab Emirates University, Al Ain, United Arab Emirates
[119] Department of Physics, New York University, New York, NY, USA
[120] Ochanomizu University, Otsuka, Bunkyo-ku, Tokyo, Japan
[121] Ohio State University, Columbus, OH, USA
[122] Homer L. Dodge Department of Physics and Astronomy, University of Oklahoma, Norman, OK, USA
[123] Department of Physics, Oklahoma State University, Stillwater, OK, USA
[124] Palacký University, Joint Laboratory of Optics, Olomouc, Czech Republic
[125] Institute for Fundamental Science, University of Oregon, Eugene, OR, USA
[126] Graduate School of Science, University of Osaka, Osaka, Japan
[127] Department of Physics, University of Oslo, Oslo, Norway
[128] Department of Physics, Oxford University, Oxford, UK
[129] LPNHE, Sorbonne Université, Université Paris Cité, CNRS/IN2P3, Paris, France
[130] Department of Physics, University of Pennsylvania, Philadelphia, PA, USA
[131] Department of Physics and Astronomy, University of Pittsburgh, Pittsburgh, PA, USA
[132] [(a)]Laboratório de Instrumentação e Física Experimental de Partículas - LIP, Lisbon, Portugal; [(b)]Departamento de Física, Faculdade de Ciências, Universidade de Lisboa, Lisbon, Portugal; [(c)]Departamento de Física, Universidade de Coimbra, Coimbra, Portugal; [(d)]Centro de Física Nuclear da Universidade de Lisboa, Lisbon, Portugal; [(e)]Departamento de Física, Escola de Ciências, Universidade do Minho, Braga, Portugal; [(f)]Departamento de Física Teórica y del Cosmos, Universidad de Granada, Granada , Spain; [(g)]Departamento de Física, Instituto Superior Técnico, Universidade de Lisboa, Lisboa, Portugal
[133] Institute of Physics of the Czech Academy of Sciences, Prague, Czech Republic
[134] Czech Technical University in Prague, Prague, Czech Republic
[135] Faculty of Mathematics and Physics, Charles University, Prague, Czech Republic
[136] Particle Physics Department, Rutherford Appleton Laboratory, Didcot, UK
[137] IRFU, CEA, Université Paris-Saclay, Gif-sur-Yvette, France
[138] Santa Cruz Institute for Particle Physics, University of California Santa Cruz, Santa Cruz, CA, USA

[139] [(a)]Departamento de Física, Pontificia Universidad Católica de Chile, Santiago, Chile; [(b)]Millennium Institute for Subatomic Physics at High Energy Frontier (SAPHIR), Santiago, Chile; [(c)]Instituto de Investigación Multidisciplinario en Ciencia y Tecnología, y Departamento de Física, Universidad de La Serena, La Serena, Chile; [(d)]Department of Physics, Universidad Andres Bello, Santiago, Chile; [(e)]Universidad San Sebastian, Recoleta, Argentina; [(f)]Instituto de Alta Investigación, Universidad de Tarapacá, Arica, Chile; [(g)]Departamento de Física, Universidad Técnica Federico Santa María, Valparaíso, Chile
[140] Department of Physics, Institute of Science, Tokyo, Japan
[141] Department of Physics, University of Washington, Seattle, WA, USA
[142] [(a)]Institute of Frontier and Interdisciplinary Science and Key Laboratory of Particle Physics and Particle Irradiation (MOE), Shandong University, Qingdao, China; [(b)]School of Physics, Zhengzhou University, Zhengzhou, China
[143] [(a)]State Key Laboratory of Dark Matter Physics, School of Physics and Astronomy, Shanghai Jiao Tong University, Key Laboratory for Particle Astrophysics and Cosmology (MOE), SKLPPC, Shanghai, China; [(b)]State Key Laboratory of Dark Matter Physics, Tsung-Dao Lee Institute, Shanghai Jiao Tong University, Shanghai, China
[144] Department of Physics and Astronomy, University of Sheffield, Sheffield, UK
[145] Department of Physics, Shinshu University, Nagano, Japan
[146] Department Physik, Universität Siegen, Siegen, Germany
[147] Department of Physics, Simon Fraser University, Burnaby, BC, Canada
[148] SLAC National Accelerator Laboratory, Stanford, CA, USA
[149] Department of Physics, Royal Institute of Technology, Stockholm, Sweden
[150] Departments of Physics and Astronomy, Stony Brook University, Stony Brook, NY, USA
[151] Department of Physics and Astronomy, University of Sussex, Brighton, UK
[152] School of Physics, University of Sydney, Sydney, Australia
[153] Institute of Physics, Academia Sinica, Taipei, Taiwan
[154] [(a)]E. Andronikashvili Institute of Physics, Iv. Javakhishvili Tbilisi State University, Tbilisi, Georgia; [(b)]High Energy Physics Institute, Tbilisi State University, Tbilisi, Georgia; [(c)]University of Georgia, Tbilisi, Georgia
[155] Department of Physics, Technion, Israel Institute of Technology, Haifa, Israel
[156] Raymond and Beverly Sackler School of Physics and Astronomy, Tel Aviv University, Tel Aviv, Israel
[157] Department of Physics, Aristotle University of Thessaloniki, Thessaloniki, Greece
[158] International Center for Elementary Particle Physics and Department of Physics, University of Tokyo, Tokyo, Japan
[159] Graduate School of Science and Technology, Tokyo Metropolitan University, Tokyo, Japan
[160] Department of Physics, University of Toronto, Toronto, ON, Canada
[161] [(a)]TRIUMF, Vancouver, BC, Canada; [(b)]Department of Physics and Astronomy, York University, Toronto, ON, Canada
[162] Division of Physics and Tomonaga Center for the History of the Universe, Faculty of Pure and Applied Sciences, University of Tsukuba, Tsukuba, Japan
[163] Department of Physics and Astronomy, Tufts University, Medford, MA, USA
[164] Department of Physics and Astronomy, University of California Irvine, Irvine, CA, USA
[165] University of West Attica, Athens, Greece
[166] Department of Physics and Astronomy, University of Uppsala, Uppsala, Sweden
[167] Department of Physics, University of Illinois, Urbana, IL, USA
[168] Instituto de Física Corpuscular (IFIC), Centro Mixto Universidad de Valencia - CSIC, Valencia, Spain
[169] Department of Physics, University of British Columbia, Vancouver, BC, Canada
[170] Department of Physics and Astronomy, University of Victoria, Victoria, BC, Canada
[171] Fakultät für Physik und Astronomie, Julius-Maximilians-Universität Würzburg, Würzburg, Germany
[172] Department of Physics, University of Warwick, Coventry, UK
[173] Waseda University, Tokyo, Japan
[174] Department of Particle Physics and Astrophysics, Weizmann Institute of Science, Rehovot, Israel
[175] Department of Physics, University of Wisconsin, Madison, WI, USA
[176] Fakultät für Mathematik und Naturwissenschaften, Fachgruppe Physik, Bergische Universität Wuppertal, Wuppertal, Germany
[177] Department of Physics, Yale University, New Haven, CT, USA
[178] Yerevan Physics Institute, Yerevan, Armenia

[a] Also at Affiliated with an Institute Formerly Covered by a Cooperation Agreement with CERN, Geneva, Switzerland

[b] Also at An-Najah National University, Nablus, Palestine
[c] Also at Borough of Manhattan Community College, City University of New York, New York, NY, USA
[d] Also at Center for Interdisciplinary Research and Innovation (CIRI-AUTH), Thessaloniki, Greece
[e] Also at Centre of Physics of the Universities of Minho and Porto (CF-UM-UP), Braga, Portugal
[f] Also at CERN, Geneva, Switzerland
[g] Also at Département de Physique Nucléaire et Corpusculaire, Université de Genève, Geneva, Switzerland
[h] Also at Departament de Fisica de la Universitat Autonoma de Barcelona, Barcelona, Spain
[i] Also at Department of Financial and Management Engineering, University of the Aegean, Chios, Greece
[j] Also at Department of Modern Physics and State Key Laboratory of Particle Detection and Electronics, University of Science and Technology of China, Hefei, China
[k] Also at Department of Physics, Ben Gurion University of the Negev, Beer Sheva, Israel
[l] Also at Department of Physics, Bolu Abant Izzet Baysal University, Bolu, Turkey
[m] Also at Department of Physics, King's College London, London, UK
[n] Also at Department of Physics, Stellenbosch University, Stellenbosch, South Africa
[o] Also at Department of Physics, University of Fribourg, Fribourg, Switzerland
[p] Also at Department of Physics, University of Thessaly, Volos, Greece
[q] Also at Department of Physics, Westmont College, Santa Barbara, USA
[r] Also at Faculty of Physics, Sofia University, 'St. Kliment Ohridski', Sofia, Bulgaria
[s] Also at Faculty of Physics, University of Bucharest, Bucharest, Romania
[t] Also at Hellenic Open University, Patras, Greece
[u] Also at Henan University, Kaifeng, China
[v] Also at Imam Mohammad Ibn Saud Islamic University, Riyadh, Saudi Arabia
[w] Also at Indian Institute of Technology (IIT), Jodhpur, India
[x] Also at Institucio Catalana de Recerca i Estudis Avancats, ICREA, Barcelona, Spain
[y] Also at Institut für Experimentalphysik, Universität Hamburg, Hamburg, Germany
[z] Also at Institute for Nuclear Research and Nuclear Energy (INRNE) of the Bulgarian Academy of Sciences, Sofia, Bulgaria
[aa] Also at Institute of Applied Physics, Mohammed VI Polytechnic University, Ben Guerir, Morocco
[ab] Also at Institute of Particle Physics (IPP), Edmonton, Canada
[ac] Also at Institute of Physics and Technology, Mongolian Academy of Sciences, Ulaanbaatar, Mongolia
[ad] Also at Institute of Physics, Azerbaijan Academy of Sciences, Baku, Azerbaijan
[ae] Also at Institute of Theoretical Physics, Ilia State University, Tbilisi, Georgia
[af] Also at Millennium Institute for Subatomic Physics at High Energy Frontier (SAPHIR), Santiago, Chile
[ag] Also at National Institute of Physics, University of the Philippines Diliman (Philippines), Quezon City, Philippines
[ah] Also at The Collaborative Innovation Center of Quantum Matter (CICQM), Beijing, China
[ai] Also at TRIUMF, Vancouver, BC, Canada
[aj] Also at Università di Napoli Parthenope, Naples, Italy
[ak] Also at University of Chinese Academy of Sciences (UCAS), Beijing, China
[al] Also at Department of Physics, University of Colorado Boulder, Boulder, CO, USA
[am] Also at University of Siena, Siena, Italy
[an] Also at Washington College, Chestertown, MD, USA
[ao] Also at Physics Department, Yeditepe University, Istanbul, Turkey
* Deceased